LARGE SCALE CLUSTERING IN THE SDSS LUMINOUS RED GALAXY SAMPLE

Eyal Kazin
Center for Cosmology and Particle Physics
New York University

In Collaboration with:
Michael Blanton, NYU
and:
Román Scoccimarro, NYU
Andreas Berlind, Vanderbilt Uni.
Cameron McBride, Vanderbilt Uni.

Today I will discuss:

- ☐ Introduction 13 minutes
  - ☐ Quantifying Clustering
  - ☐ LRGs- Why (should) we like these galaxies so much?
  - ☐ The Sloan Digital Sky Survey
- ☐ Baryonic Acoustic Feature 30 minutes
- ☐ Introduction to Redshift Distortions 2 minutes
- ☐ Redshift Distortions in Clustering 5 minutes

Large-Scale Structure

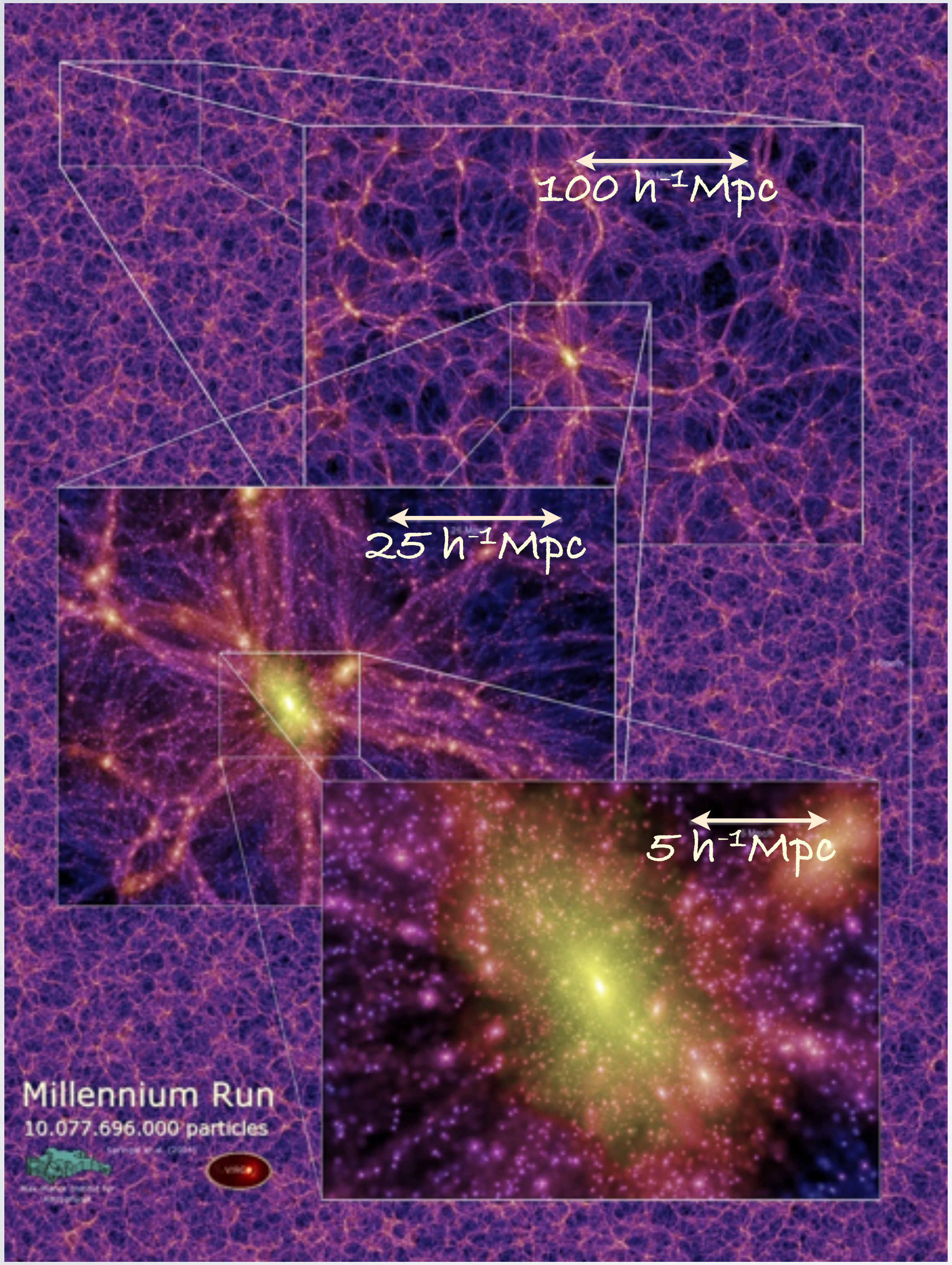

The Millennium Simulation Project

Dark Matter Distribution

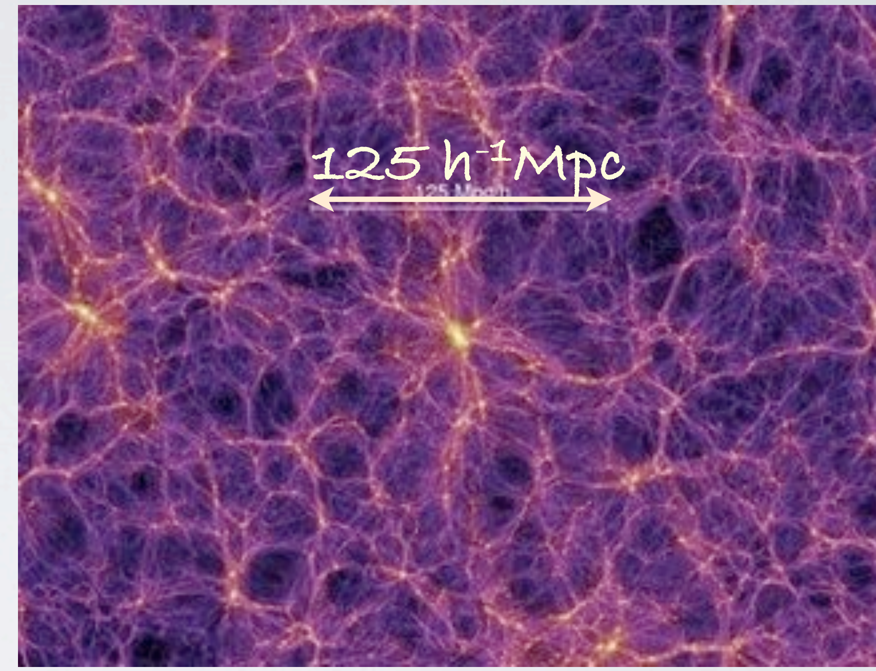

Mock Galaxy Distribution

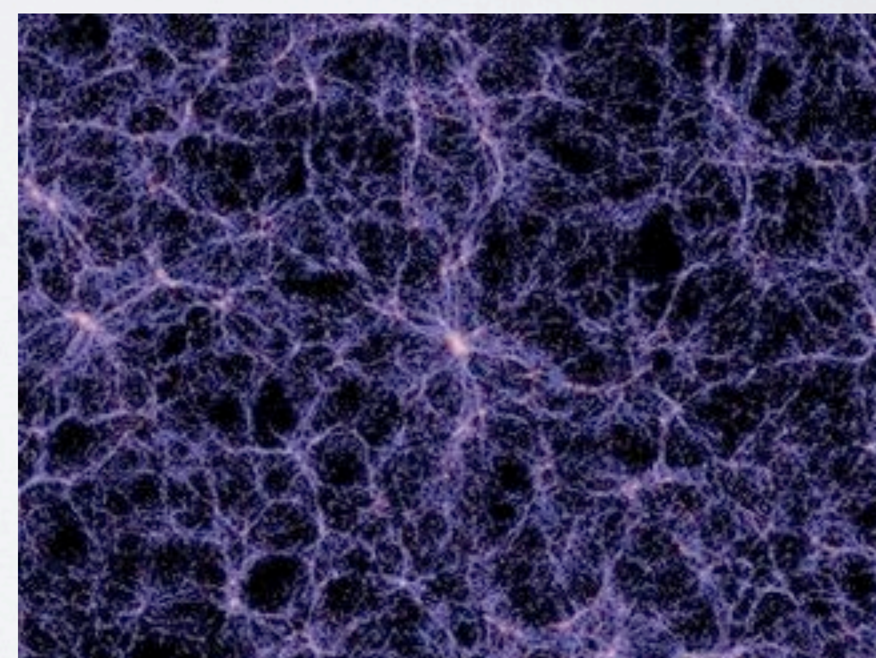

Springel et al. (2005)

Quantifying Clustering

$$\rho(x) = \bar{\rho}(1+\delta(x))$$

ρ- density

δ- overdensity

$\delta \geq -1$

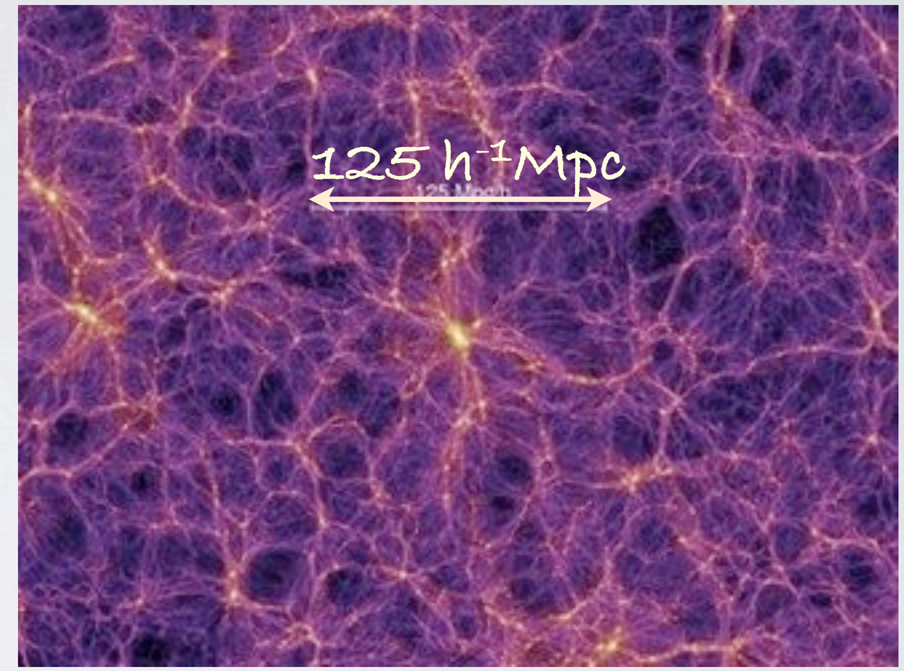

Springel et al. (2005)

2 point functions

correlation function $\xi(r) \equiv \langle \delta(x)\delta(x+r) \rangle_{volume}$

Power Spectrum $P(k) \equiv \int d^3x e^{-ikr} \xi(r)$

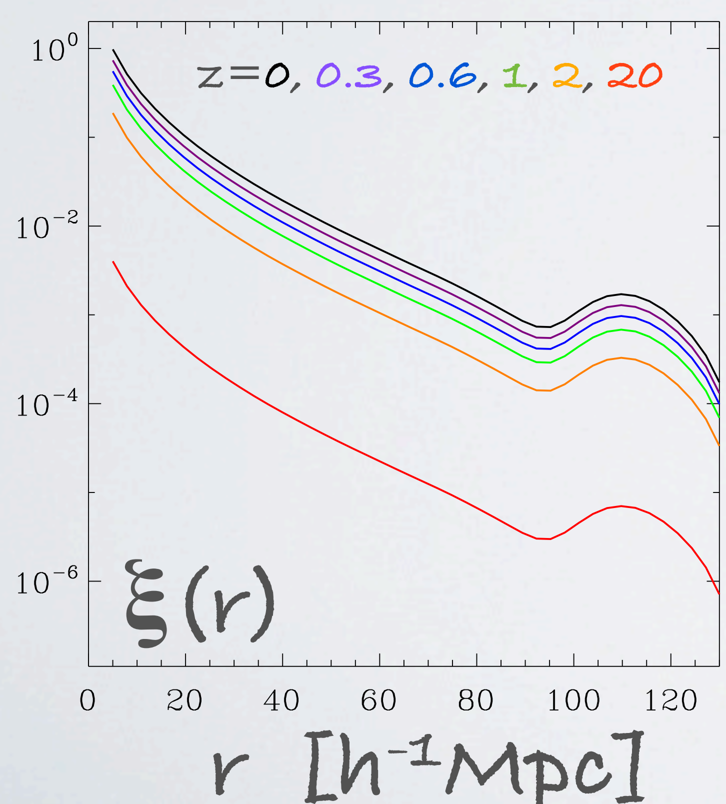

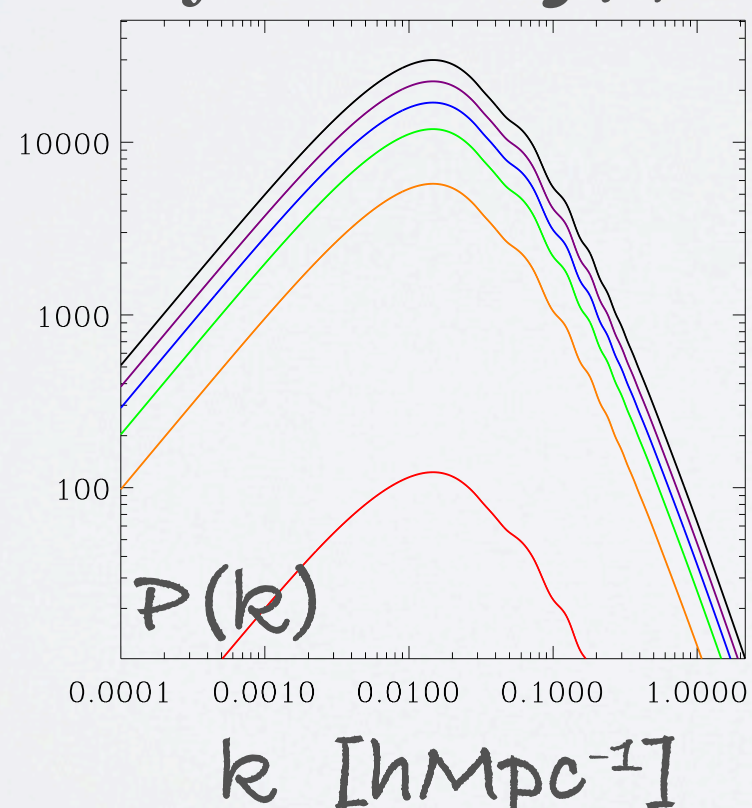

Luminous Red Galaxies

From a talk by Max Tegmark

Padmanabhan et al. (2007)

based on Bruzual&Charlot (2003) model

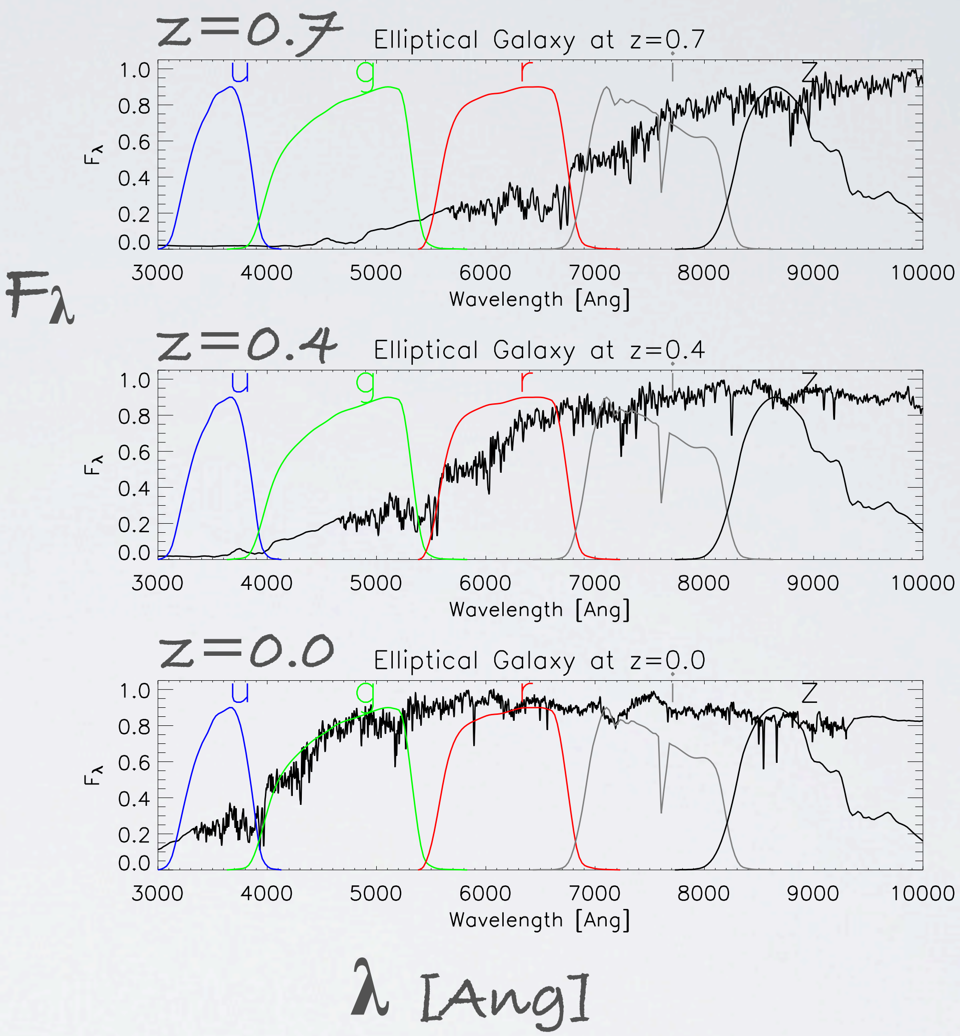

- Luminous ➢ Enable large volume limited samples
- Not too rare $n(z) \sim 3 \cdot 10^{-4}\ (h\mathrm{Mpc}^{-1})^3$
- Trace Matter well, "bias" (clustering gain) $b_{Lin} \sim 2$
- Easy to identify by color cuts, spectra

$\delta_{gal} \approx b_{Lin}\delta$

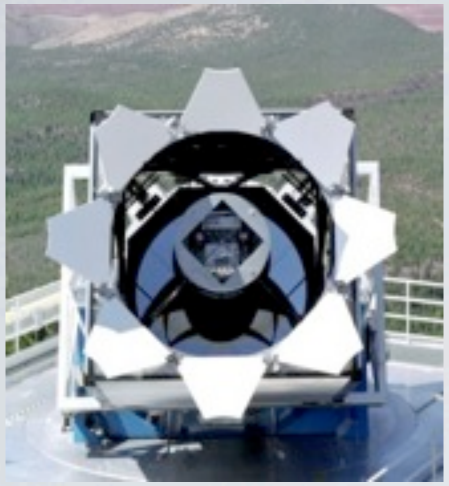

The Sloan Digital Sky Survey LRG Sample

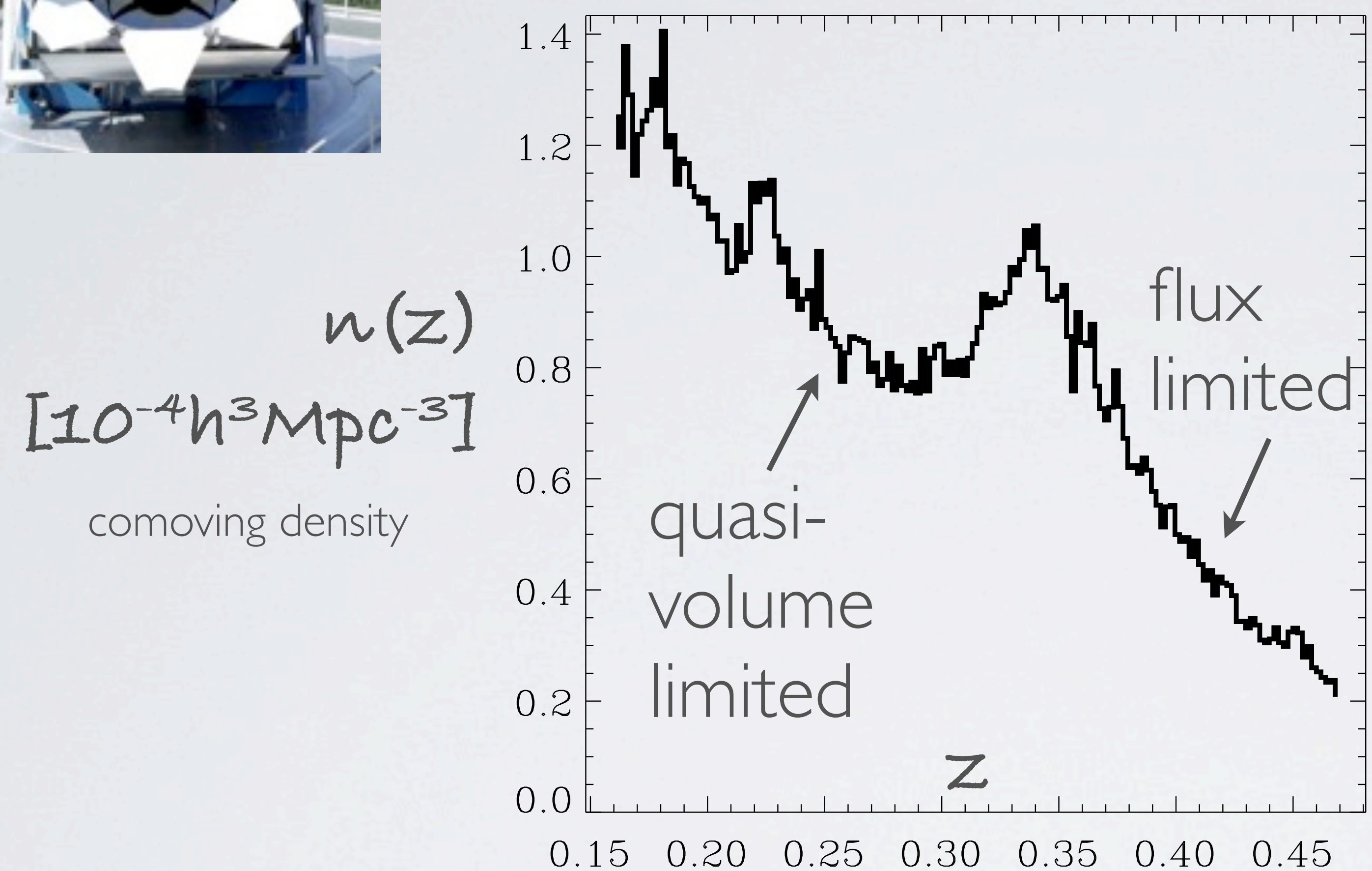

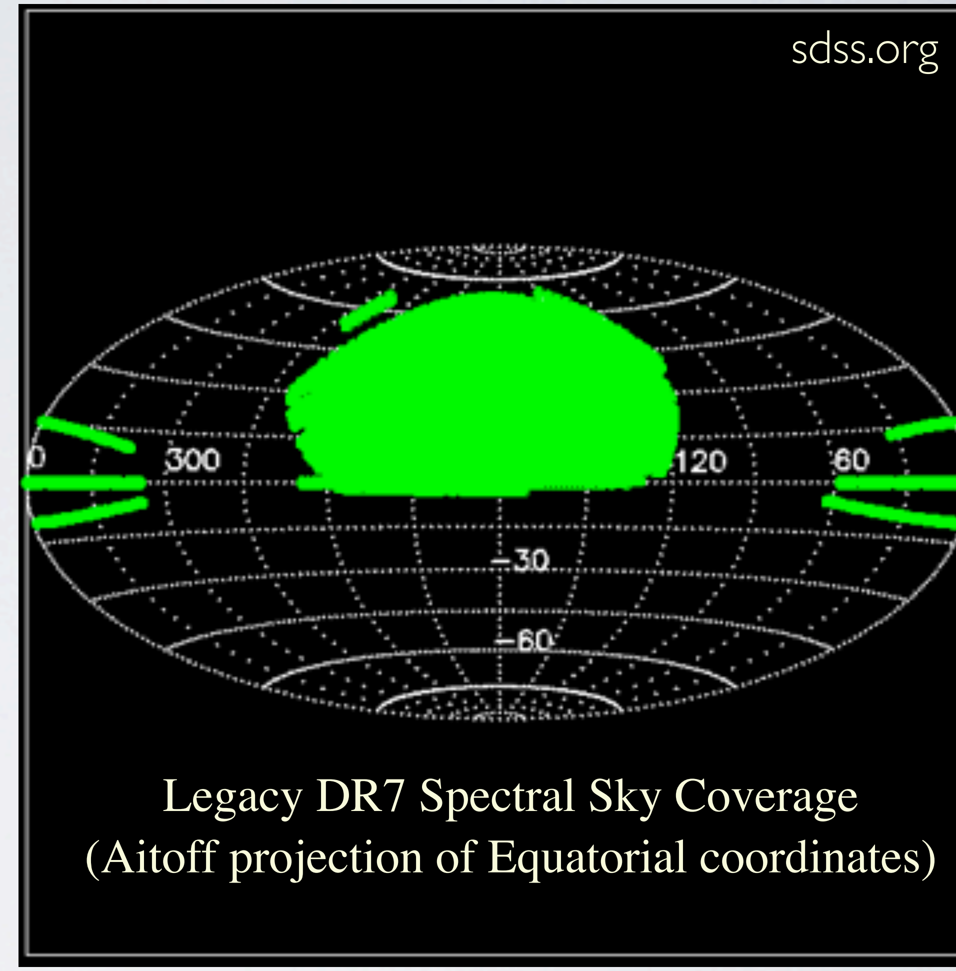

Legacy DR7 Spectral Sky Coverage (Aitoff projection of Equatorial coordinates)

- >100,00 LRGs between $0.16<z<0.47$
- Sky Coverage ~8,000 degree^2
- Comoving Volume 1.6 h^{-3}Gpc^3 of which:

  quasi-volume Limited until

  $z<0.36$ (0.66 h^{-3}Gpc^3)

Today I will discuss:

- [ ] Introduction 13 minutes
  - [x] Quantifying Clustering
  - [x] LRGs- Why (should) we like these galaxies so much?
  - [x] The Sloan Digital Sky Survey
- [ ] Baryonic Acoustic Feature 30 minutes
- [ ] Introduction to Redshift Distortions 2 minutes
- [ ] Redshift Distortions in Clustering 5 minutes

The Baryonic Acoustic Feature
Linear Theory

CMB T-T   Larson et al. (2010)

Feature in the early universe:

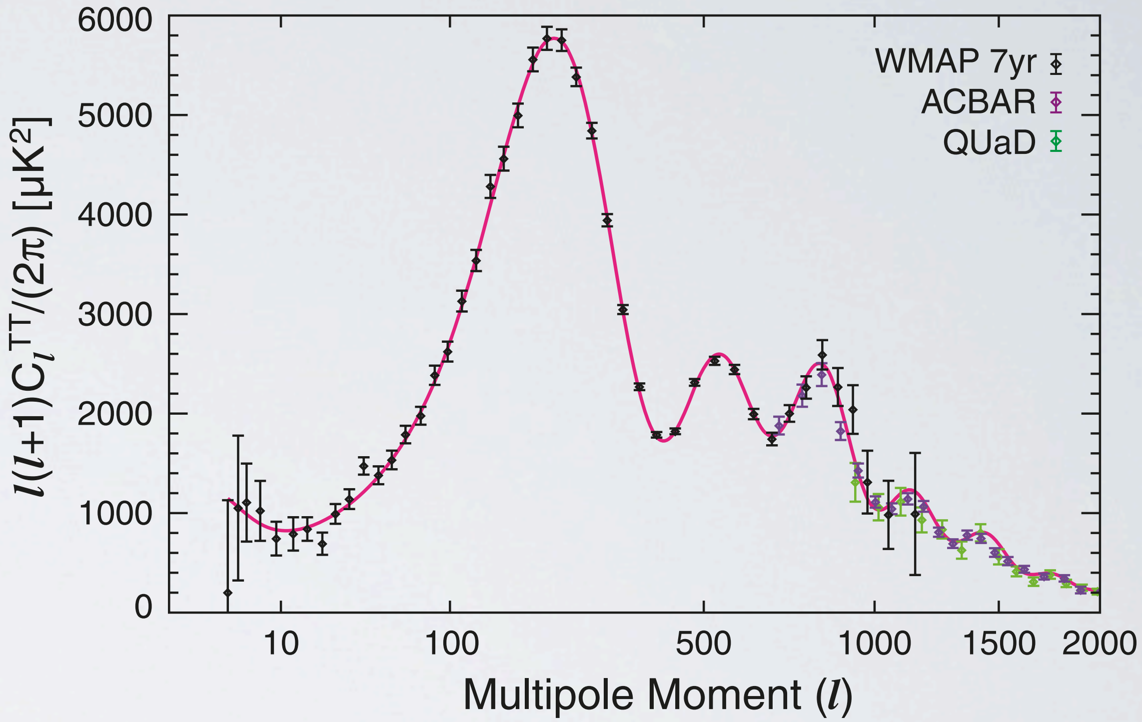

Baryonic Acoustic Origins

Plots by Daniel Eisenstein

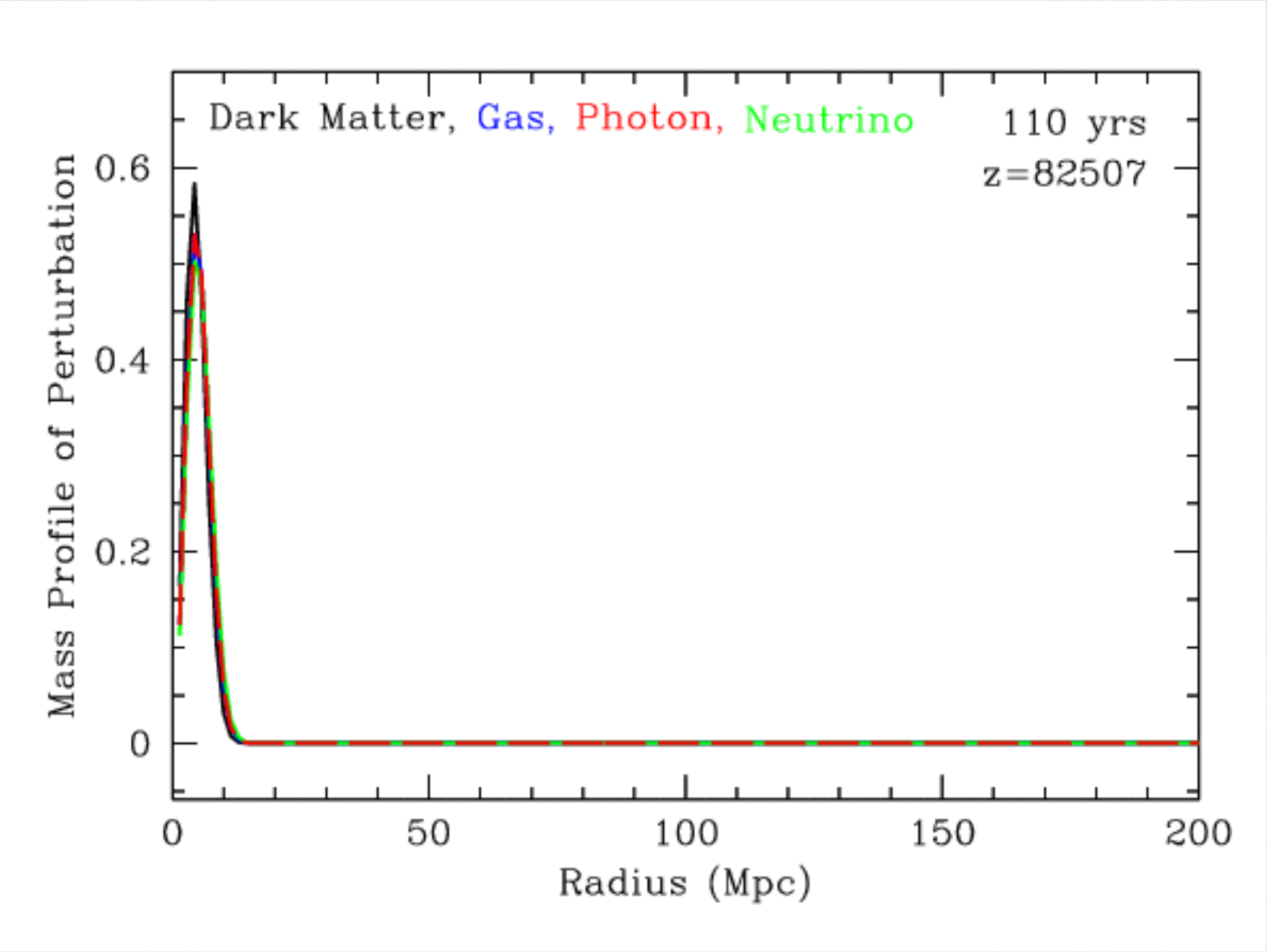

Baryonic Acoustic Origins

Plots by Daniel Eisenstein

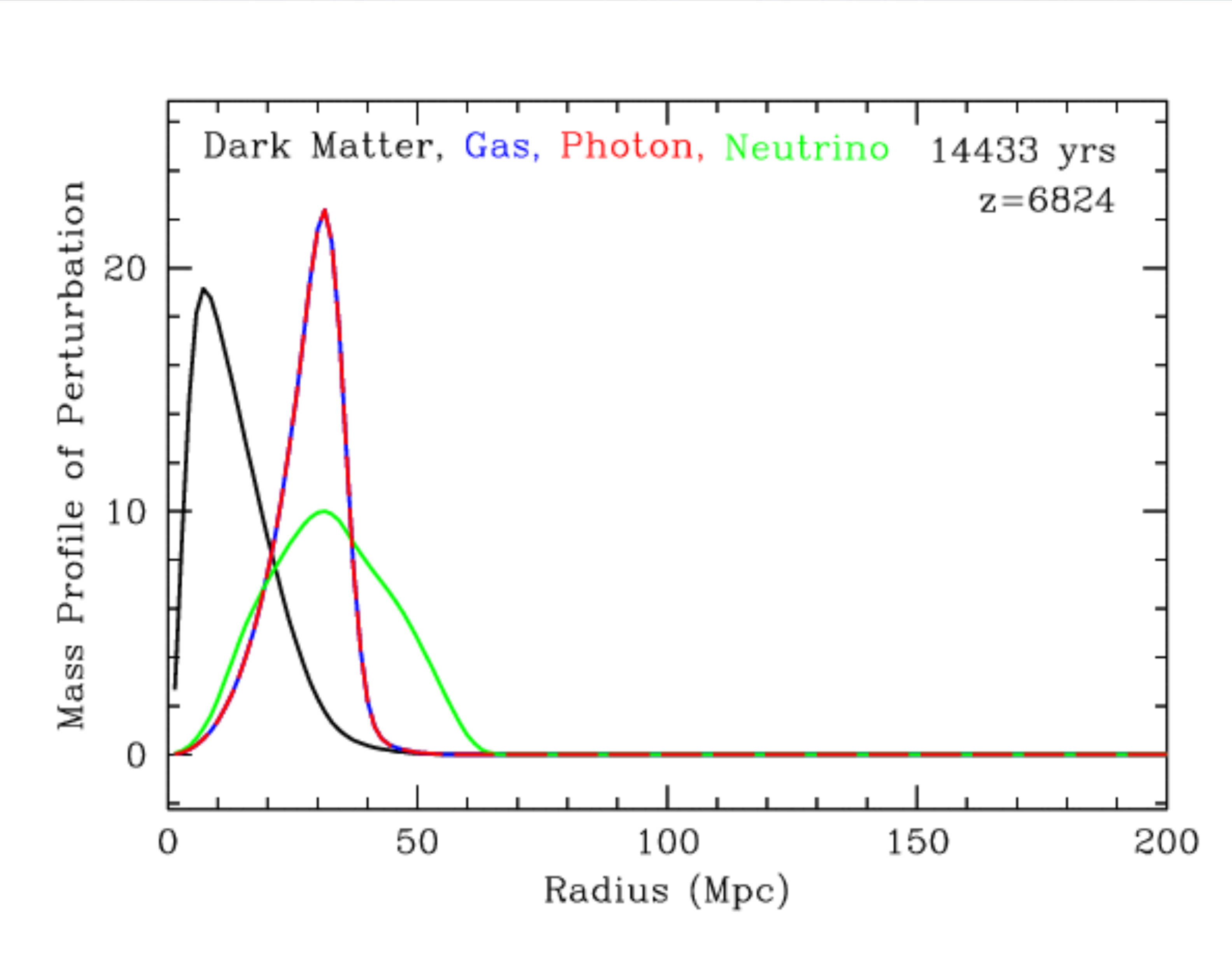

Baryonic Acoustic Origins

Plots by Daniel Eisenstein

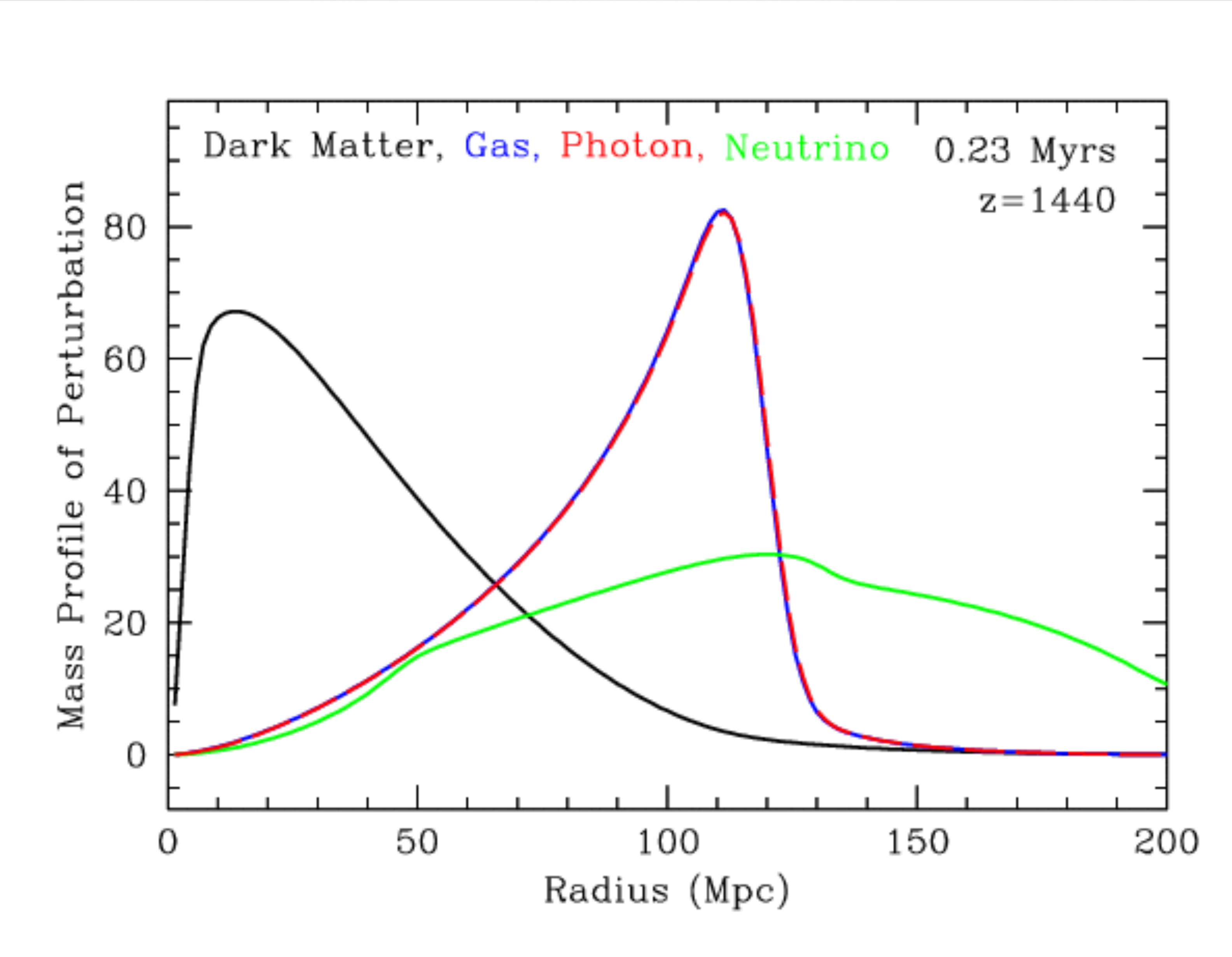

Baryonic Acoustic Origins

Plots by Daniel Eisenstein

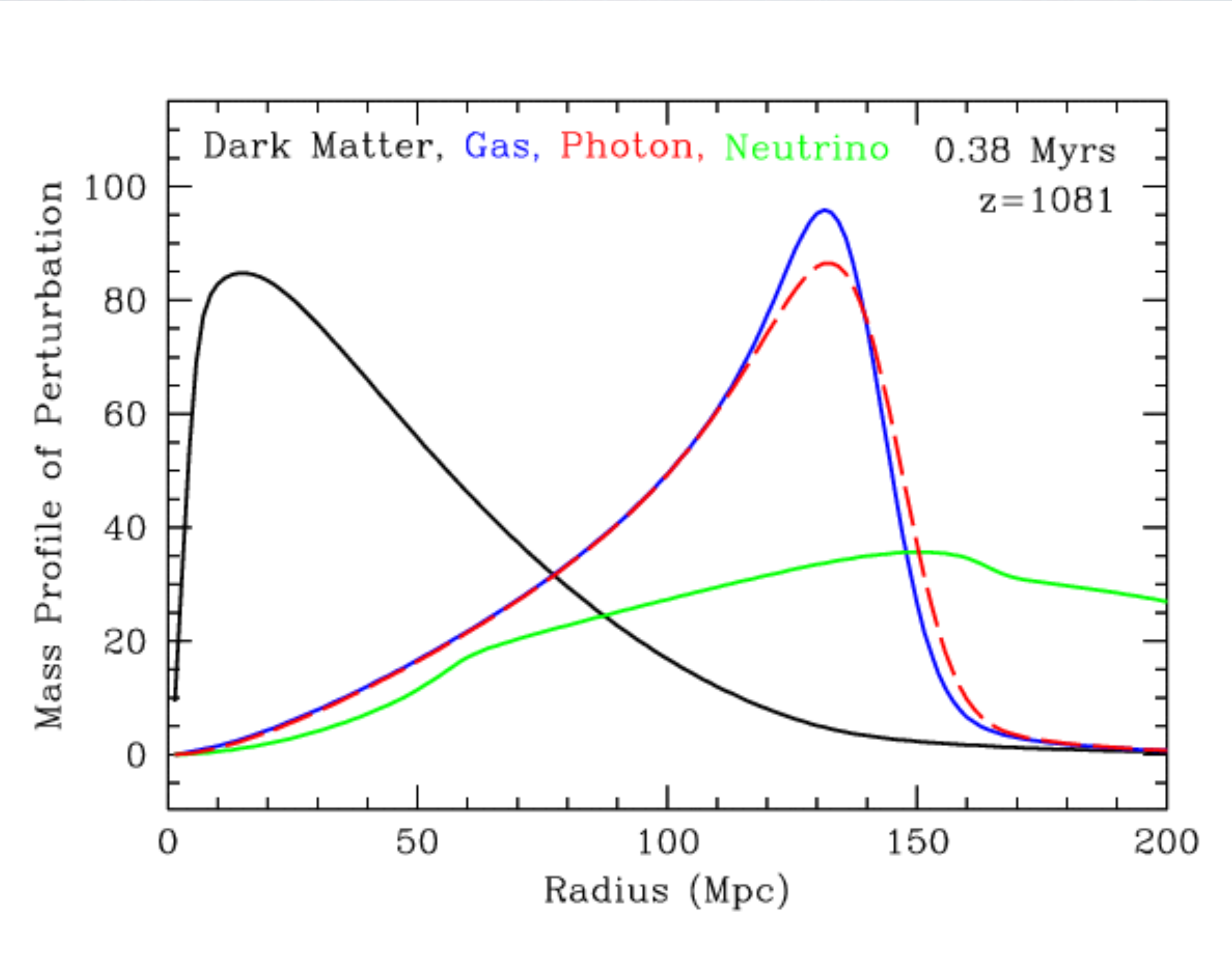

Baryonic Acoustic Origins

Plots by Daniel Eisenstein

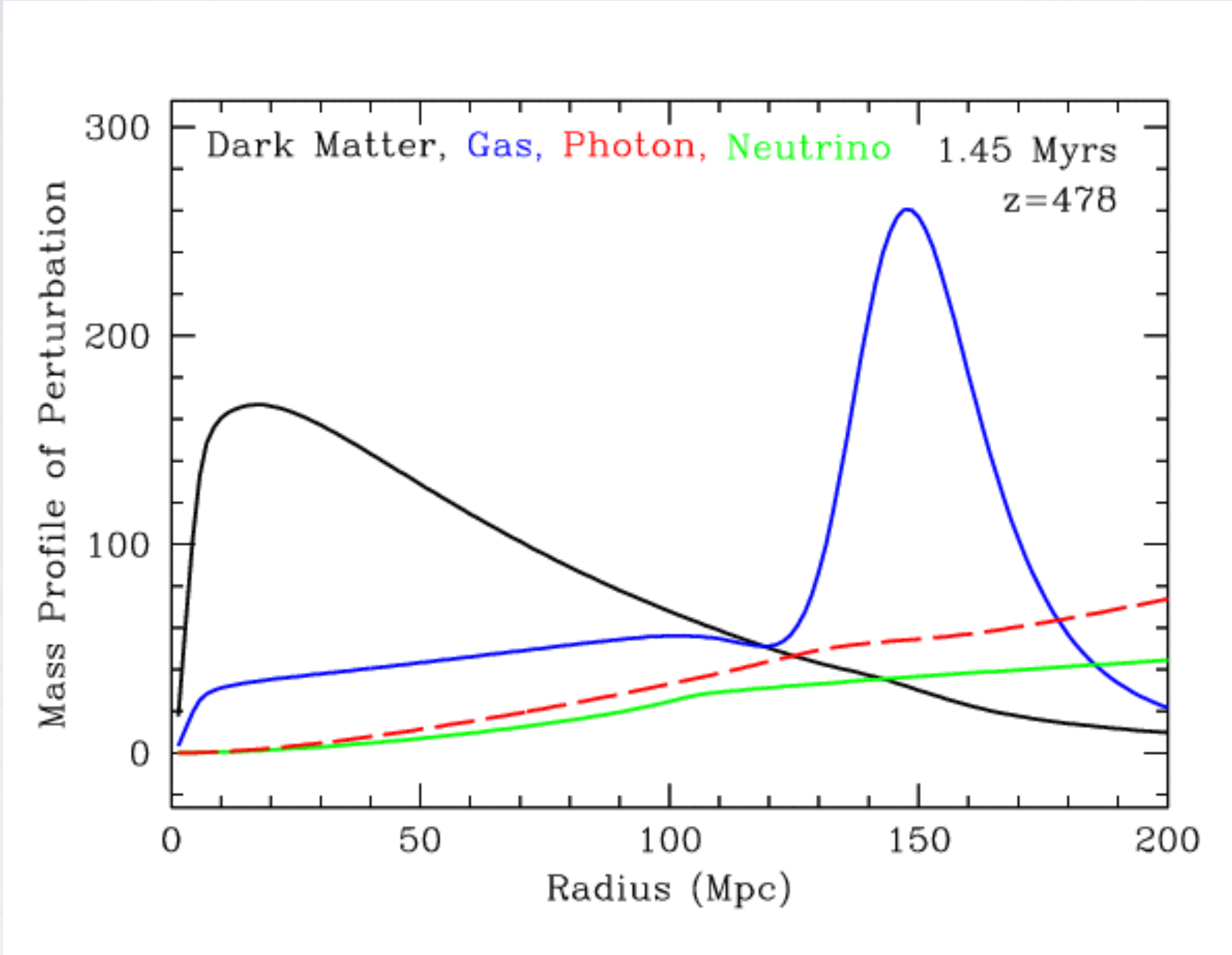

Baryonic Acoustic Origins

Plots by Daniel Eisenstein

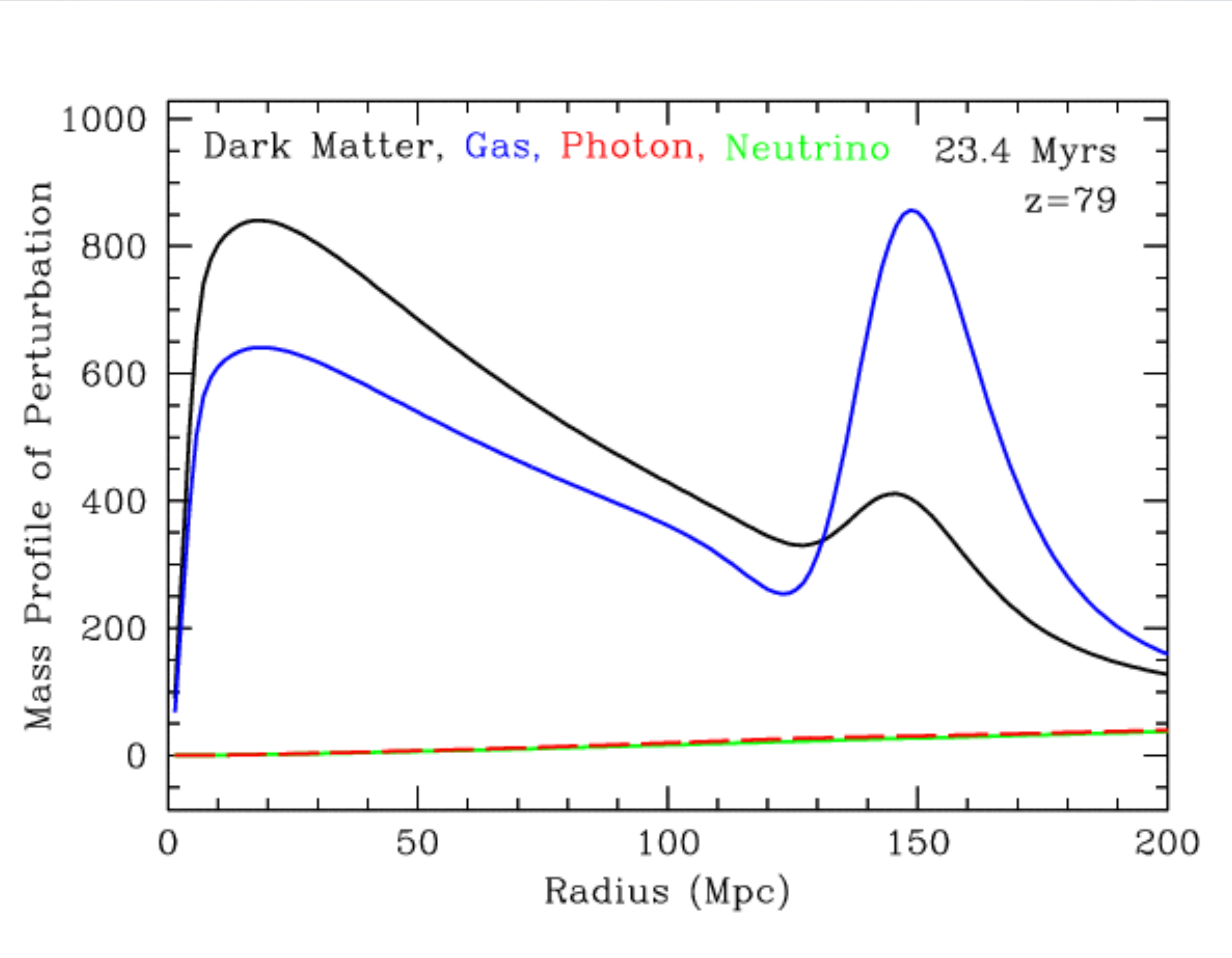

Baryonic Acoustic Origins

Plots by Daniel Eisenstein

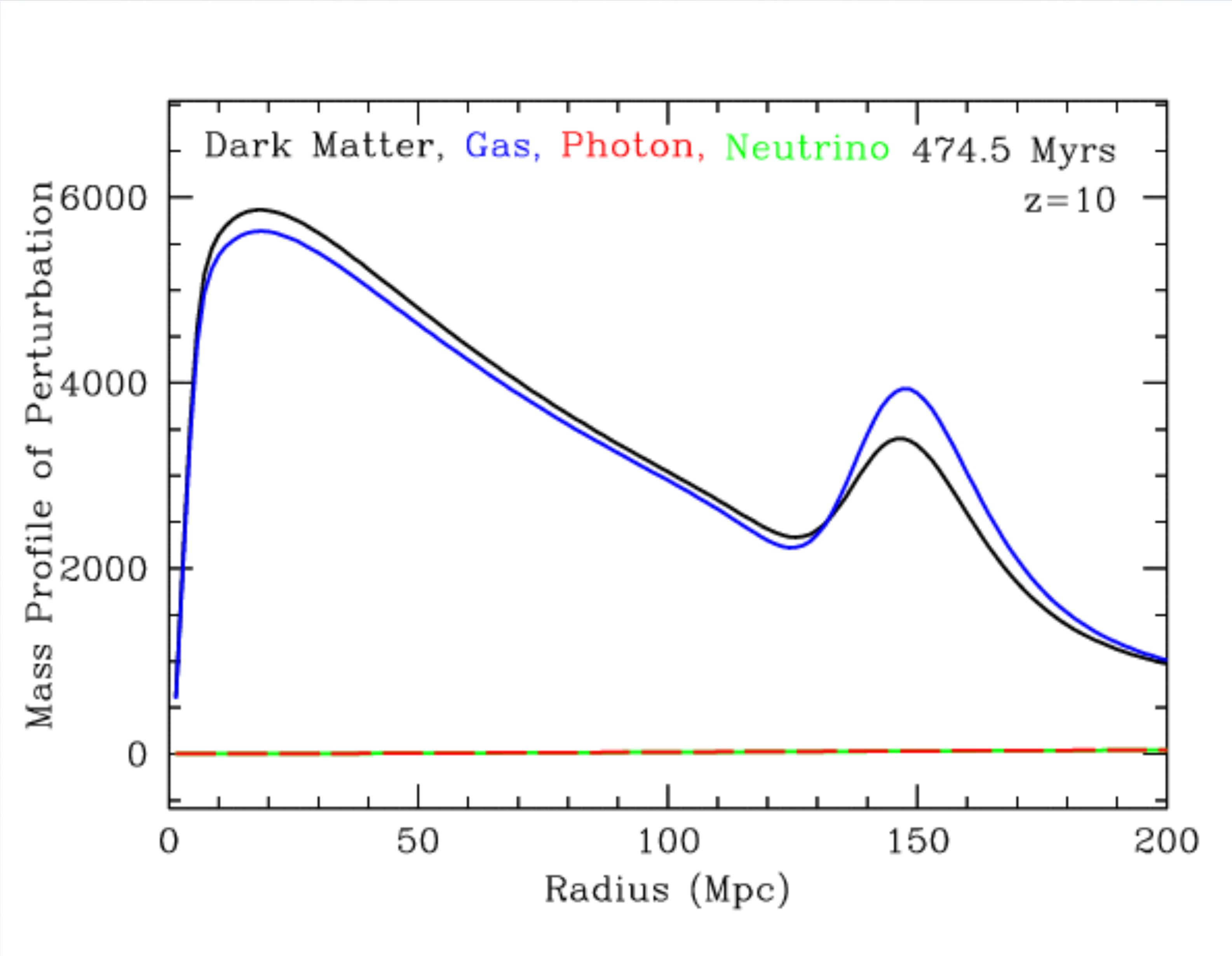

Baryonic Acoustic Origins

Plots by Daniel Eisenstein

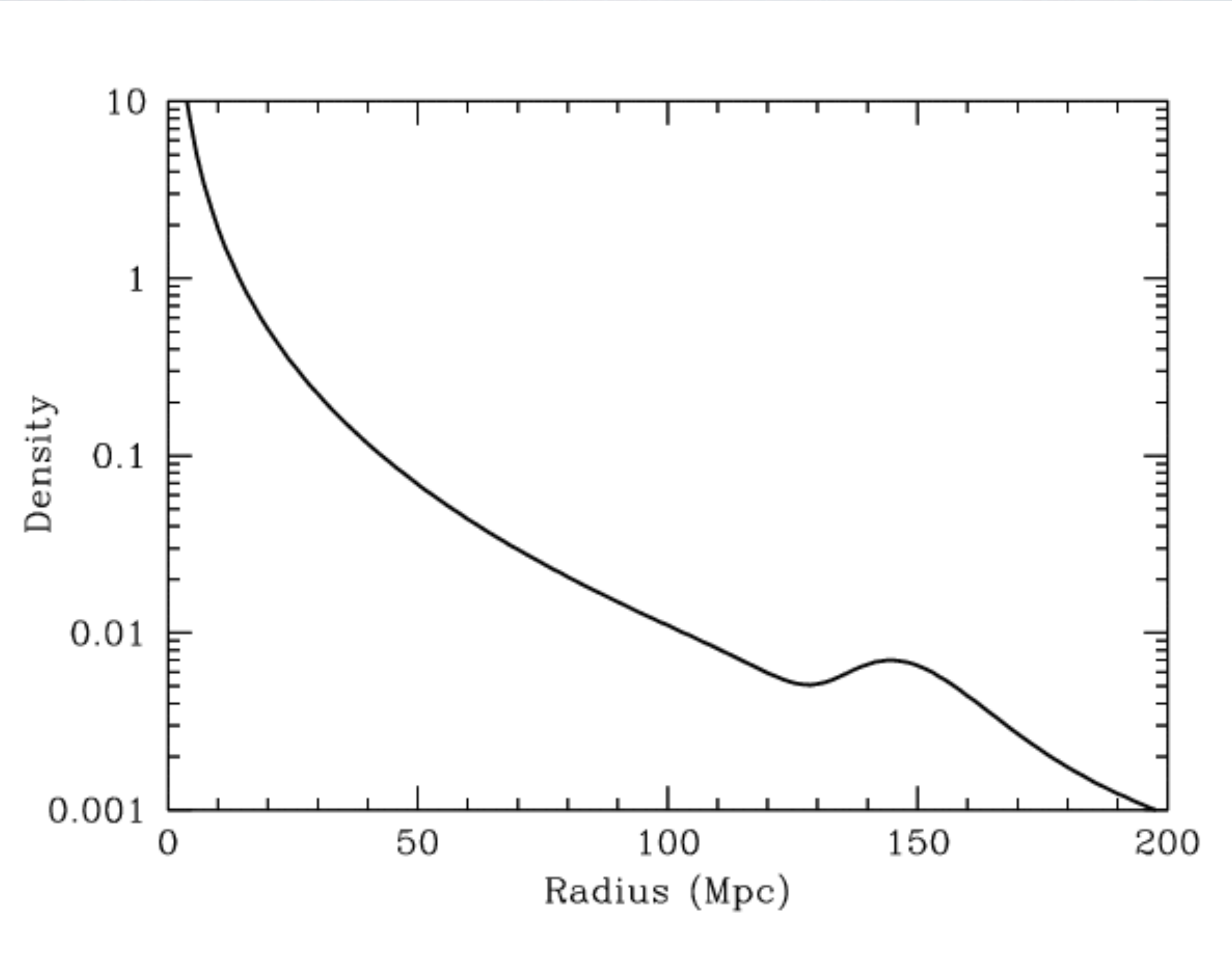

The Baryonic Acoustic Feature
Linear Theory

Feature in the early universe:

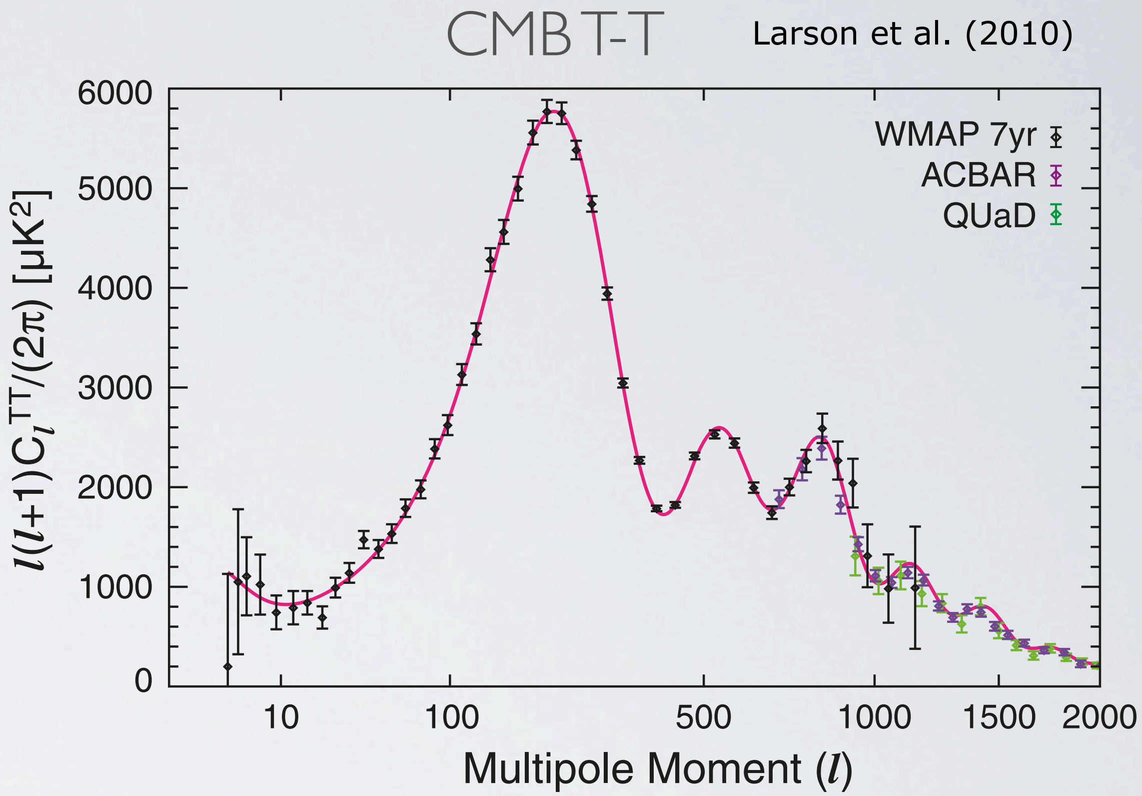

Feature in the late universe:

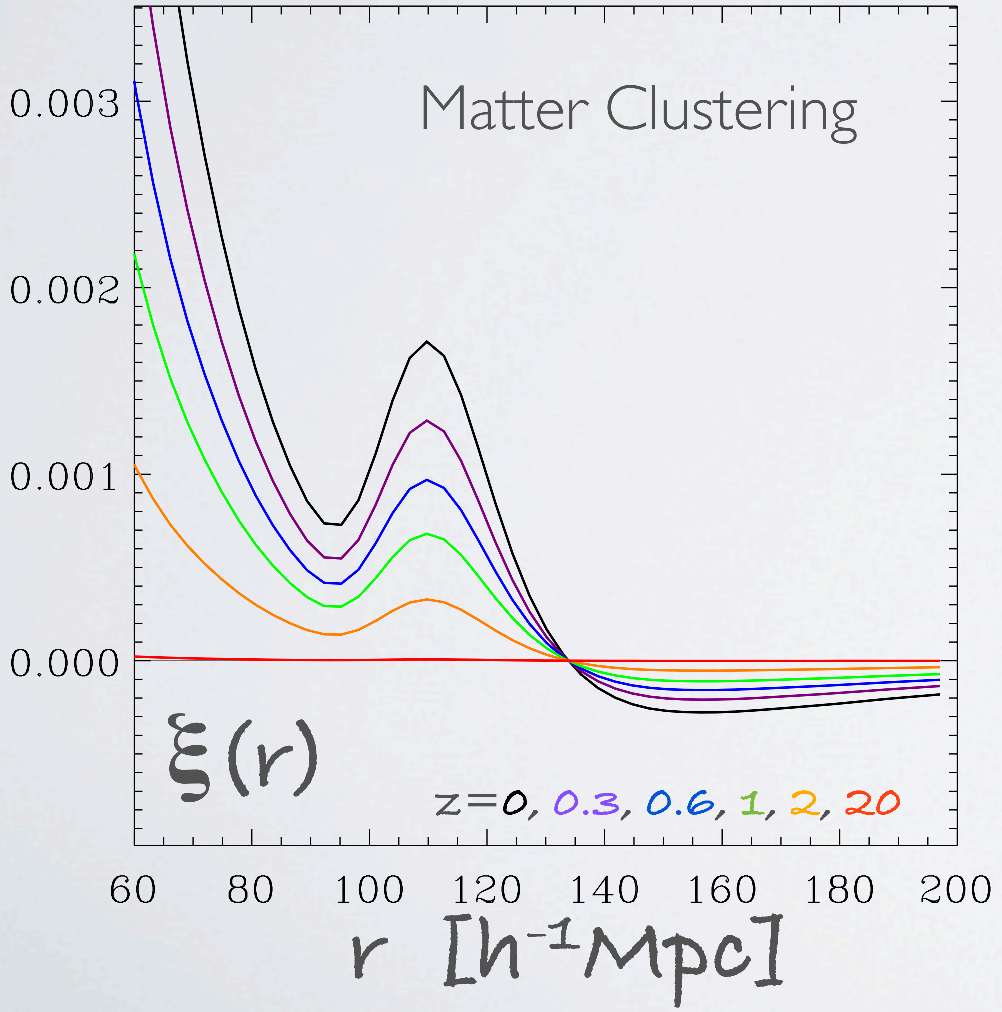

The Baryonic Acoustic Feature
Linear Theory

Feature in the early universe:

CMB T-T

Larson et al. (2010)

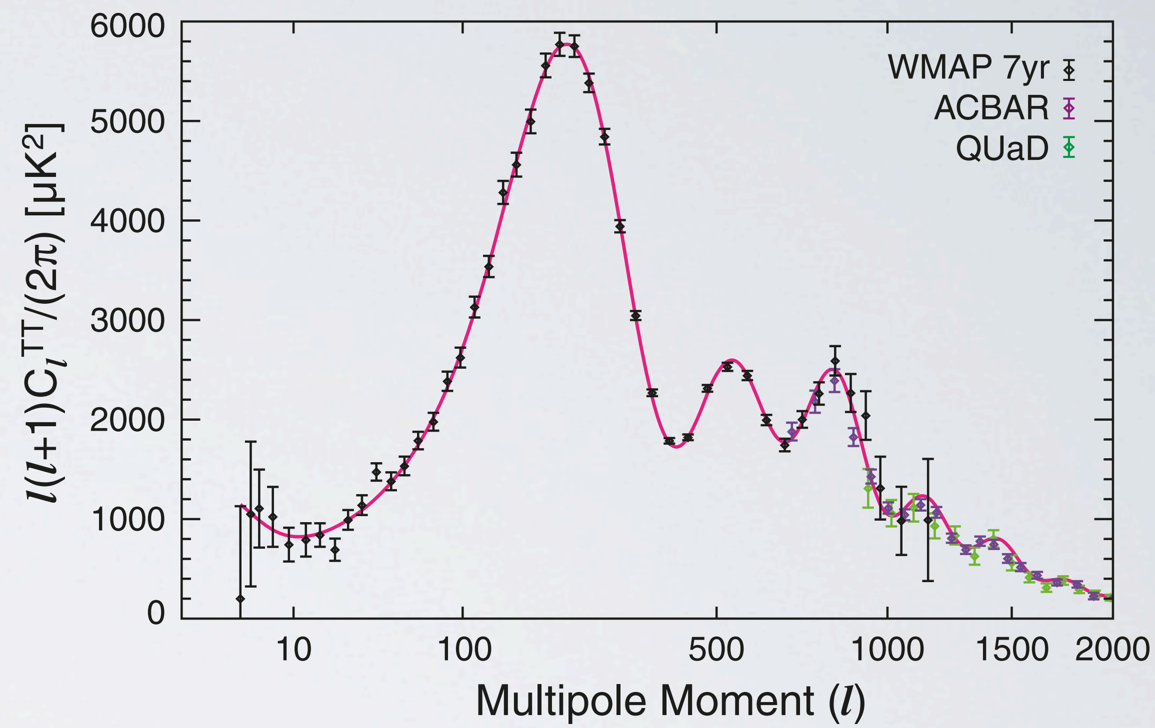

Feature in the late universe:

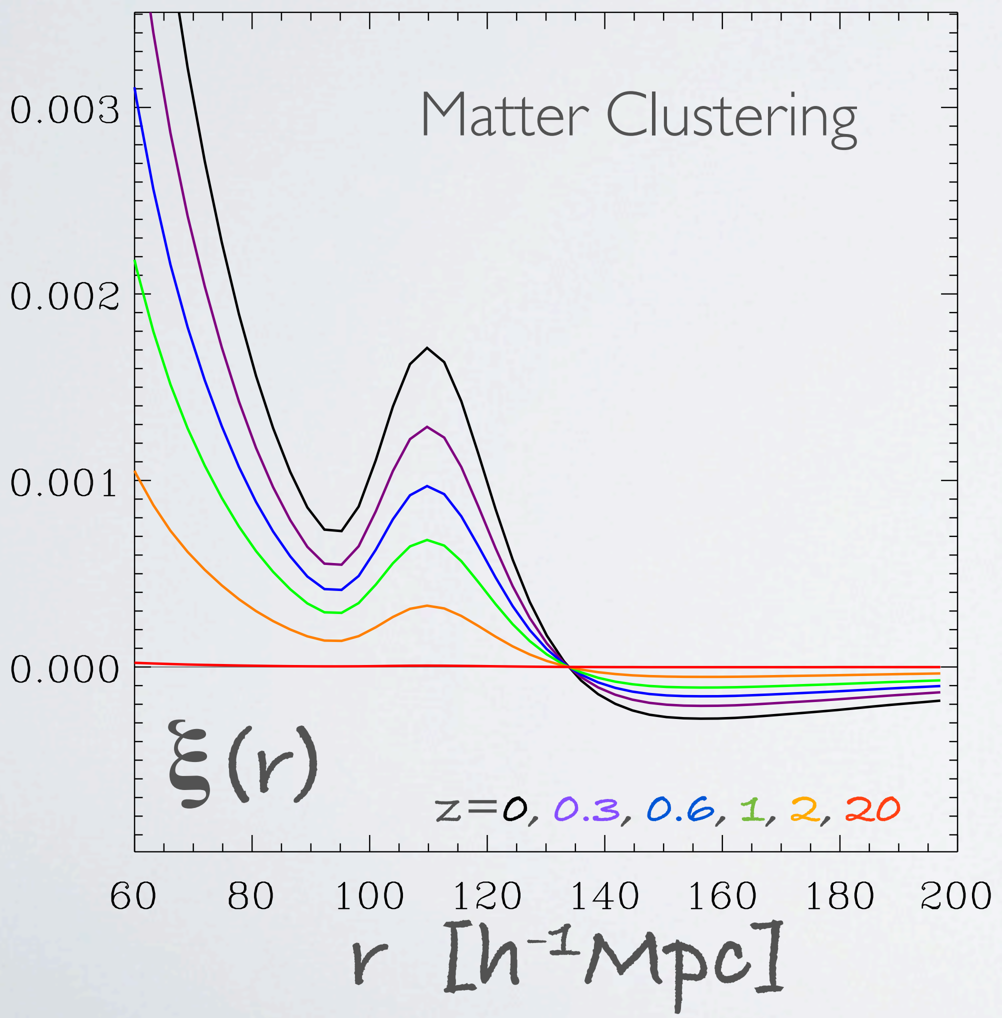

sound horizon

$$r_s(z_{dec}) = \int_0^{\tau_{dec}} c_s \, d\tau = \int_{\text{inifinity}}^{z_{dec}} c_s / H(z') \, dz'$$

The Baryonic Acoustic Feature
Linear Theory

CMB T-T   Larson et al. (2010)

Feature in the early universe:

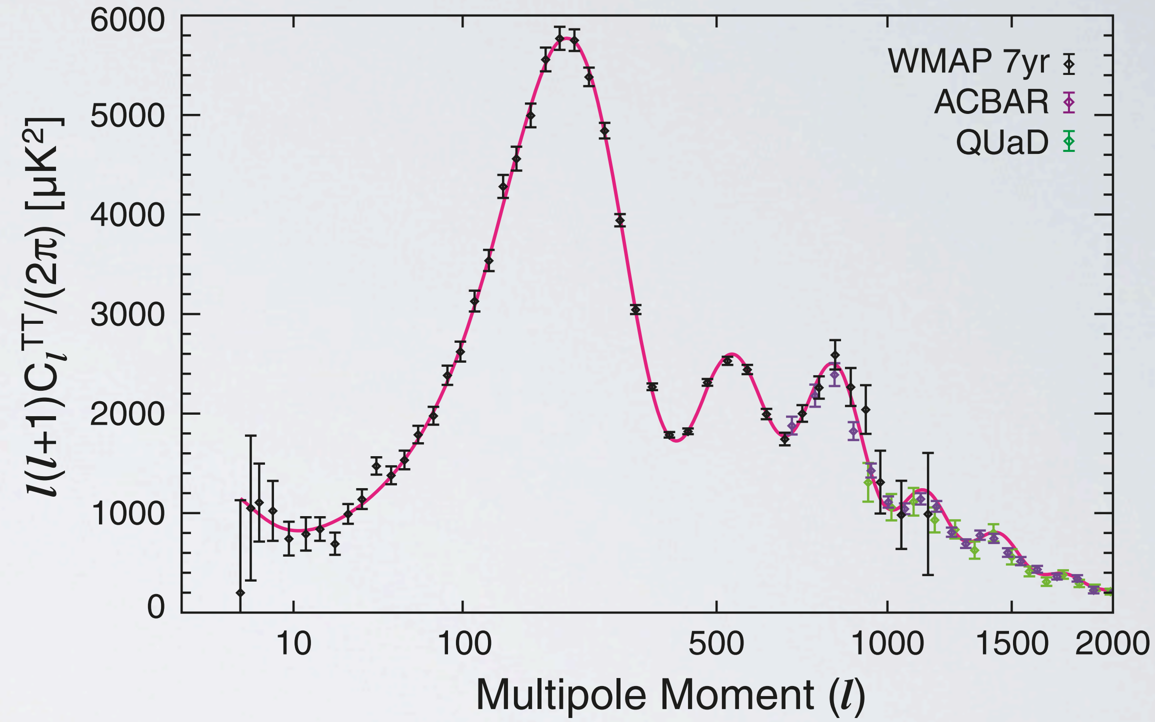

Feature in the late universe:

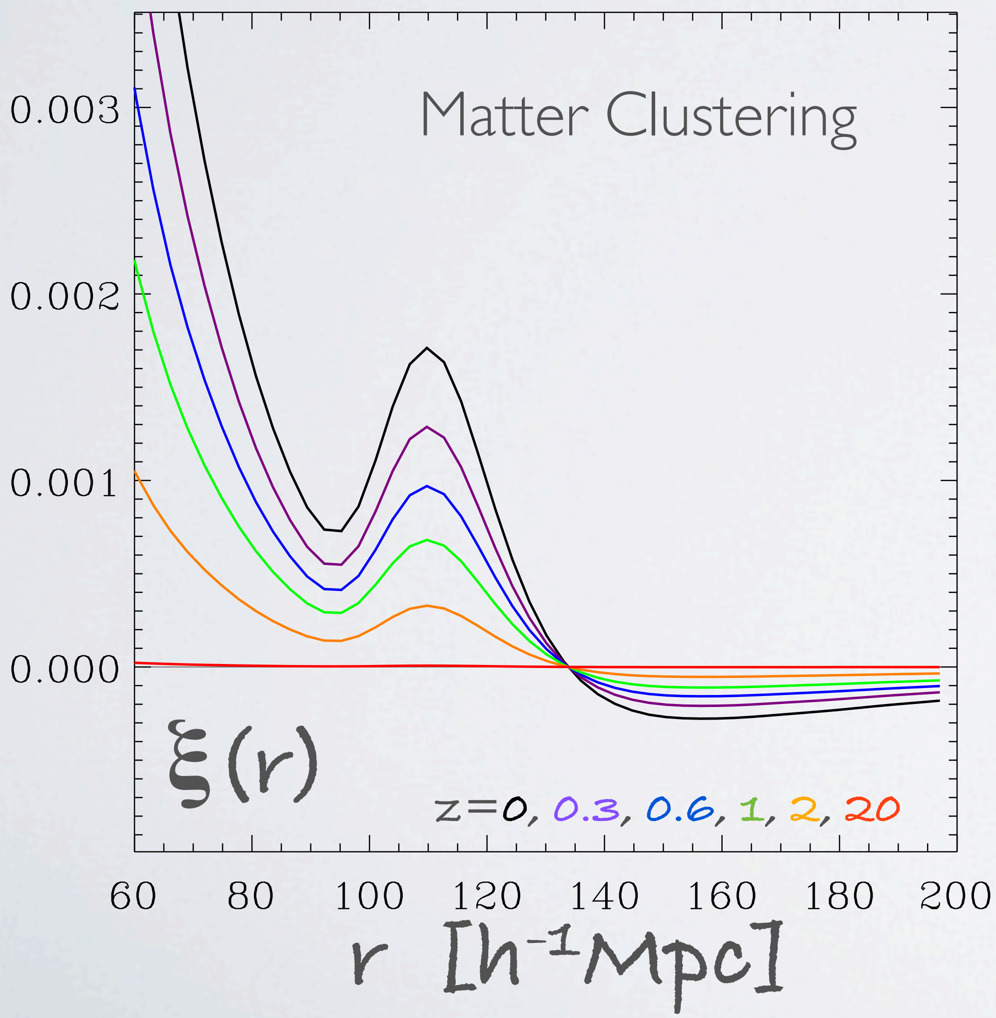

sound horizon

$$r_s(z_{dec}) = \int_0^{\tau_{dec}} c_s \, d\tau = \int_{\text{inifinity}}^{z_{dec}} c_s / H(z') \, dz'$$

z_{dec}, τ_{dec} conformal time and redshift at photon-baryon decoupling

$$d\tau \equiv (1+z)\,dt = 1/(H(z))\,dz$$

The Baryonic Acoustic Feature
Linear Theory

CMB T-T   Larson et al. (2010)

Feature in the early universe:

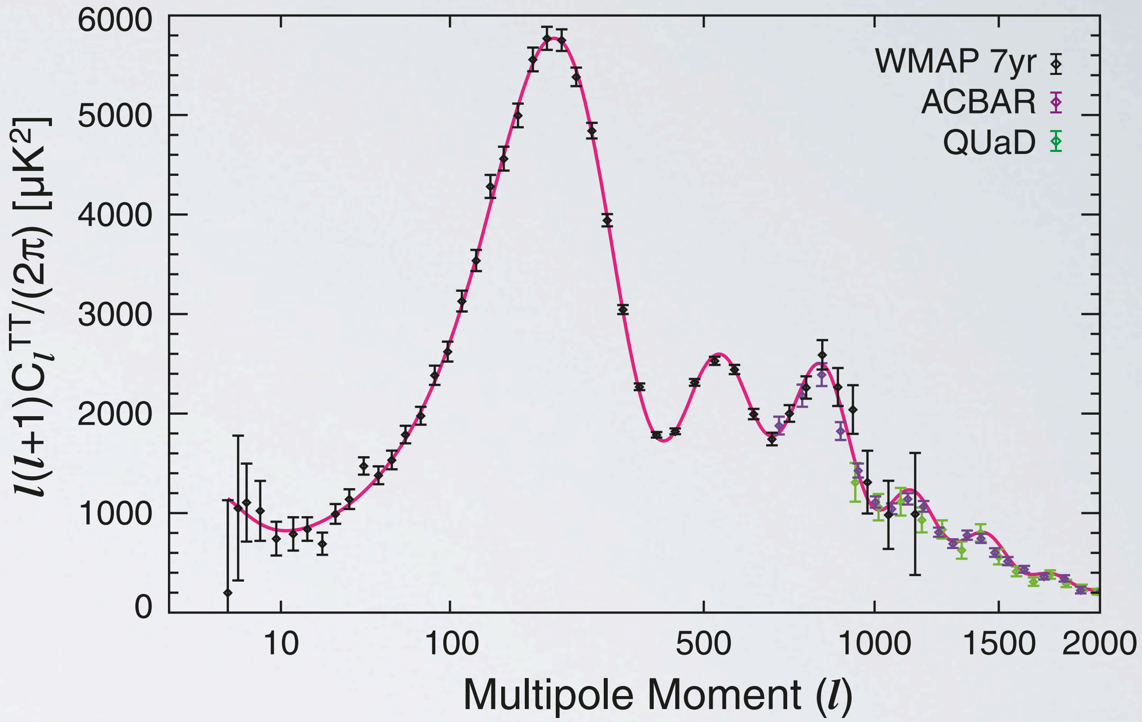

Feature in the late universe:

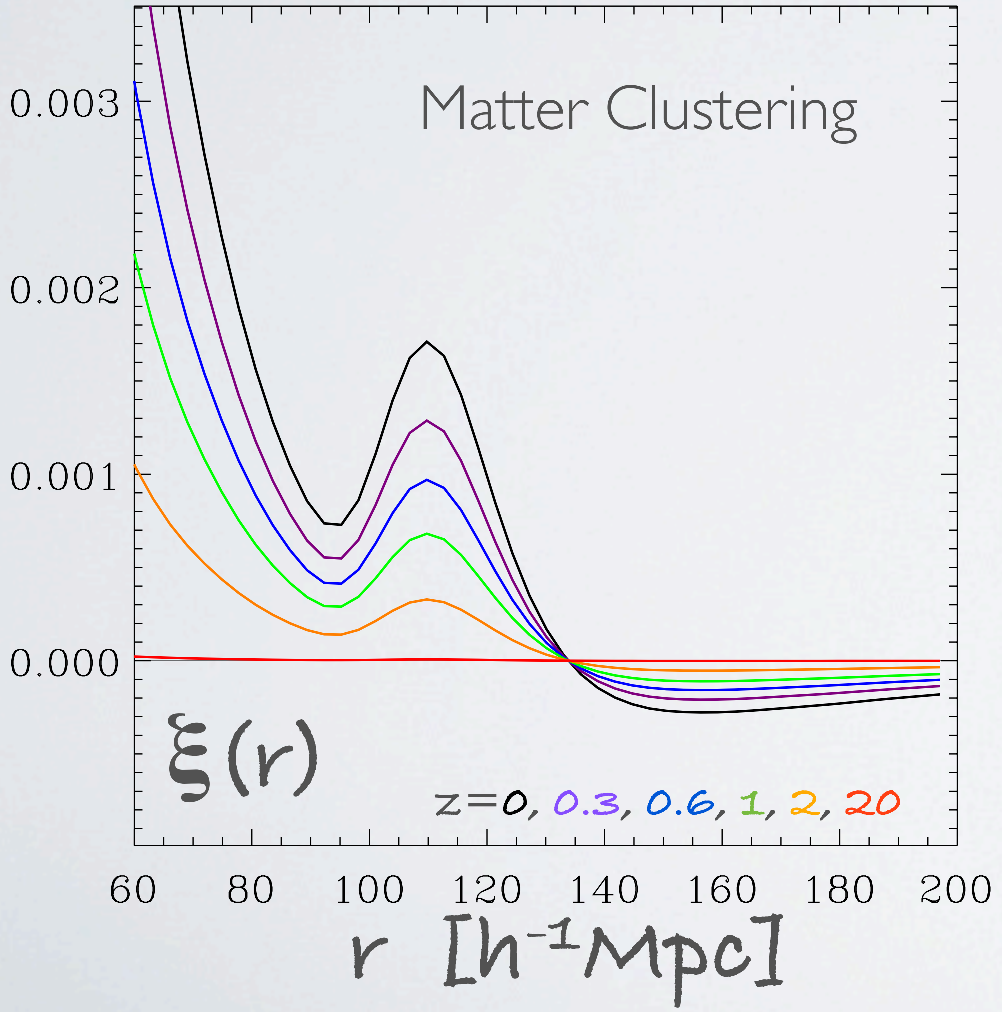

sound horizon

$$r_s(z_{dec}) = \int_0^{\tau_{dec}} c_s d\tau = \int_{inifinity}^{z_{dec}} c_s / H(z') dz'$$

z_{dec}, τ_{dec} conformal time and redshift at photon-baryon decoupling

$$d\tau \equiv (1+z)dt = 1/(H(z))dz$$

sound speed $c_s(z) = c/\sqrt{[3(1+R)]}$

baryon to photon ratio $R(z) \equiv 0.75\rho_b/\rho_\gamma$

The Baryonic Acoustic Feature in Late Universe (reality check)

Deviations from linear theory

(laundry list)

- Nonlinear clustering
- Galaxy bias $\delta_{gal} \approx b_{Lin}\delta$
- Redshift Distortions
- Assuming cosmology

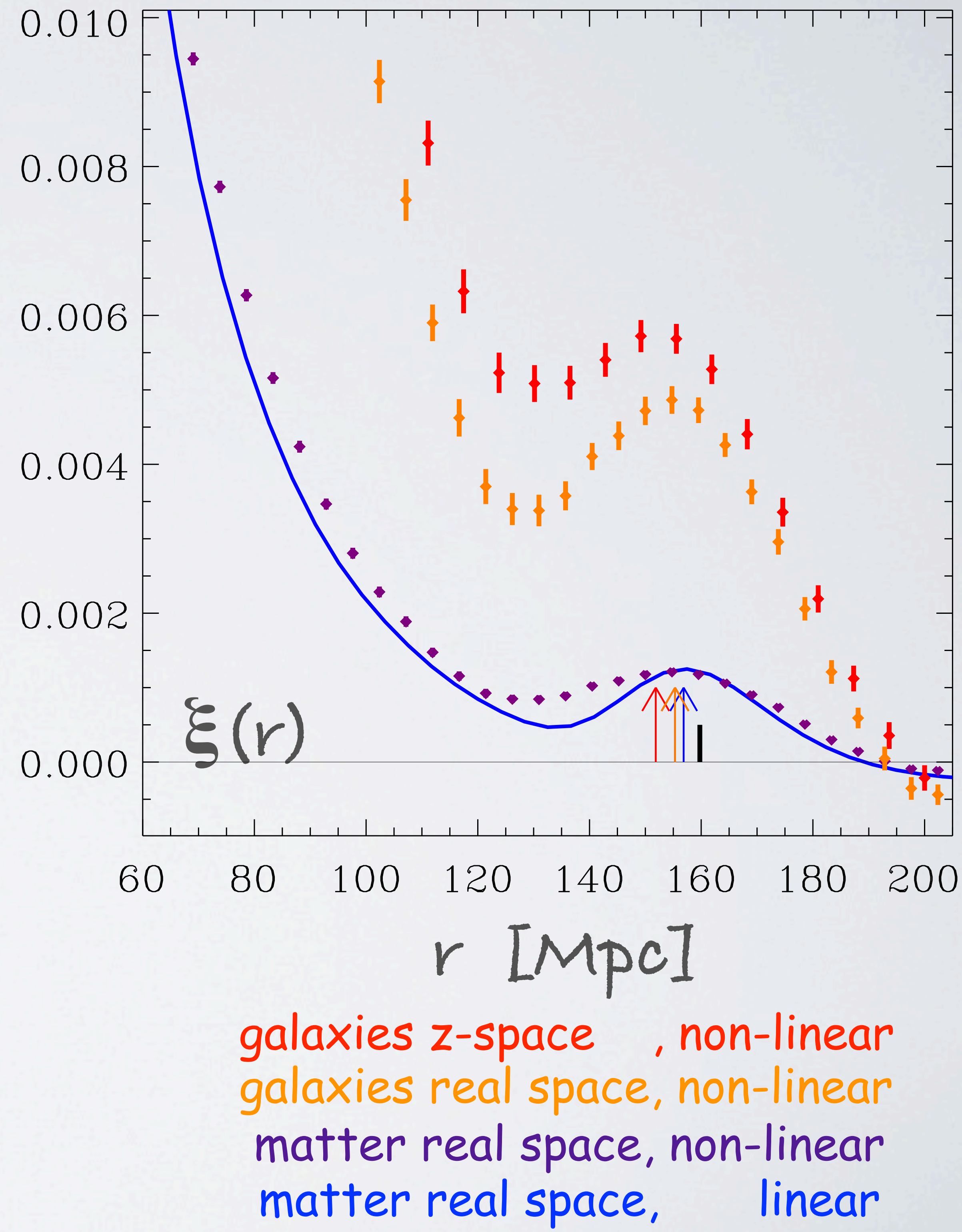

The Baryonic Acoustic Feature in Late Universe (reality check)

Deviations from linear theory

(laundry list)

- Nonlinear clustering
- Galaxy bias $\delta_{gal} \approx b_{Lin}\delta$
- Redshift Distortions
- Assuming cosmology

S/N (ξ/σ) depends on

- Volume of sample
- Density of sample n

$\sigma \propto (\sqrt{V^{-1}})(P(k)+n^{-1})$

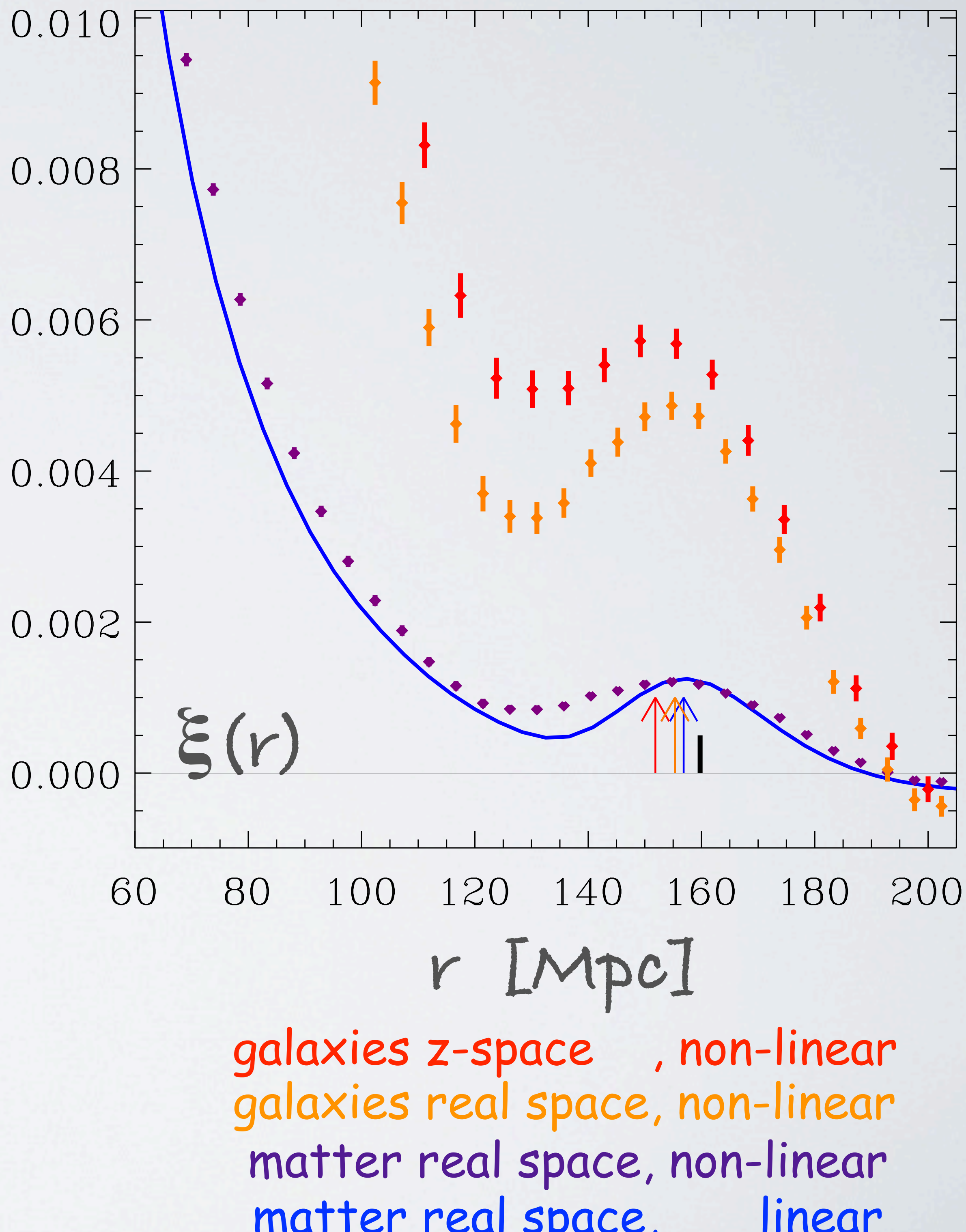

Baryonic Acoustic Feature in SDSS LRGs
MONOPOLE

2005: Detection!

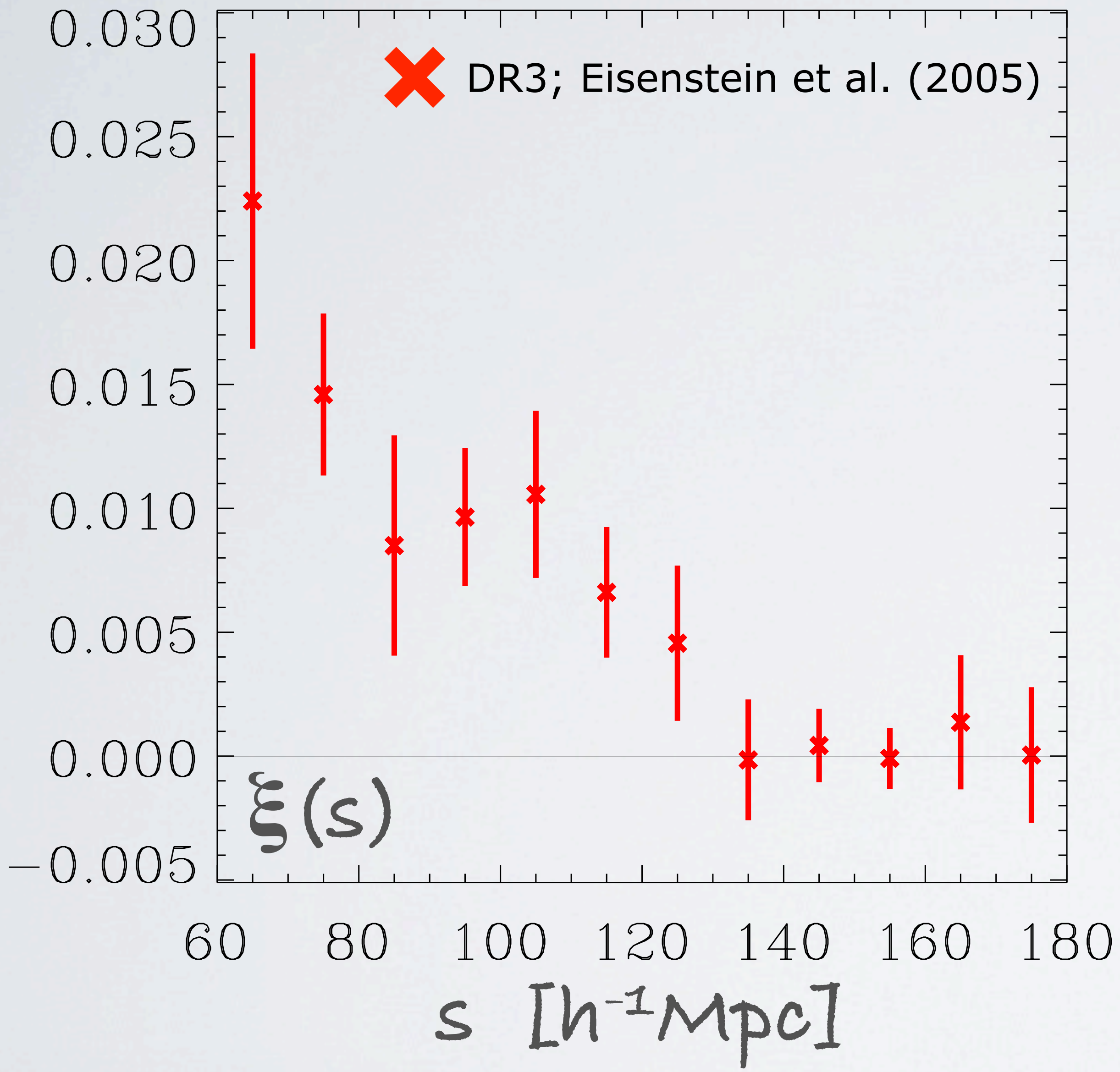

Baryonic Acoustic Feature in SDSS LRGs
MONOPOLE

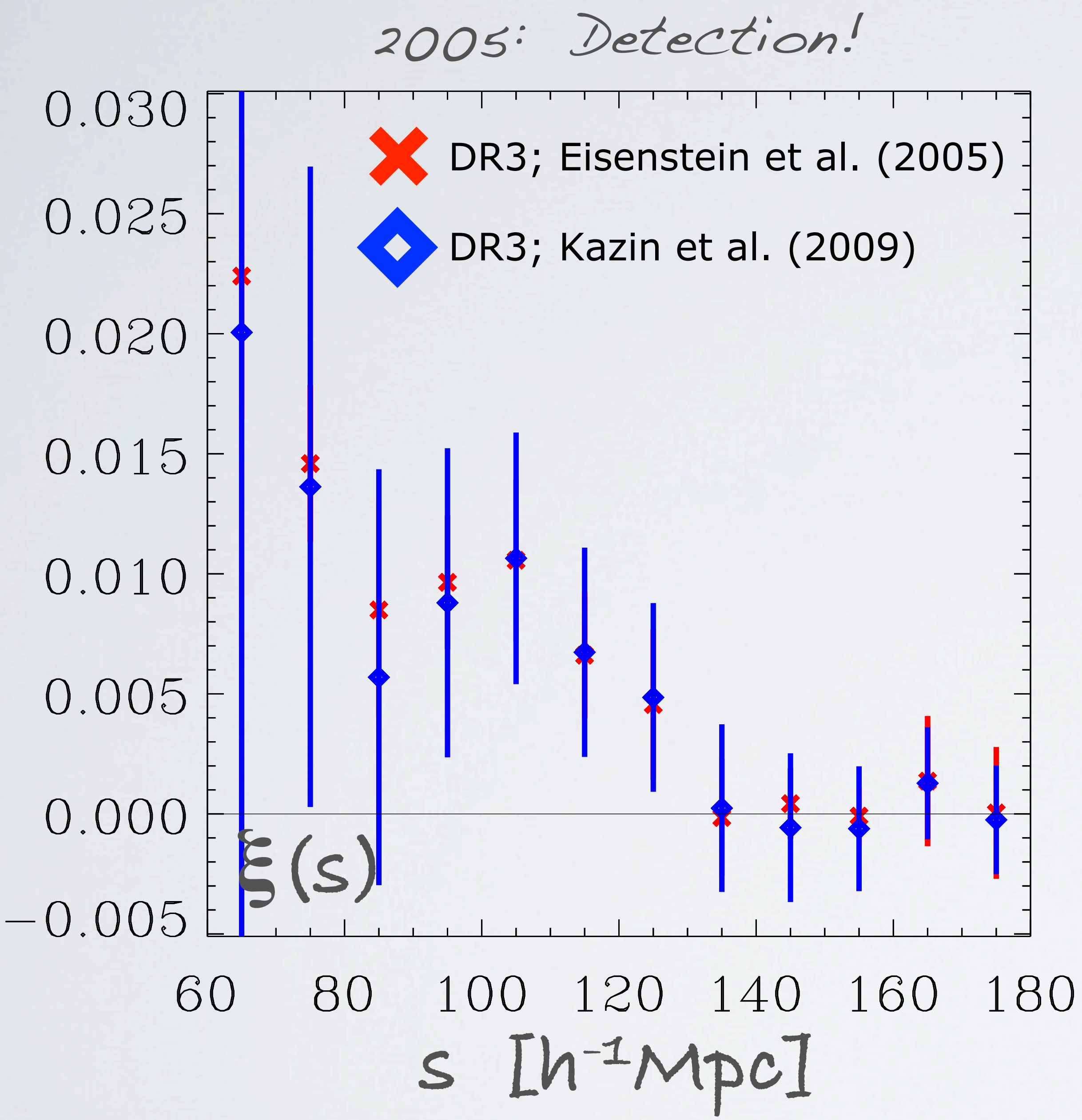

Baryonic Acoustic Feature in SDSS LRGs
MONOPOLE

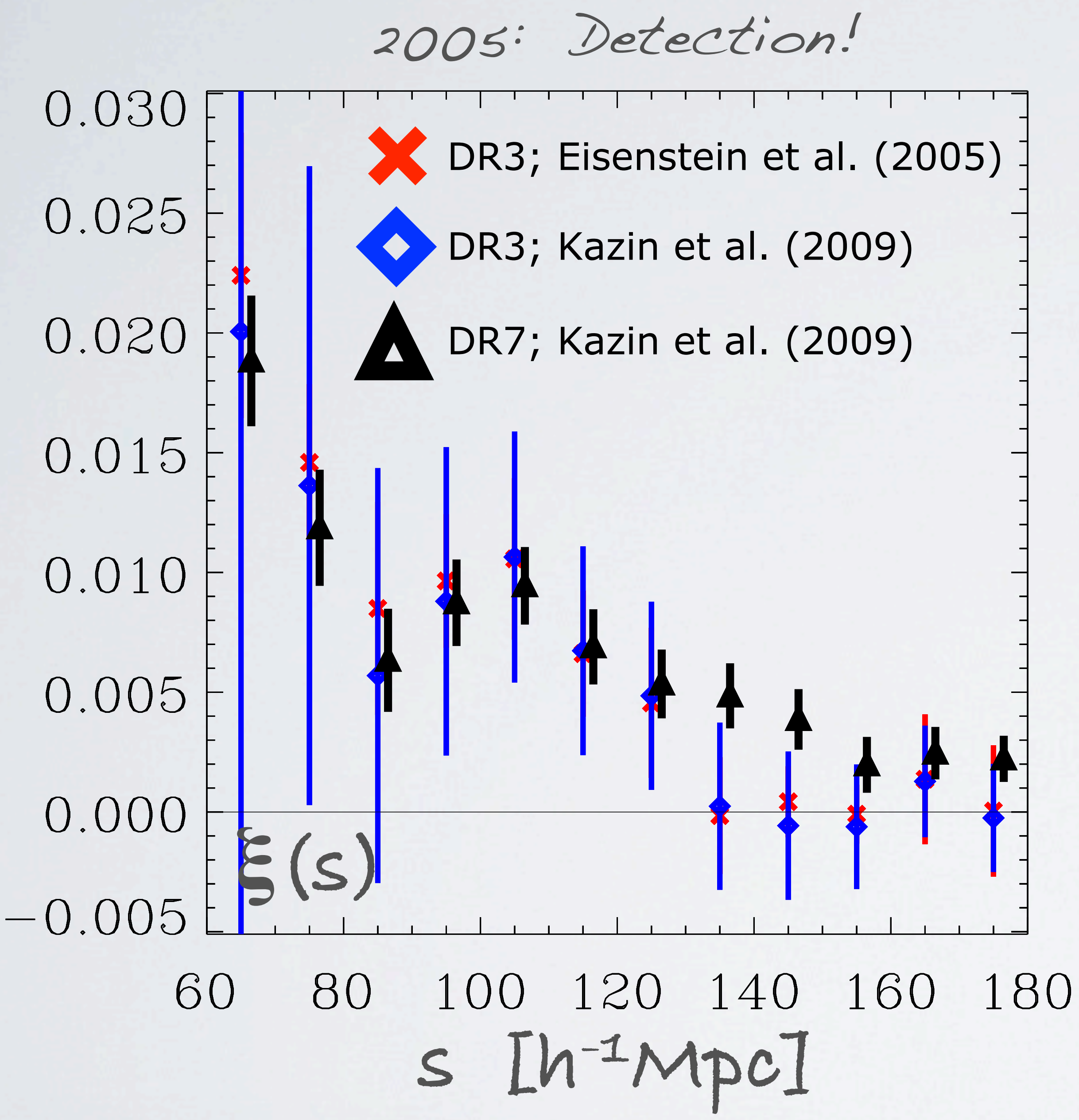

Baryonic Acoustic Feature in SDSS LRGs
MONOPOLE

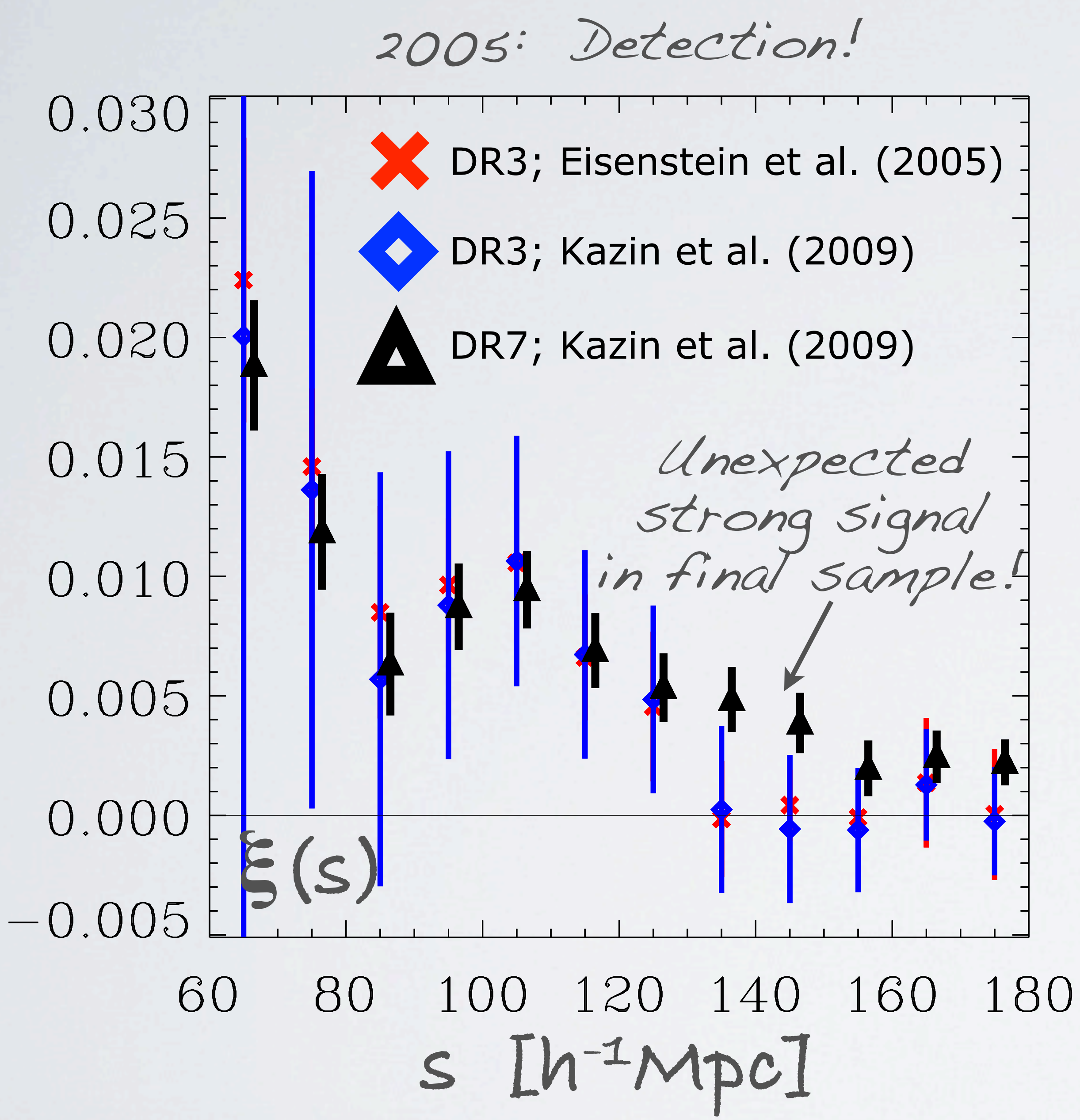

Unexplained strong signal on large scales when analyzing volumes larger than DR3

Baryonic Acoustic Feature in SDSS LRGs MONOPOLE

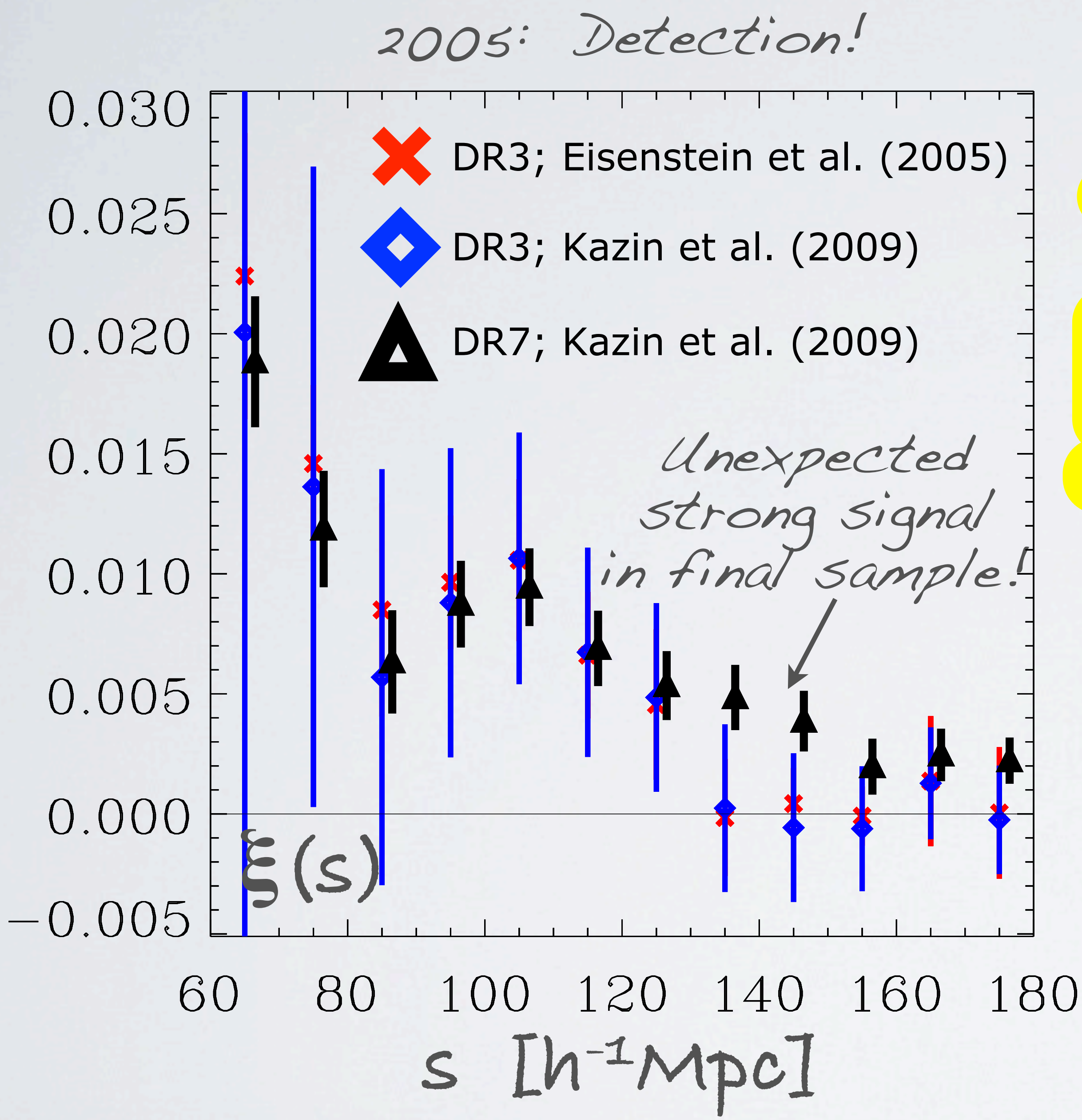

Unexplained strong signal on large scales when analyzing volumes larger than DR3

From Blake et al. (2007)

- We measure a hint of excess power relative to the best-fitting cosmological model on the largest scales (the lowest multipole bands in the four redshift slices in Figure 10). If confirmed, this excess power has a range of possible causes: (1) residual systematic errors; (2) cosmic variance; (3) large-scale galaxy biasing mechanisms; (4) new early-Universe physics.

Baryonic Acoustic Feature in SDSS LRGs MONOPOLE

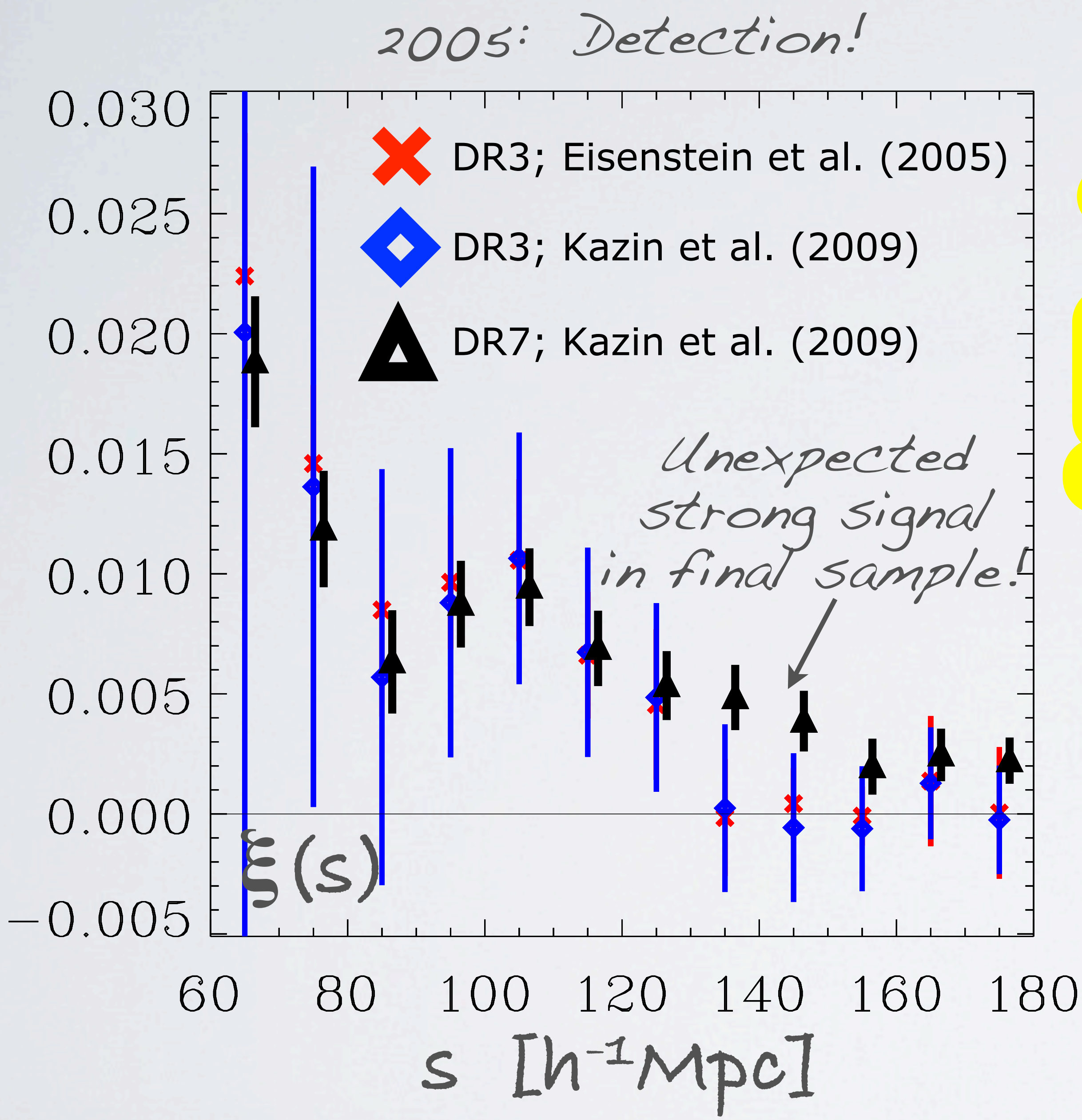

From Blake et al. (2007)

- We measure a hint of excess power relative to the best-fitting cosmological model on the largest scales (the lowest multipole bands in the four redshift slices in Figure 10). If confirmed, this excess power has a range of possible causes: (1) ~~residual systematic errors~~; (2) cosmic variance; (3) large-scale galaxy biasing mechanisms; (4) new early-Universe physics.

Unexplained strong signal on large scales when analyzing volumes larger than DR3

Large scale signal difference- Not due to systematics

LasDamas Mock Simulations

Andereas Berlind
Michael Busha
Jeff Gardner
Cameron McBride
Román Scoccimarro
Frank van den Bosch
Risa Wechsler

http://lss.phy.vanderbilt.edu/lasdamas/

- Large Suite of DM sims
- We use: 160 SDSS-II mock LRG realizations
- Emphasize on many observational effects:
  - Light-cone, z-space
  - SDSS-II geometry
  - Radial selection function
- Results in **most realistic uncertainties** of clustering measurements to date

McBride et al. ; in prep.

Baryonic Acoustic Feature in SDSS LRGs MONOPOLE

SDSS-III (BOSS) Prediction

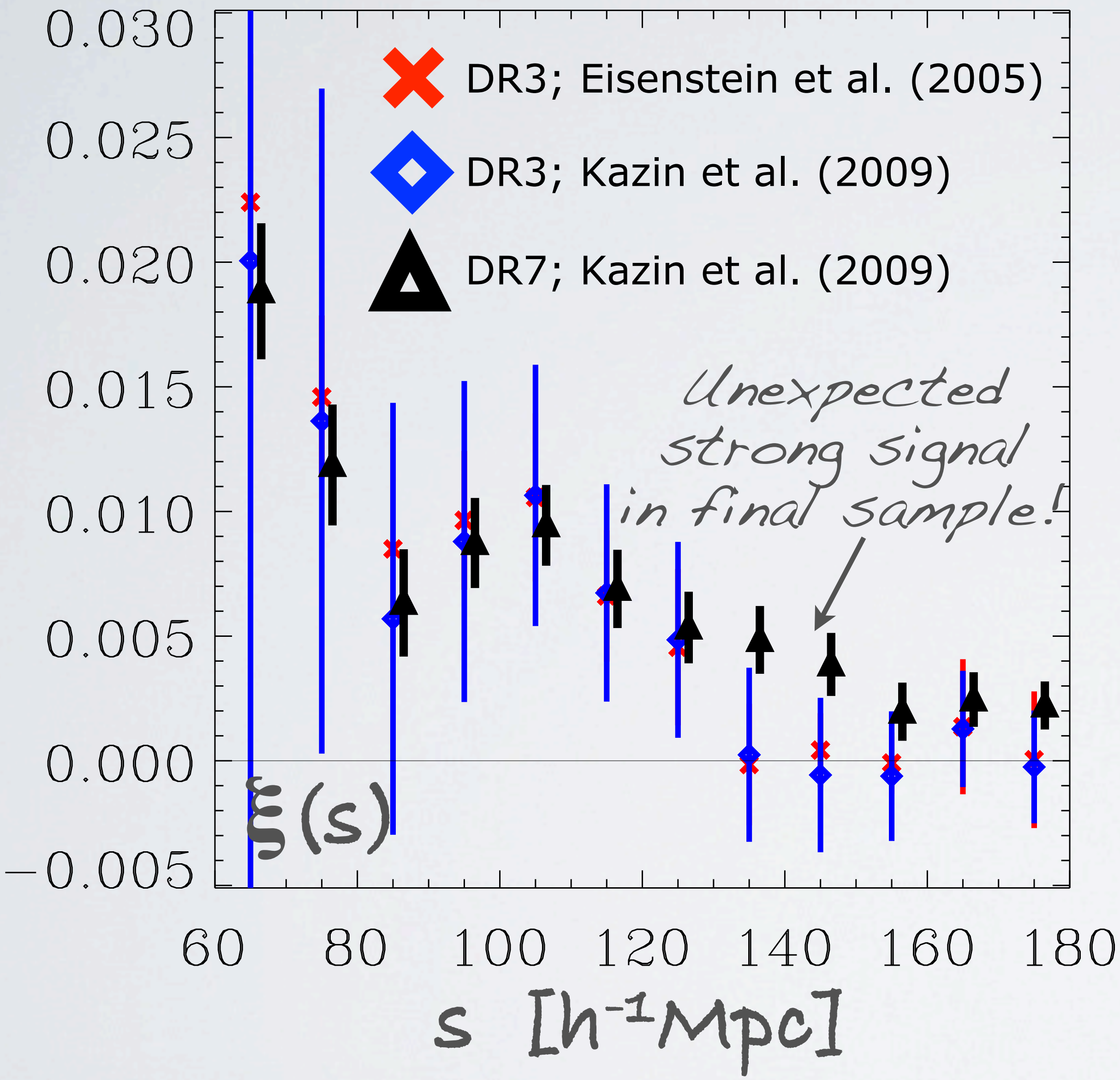

SDSS-II Results

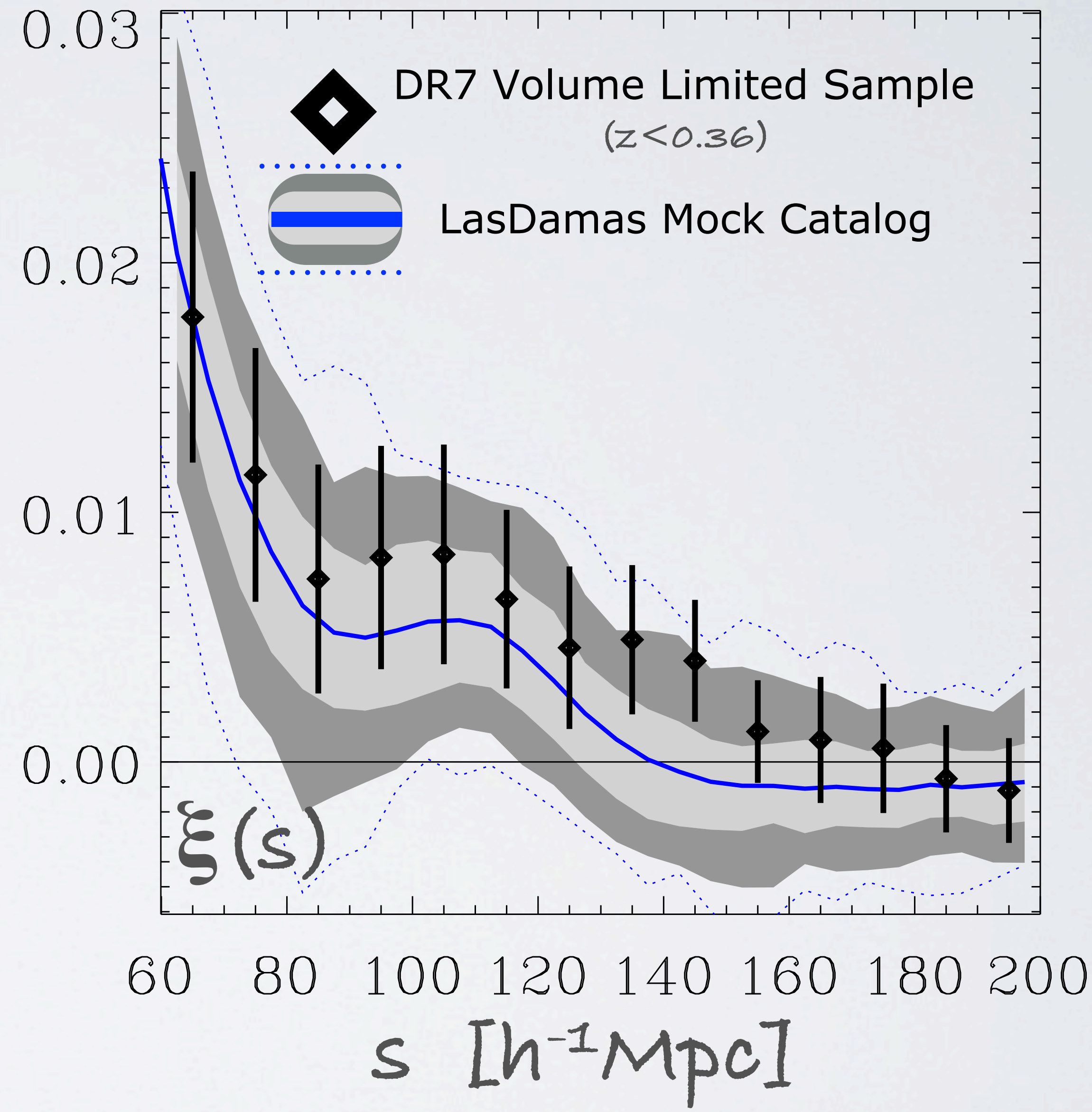

Unexplained strong signal on large scales when analyzing larger volumes than DR3

Large scale signal difference- Not due to systematics

Baryonic Acoustic Feature in SDSS LRGs MONOPOLE

SDSS-III (BOSS) Prediction

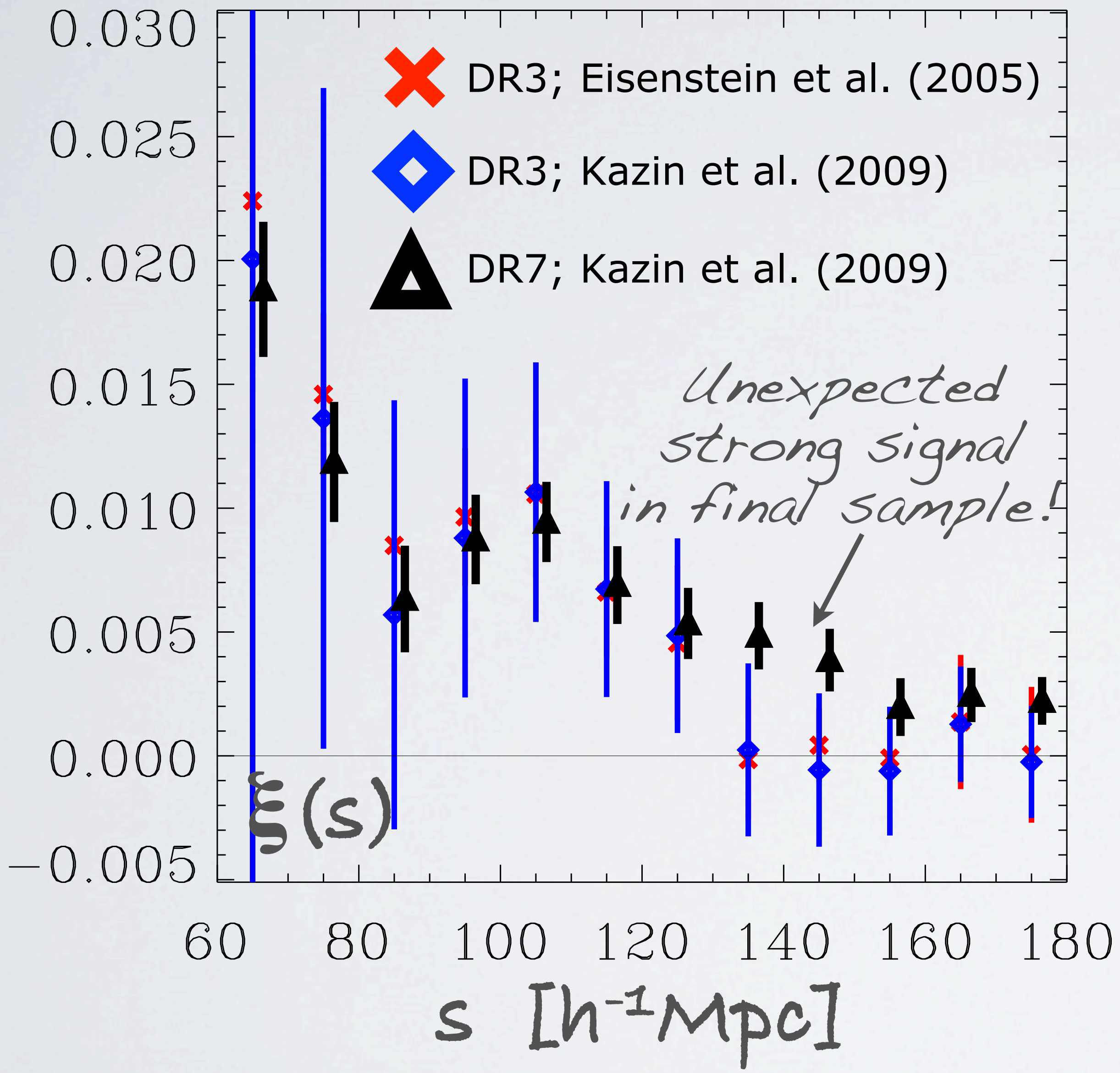

SDSS-II Results

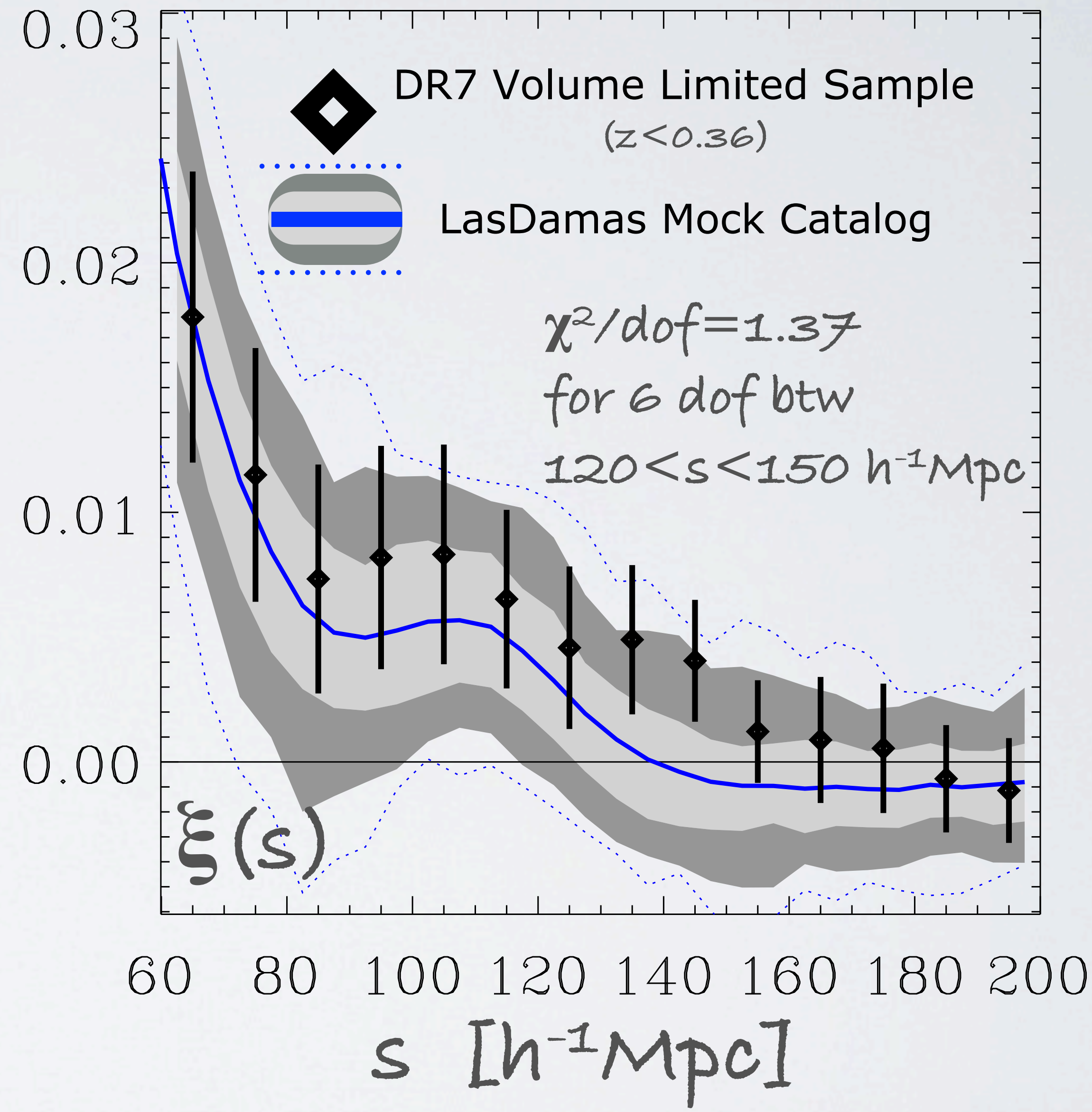

Unexplained strong signal on large scales when analyzing larger volumes than DR3

- Large scale signal difference- Not due to systematics
- ΛCDM is consistent with data within **1.5σ**

Baryonic Acoustic Feature in SDSS LRGs
MONOPOLE

SDSS-III (BOSS) Prediction

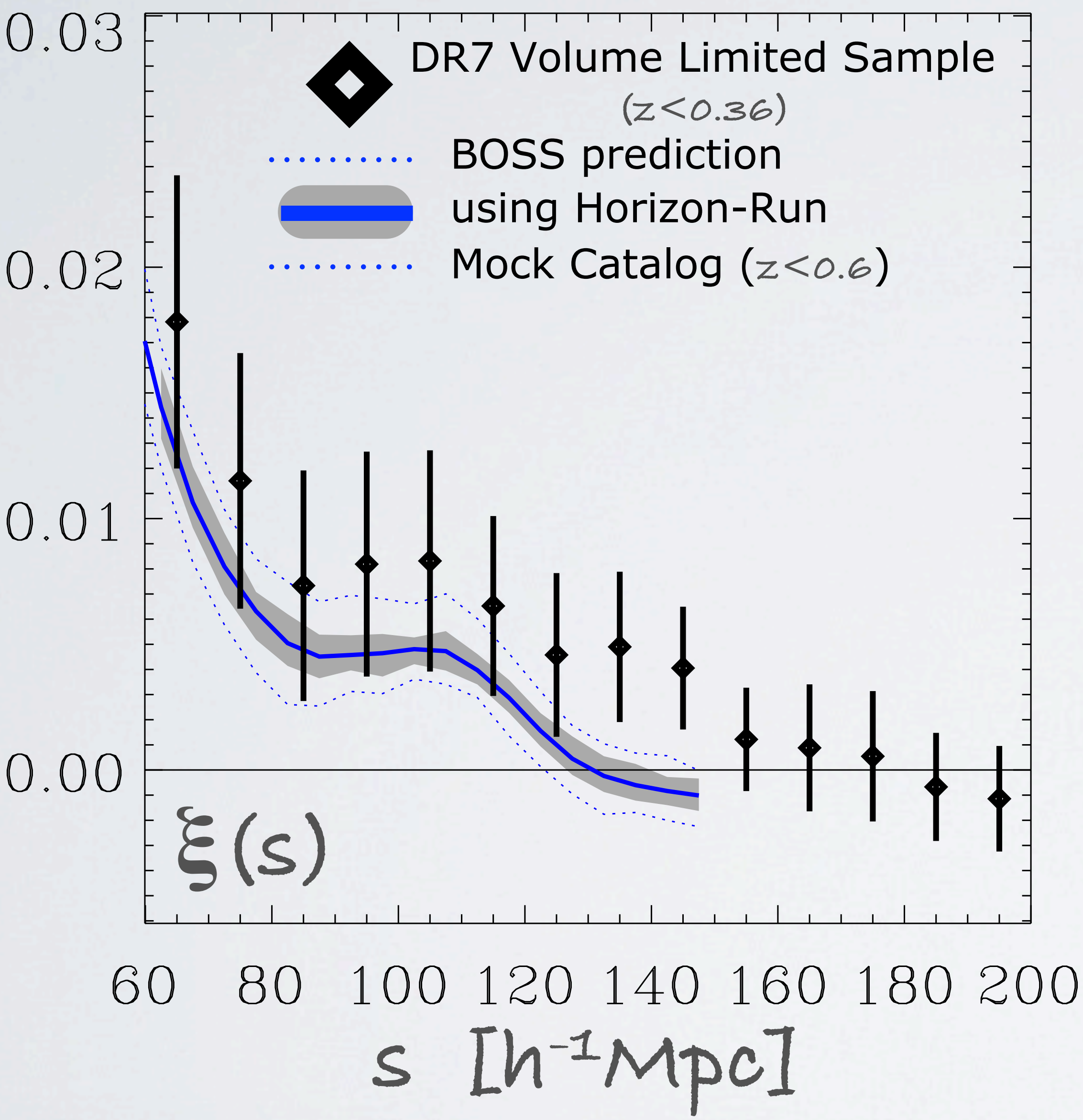

SDSS-II Results

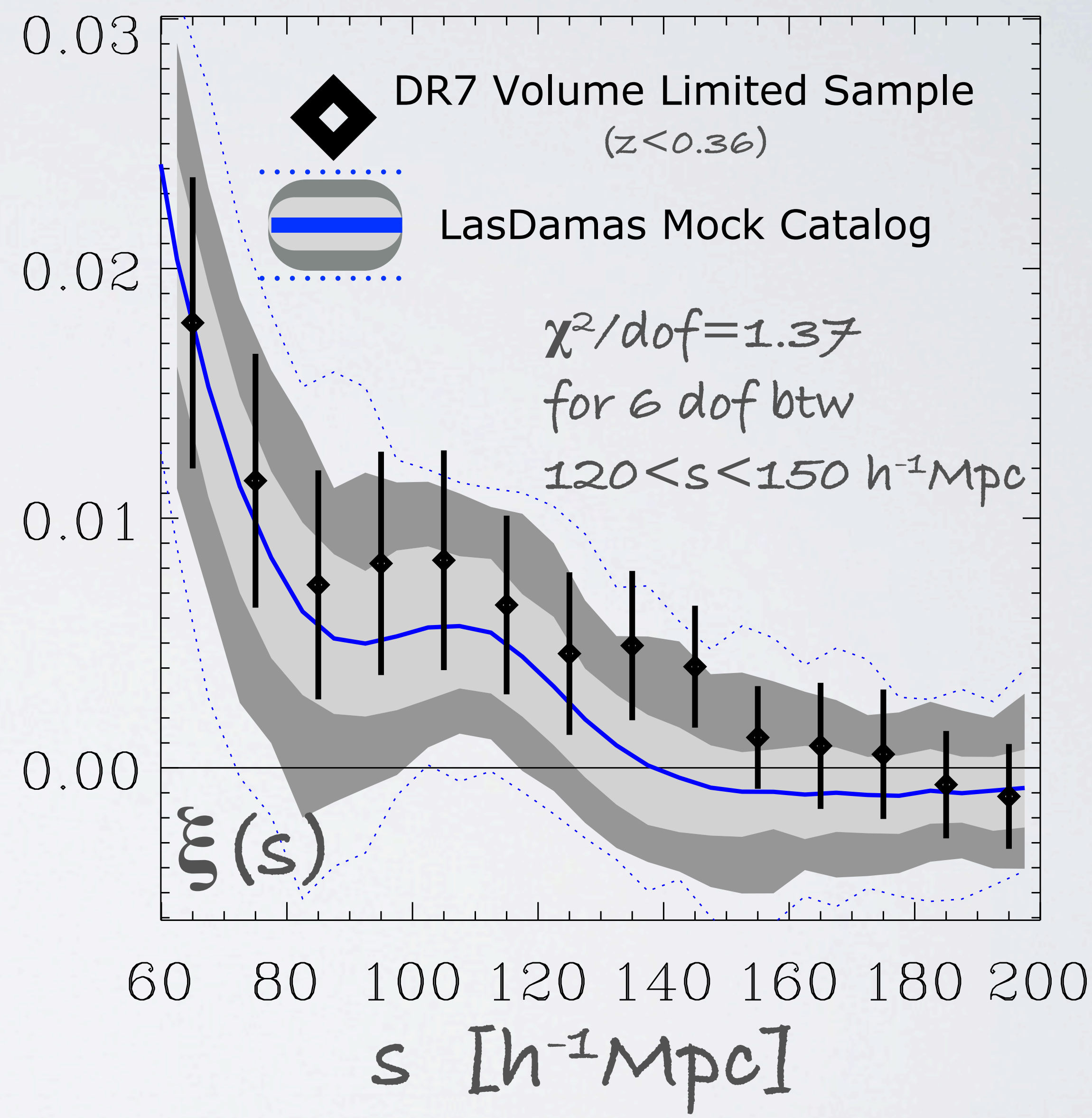

- Large scale signal difference- Not due to systematics
- ΛCDM is consistent with data within 1.5σ

Baryonic Acoustic Feature in SDSS LRGs MONOPOLE

SDSS-III (BOSS) Prediction

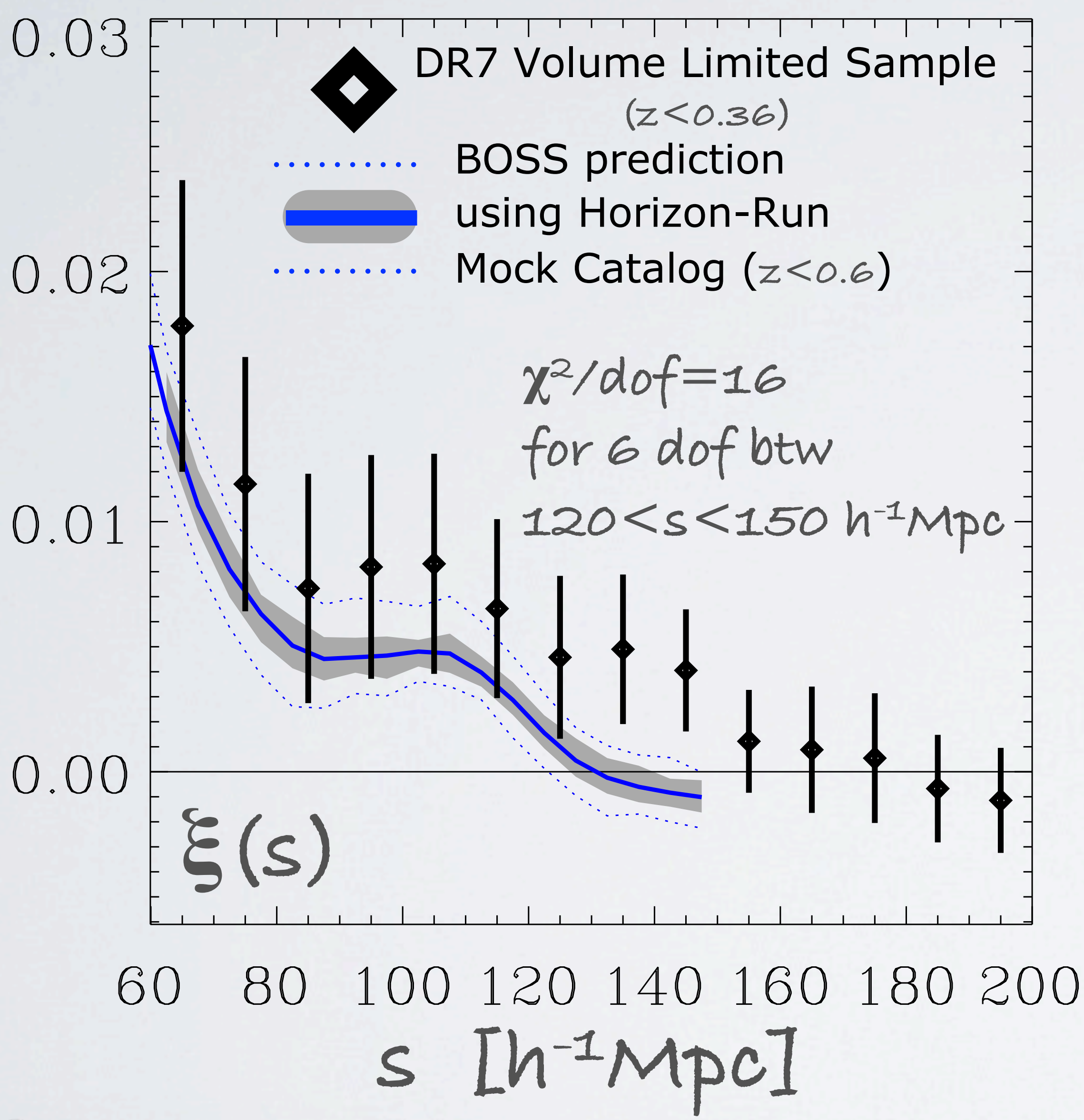

SDSS-II Results

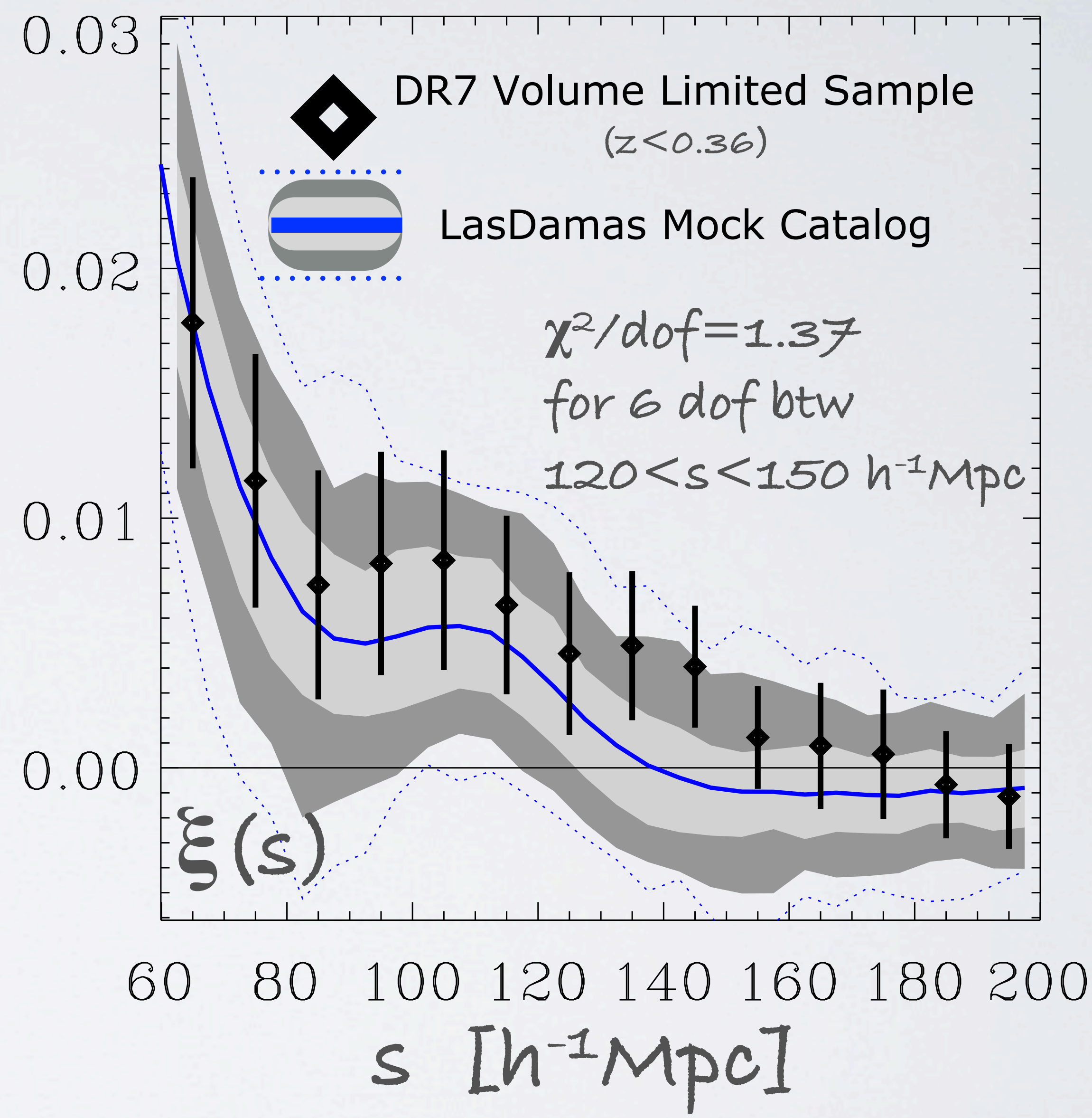

- According to ΛCDM, strong signal should not appear at a high CL
- Large scale signal difference- Not due to systematics
- ΛCDM is consistent with data within 1.5σ

Baryonic Acoustic Feature in SDSS LRGs MONOPOLE

- SDSS-II volume mock catalogs indicate a >10% chance of not detecting an apparent signature
  -based on mock catalogs provided by LasDamas (McBride et al.; in prep) and Horizon-Run mocks (Kim et al. 2009)-

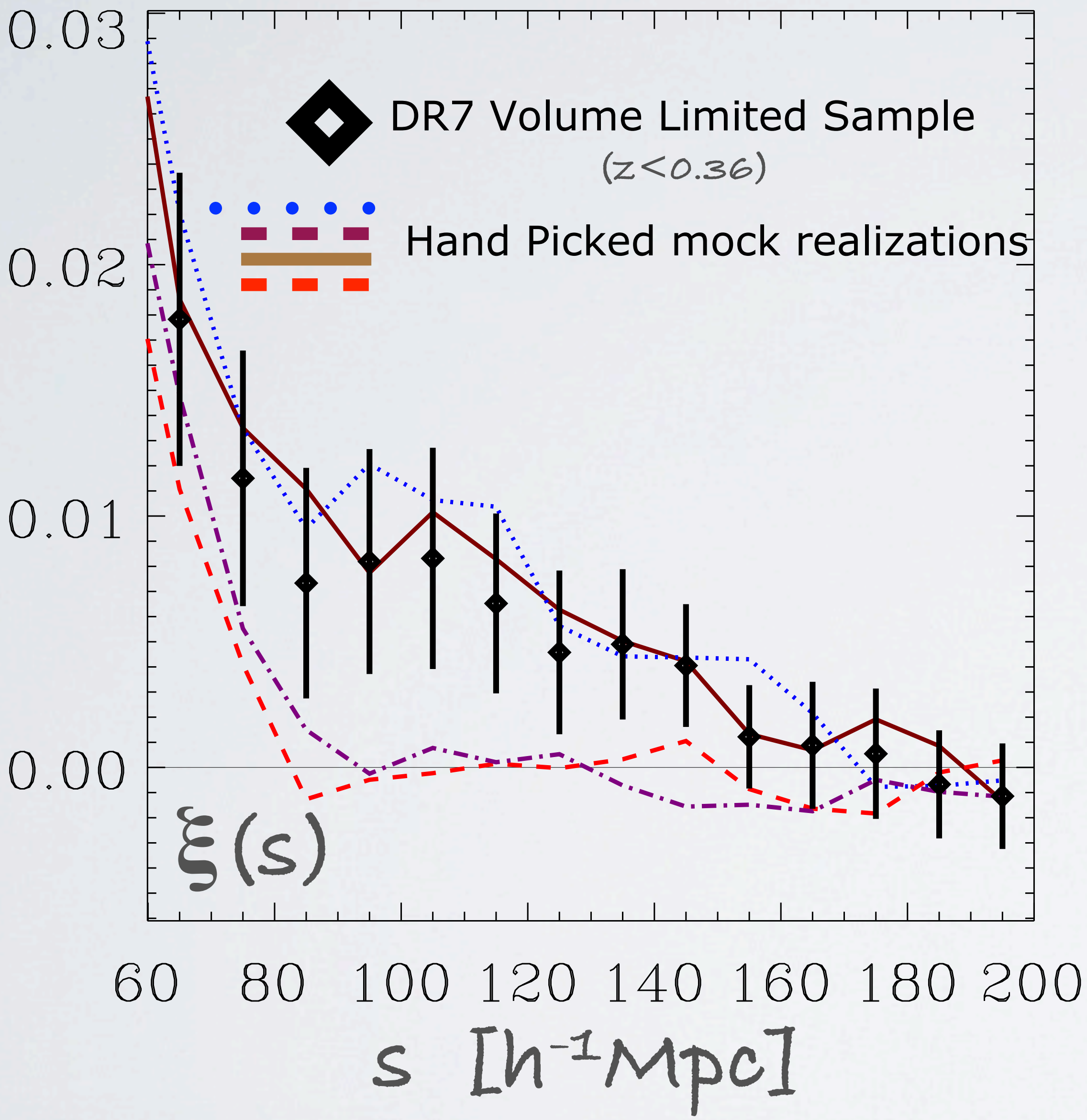

Baryonic Acoustic Feature in SDSS LRGs MONOPOLE

- SDSS-II volume mock catalogs indicate a >10% chance of not detecting an apparent signature
  -based on mock catalogs provided by LasDamas (McBride et al.; in prep) and Horizon-Run mocks (Kim et al. 2009)-

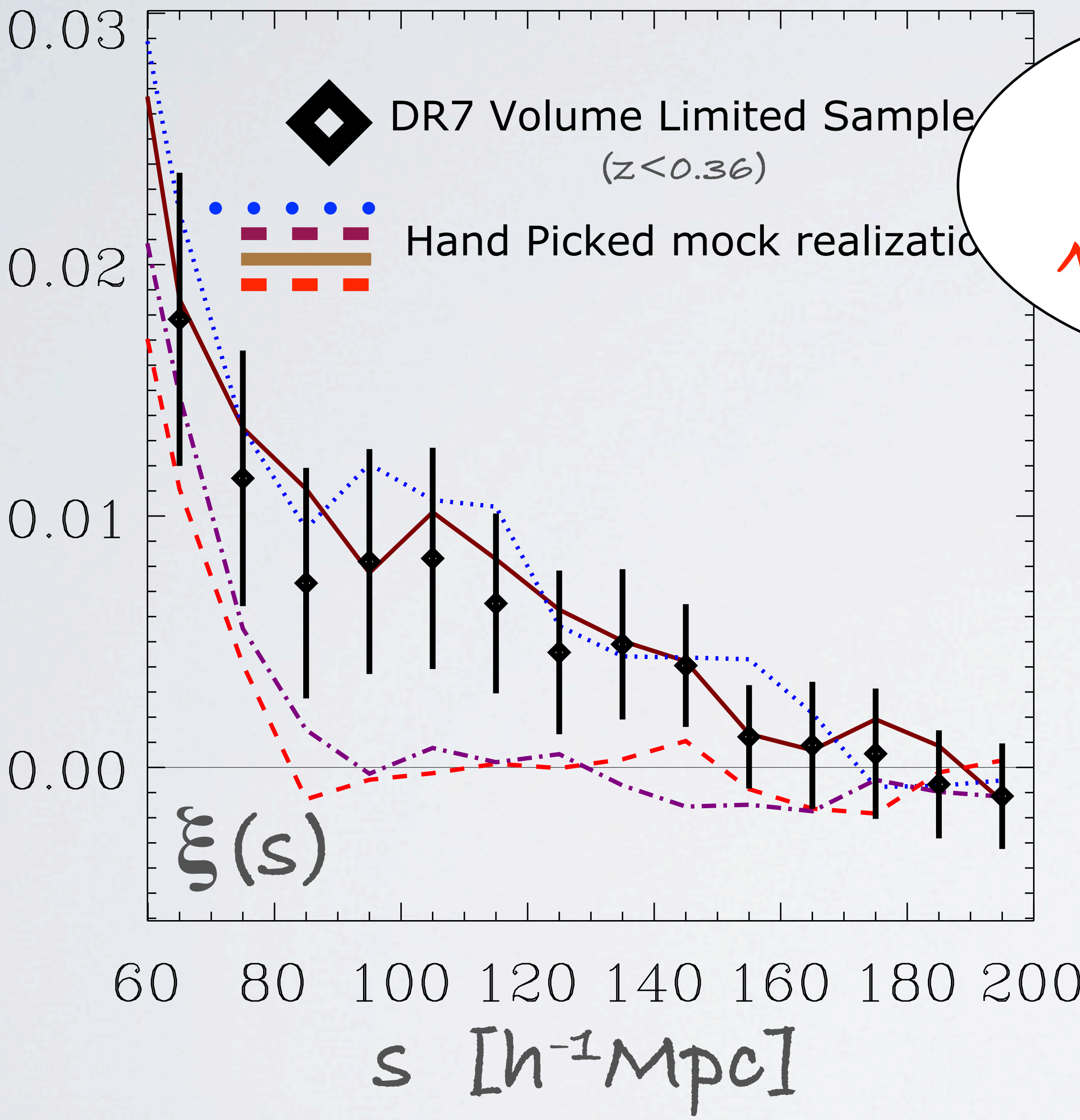

Baryonic Acoustic Feature in SDSS LRGs MONOPOLE

- SDSS-II volume mock catalogs indicate a >10% chance of not detecting an apparent signature
  -based on mock catalogs provided by LasDamas (McBride et al.; in prep) and Horizon-Run mocks (Kim et al. 2009)-

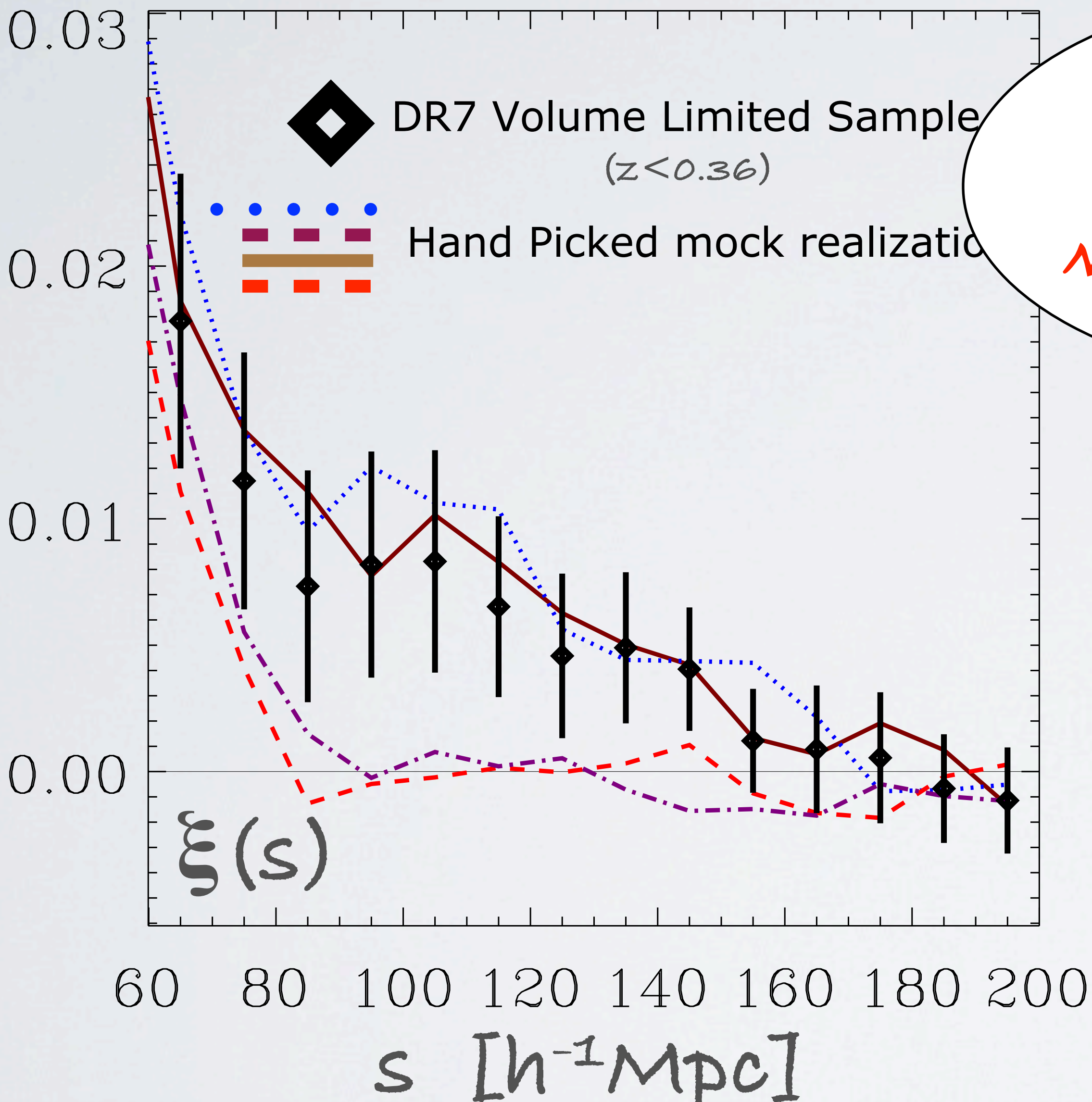

- ~45% (75 of 160) of realizations do show indication of a clear peak

Baryonic Acoustic Feature in SDSS LRGs MONOPOLE

- SDSS-II volume mock catalogs indicate a >10% chance of not detecting an apparent signature
  -based on mock catalogs provided by LasDamas (McBride et al.; in prep) and Horizon-Run mocks (Kim et al. 2009)-

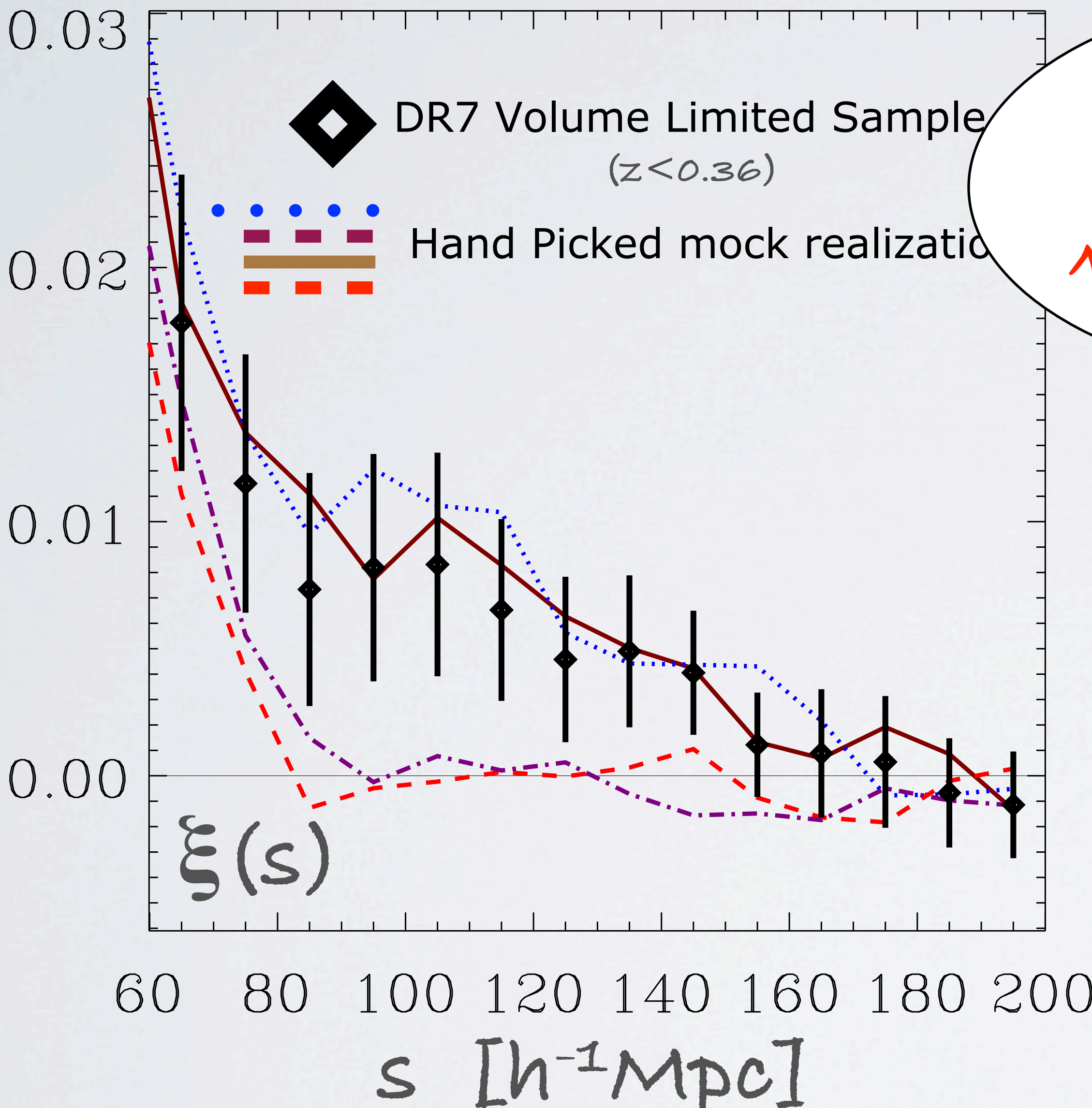

- ~45% (75 of 160) of realizations do show indication of a clear peak
- SDSS-II LRGs **do** reveal a Baryonic Acoustic Feature
  in various redshifts and luminosity cuts

The Baryonic Acoustic Feature as a Standard Ruler

- Early Universe (z_{dec}~1090):
  CMB temp fluctuations determines
  r_s~147 Mpc ($\delta r_s/r_s$ ~1.3%; Komatsu et al. 2009)
- Late Universe :
  Galaxy Clustering (z~ 0.3, 0.6)
  QSOs Lyman-α Forest (z~ 2.5)

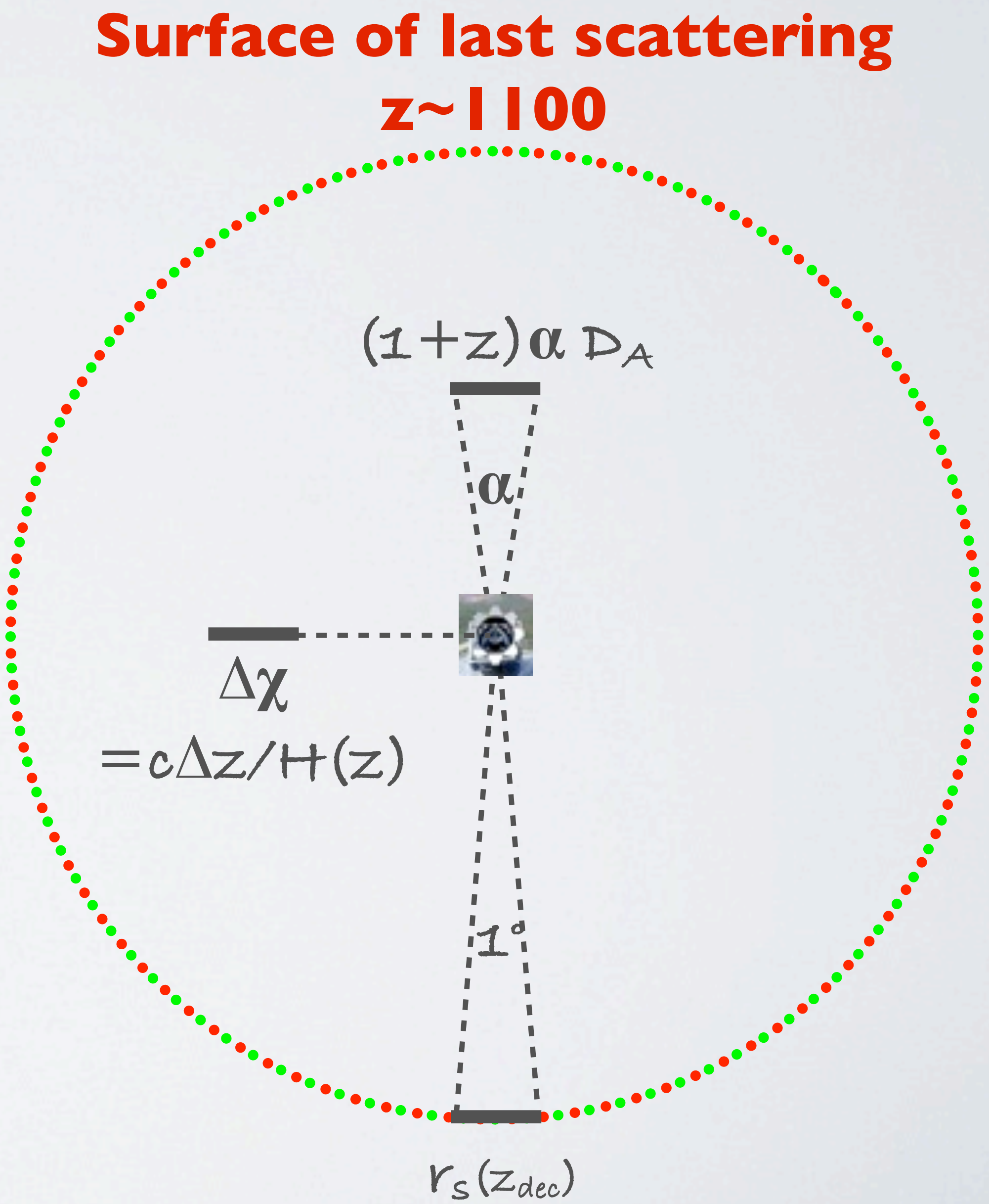

Baryonic Acoustic Feature on (and off) the Line of Sight

defining

$d = cz/H_0$ Hubble's Law for proper distance

$\chi = c\int dz'/H(z')$ comoving distance $\chi = d(1+z)$

$D_A = \chi/(1+z)$ angular distance (not comoving!)

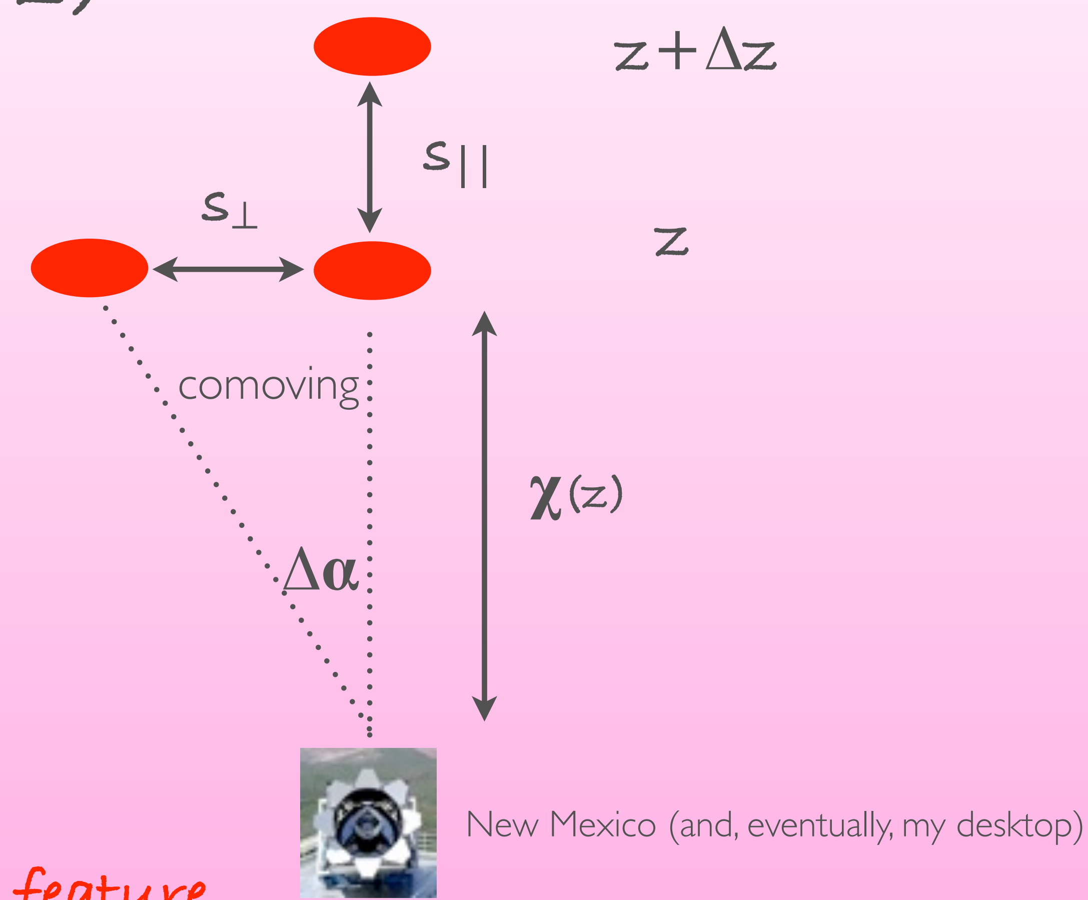

measuring

transverse feature $s_\perp = \Delta\alpha D_A(1+z)$

line of sight feature $s_{||} = \Delta\chi$

yields ...

$$\int dz'/H(z') = s_\perp/\Delta\alpha/c$$

$$H(\langle z\rangle) \sim c\Delta z/s_{||}$$

measurable with BA feature
known knowns...

meaning

$s_\perp$ constrains integral (a lot of degeneracy)

$s_{||}$ constrains H at a specific redshift!
Can constrain expansion rate!!

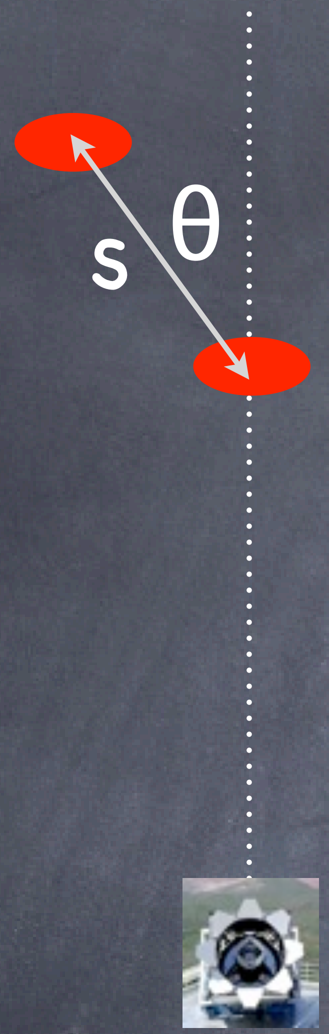

BUT....

Line of sight signal is **Noisy**

(I will show this soon... promise...)

SO....

by using the

angle averaged signal

$\langle\xi\rangle$ (aka **<u>monopole</u>**),

$$\langle\xi\rangle \equiv \int \xi(s,\theta)\sin(\theta)d\theta$$

we measure the **<u>Volume Average (effective) Distance</u>**

$$D_V(z)=[(1+z)^2 D_A{}^2 c/H(z)]^{1/3}$$

$$\propto [s_\perp{}^2 s_{||}]^{1/3}$$

meaning $\langle\xi\rangle$ constrains $D_A{}^2/H(z)$

Pinpointing Baryonic Acoustic Feature Peak in SDSS LRGs Monopole

$\xi^{model} = \lambda \xi^{NL\text{-}theory}(\alpha \cdot s)$

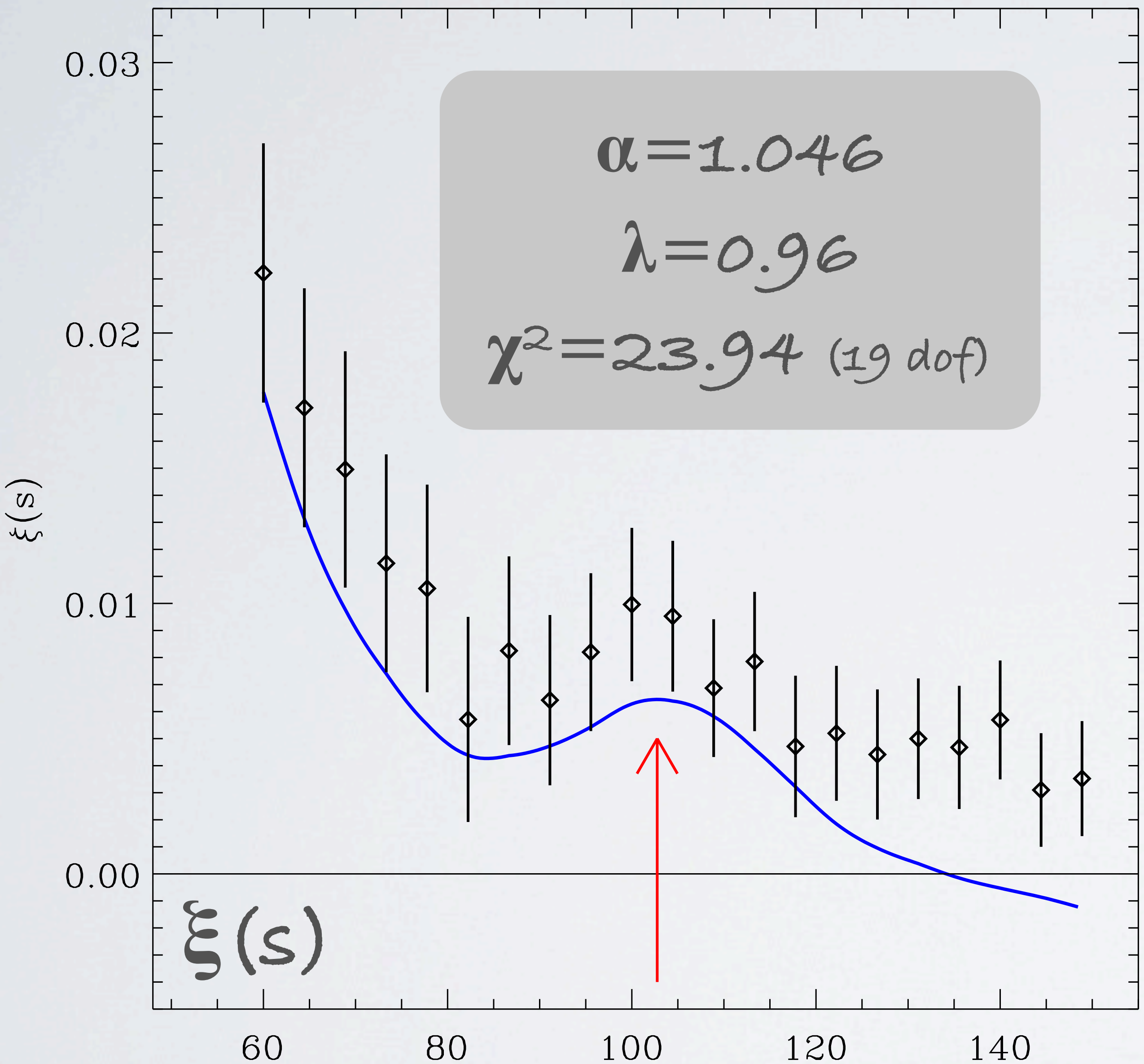

$s \; [h^{-1}Mpc]$

- Peak position measured at

$s_p = 101.6 \pm 3.0 \; h^{-1}Mpc$

Peak Position Distribution in mocks

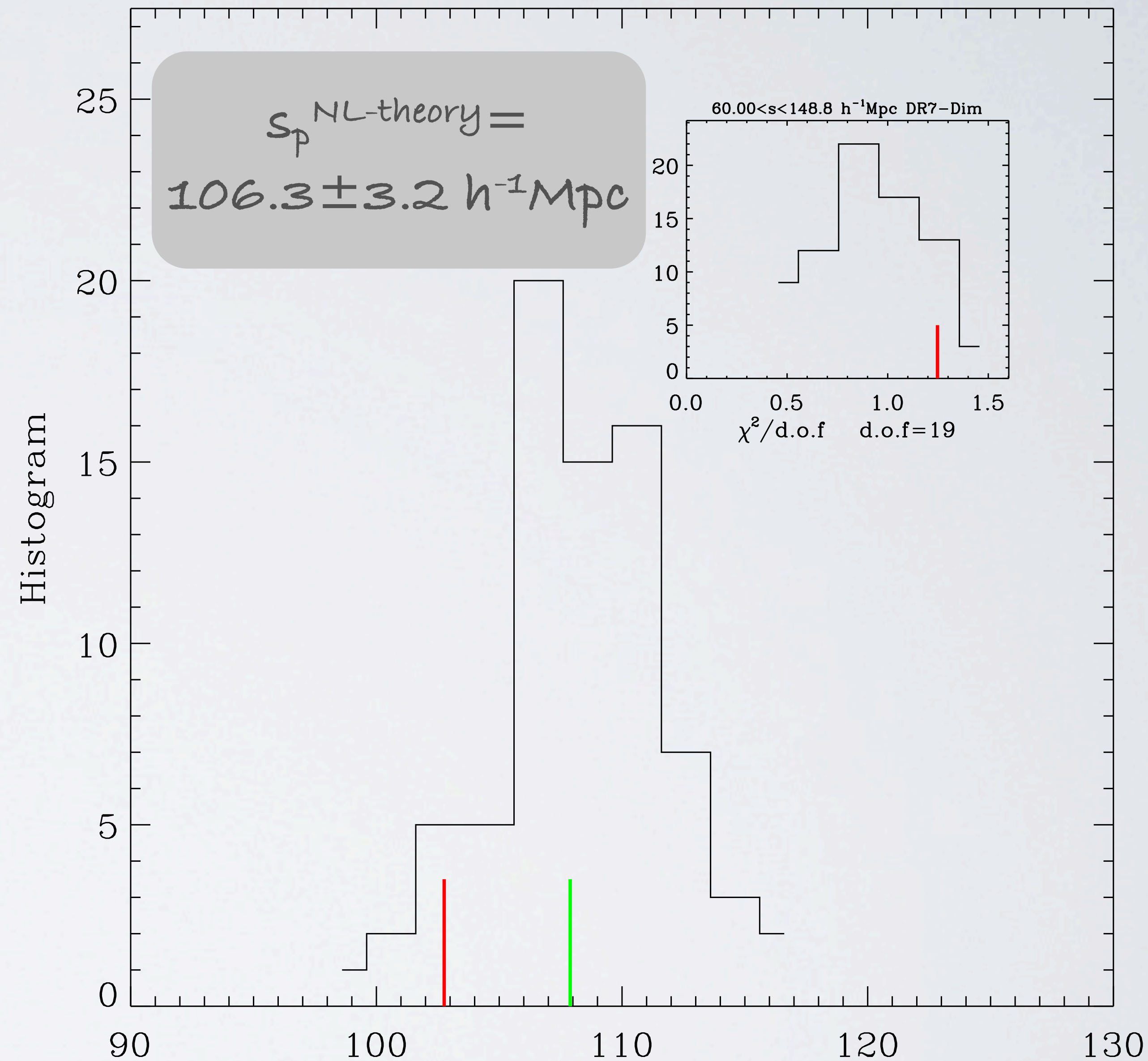

$s_p \; [h^{-1}Mpc]$

- 1σ uncertainties due to sample variance

Baryonic Acoustic Feature in SDSS LRGs
Monopole as a Standard Ruler

- Peak position yields
  $r_s/D_V=0.1389\pm0.043^{*}@\langle z\rangle=0.278$
- Applying $r_s=153.3$ Mpc (WMAP5; Komatsu et al.) we obtain:
  $D_V(\langle z\rangle=0.278)=1103\pm43$ Mpc
- Consistent with
  $\Omega_{M0}=[0.25\text{-}0.34]$,
  $h=[0.63\text{-}0.73]$

pseudo Hubble-Diagram

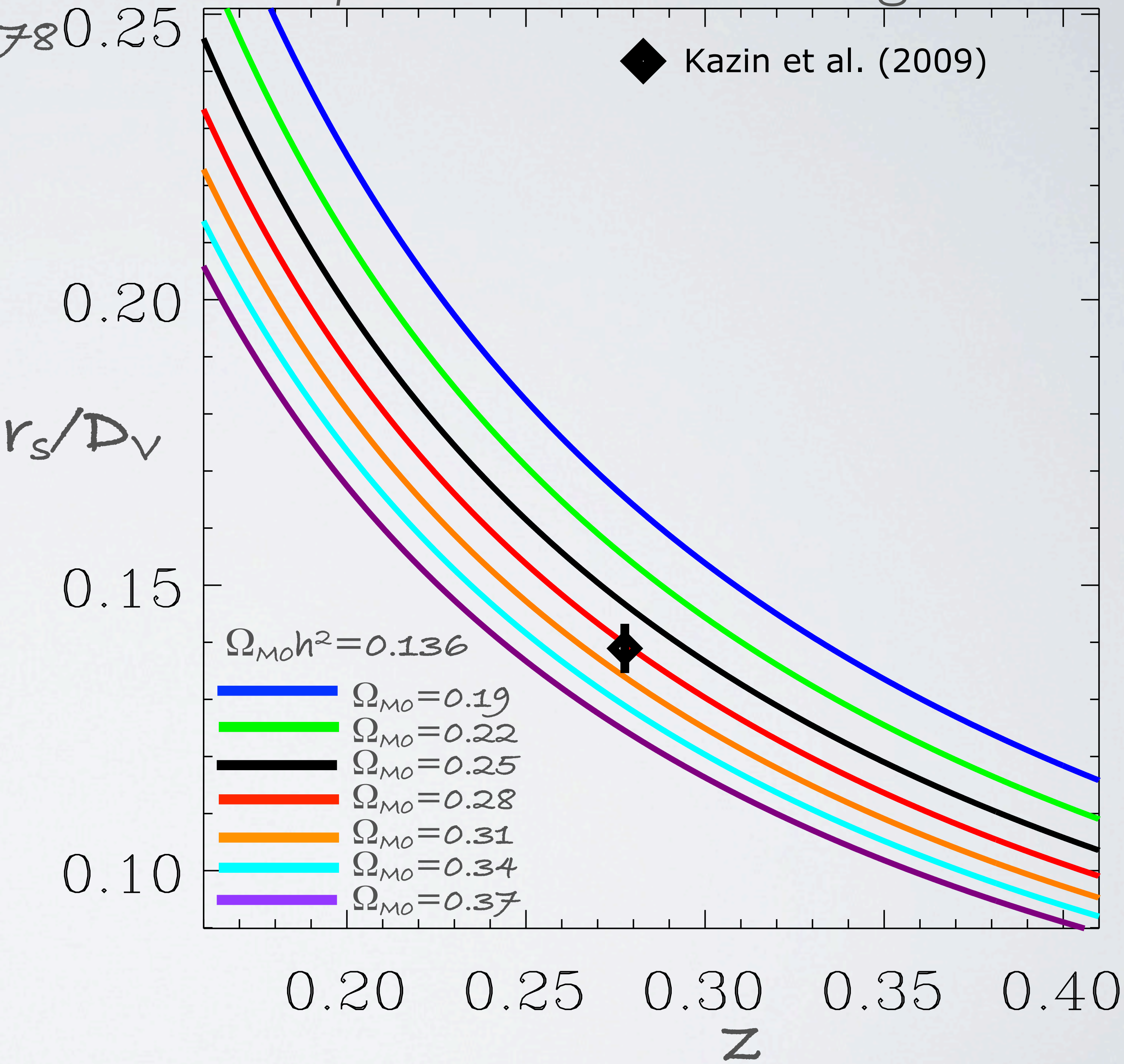

* Method:

$$(D_V/r_s)^{real}=(D_V/r_s)^{fiducial}(s_p^{\ fiducial}/s_p^{\ SDSS})$$

Baryonic Acoustic Feature in SDSS LRGs
Monopole as a Standard Ruler

- Peak position yields
  $r_s/D_V = 0.1389 \pm 0.043^* @\langle z\rangle = 0.278$
- Applying $r_s = 153.3$ Mpc (WMAP5; Komatsu et al.) we obtain:
  $D_V(\langle z\rangle = 0.278) = 1103 \pm 43$ Mpc
- Consistent with
  $\Omega_{M0} = [0.25-0.34]$,
  $h = [0.63-0.73]$

pseudo Hubble-Diagram

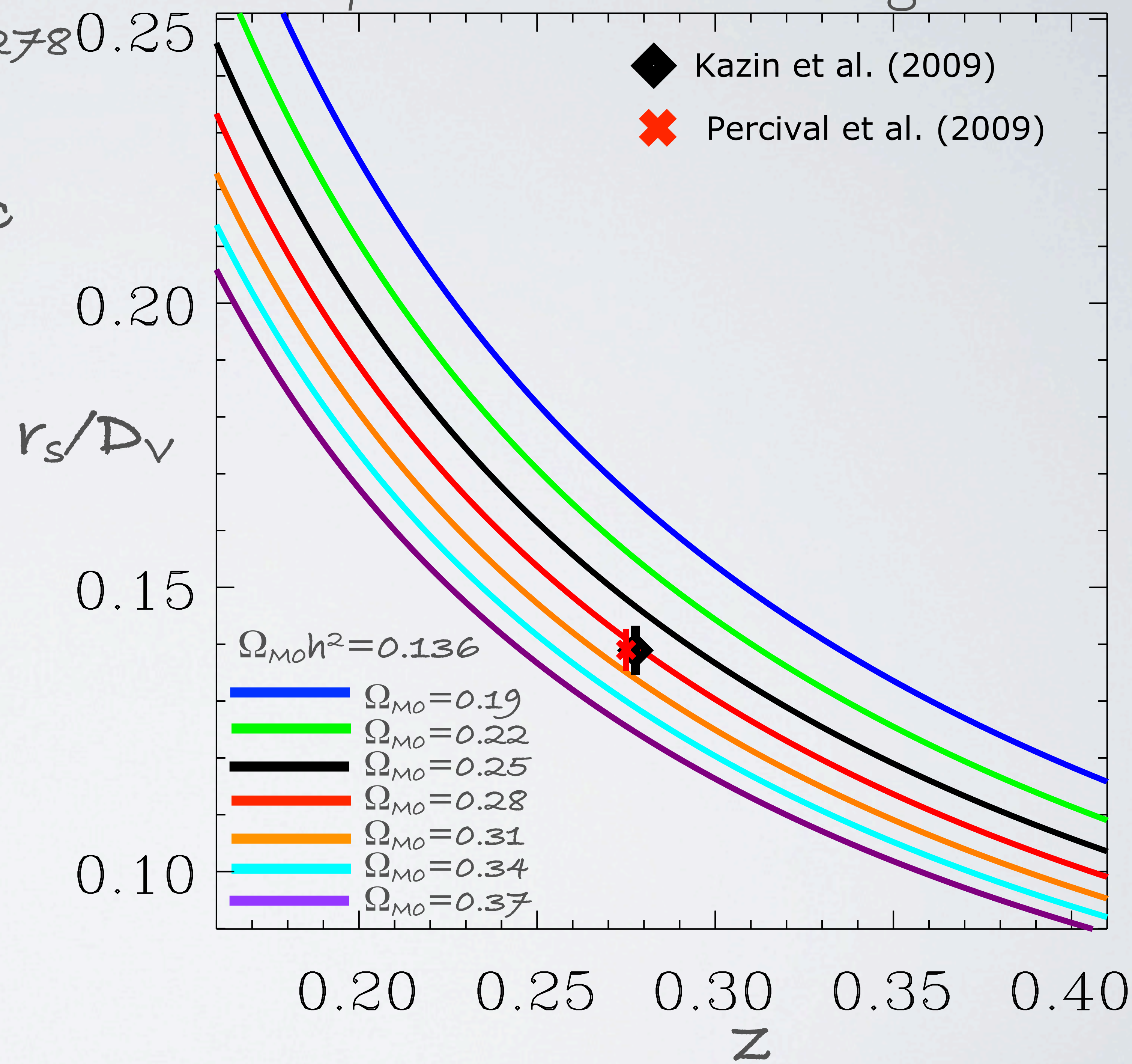

* Method:

$$(D_V/r_s)^{real} = (D_V/r_s)^{fiducial}(s_p^{\ fiducial}/s_p^{\ SDSS})$$

Baryonic Acoustic Feature in SDSS LRGs Monopole as a Standard Ruler

- Peak position yields
  $r_s/D_V = 0.1389 \pm 0.043^* @\langle z\rangle = 0.278$
- Applying $r_s = 153.3$ Mpc (WMAP5; Komatsu et al.) we obtain:
  $D_V(\langle z\rangle = 0.278) = 1103 \pm 43$ Mpc
- Consistent with
  $\Omega_{M0} = [0.25\text{-}0.34]$,
  $h = [0.63\text{-}0.73]$

pseudo Hubble-Diagram

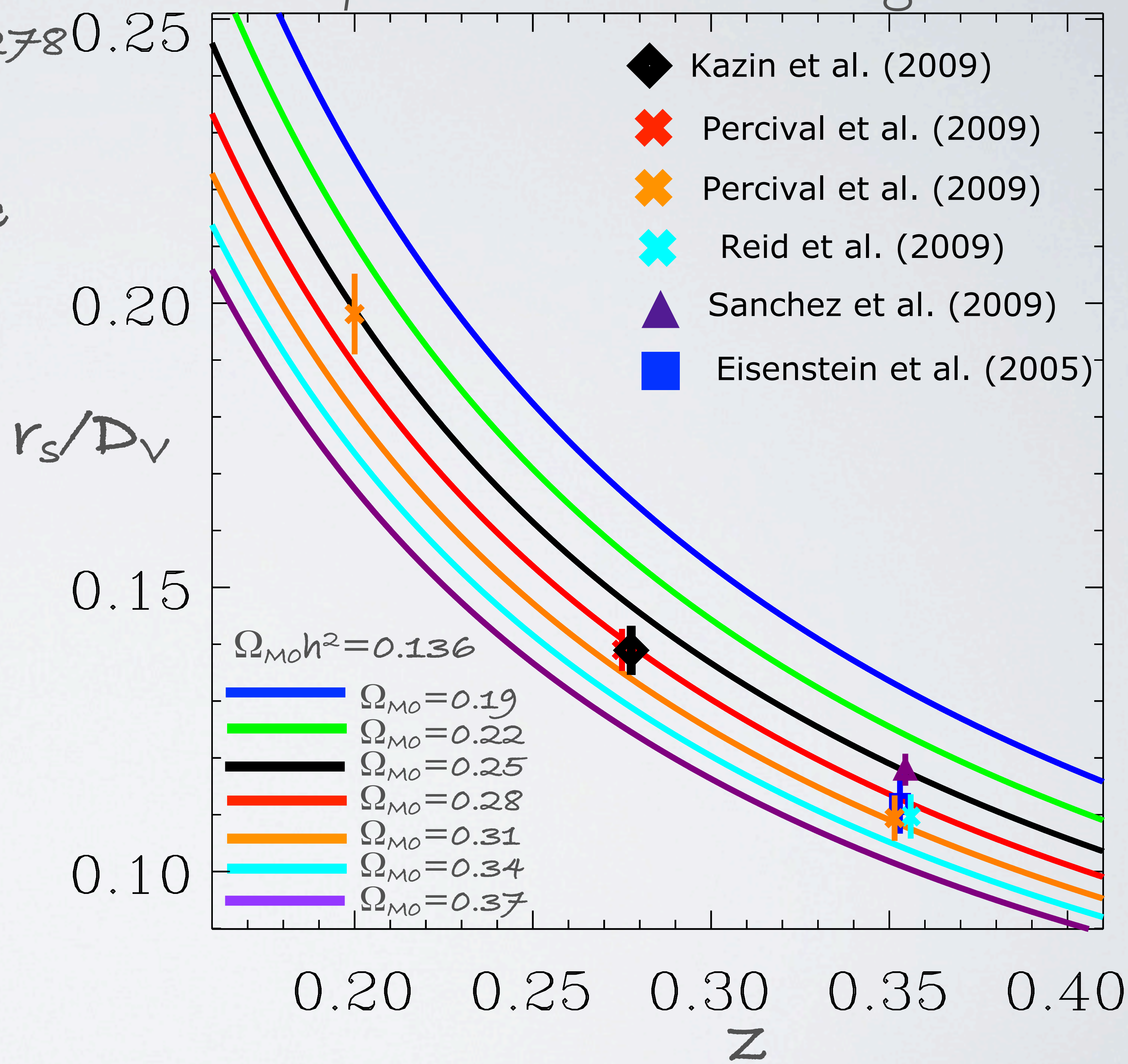

*Method:

$$(D_V/r_s)^{real} = (D_V/r_s)^{fiducial}(s_p^{\ fiducial}/s_p^{\ SDSS})$$

Baryonic Acoustic Feature in SDSS LRGs
Monopole as a Standard Ruler

- Peak position yields
  $r_s/D_V=0.1389\pm0.043^{*}@\langle z\rangle=0.278$
- Applying $r_s=153.3$ Mpc (WMAP5; Komatsu et al.) we obtain:
  $D_V(\langle z\rangle=0.278)=1103\pm43$ Mpc
- Consistent with
  $\Omega_{M0}=[0.25\text{-}0.34]$,
  $h=[0.63\text{-}0.73]$

- Comparisons with other studies of a similar sample show that r_s/D_V is not prone to data analysis systematics

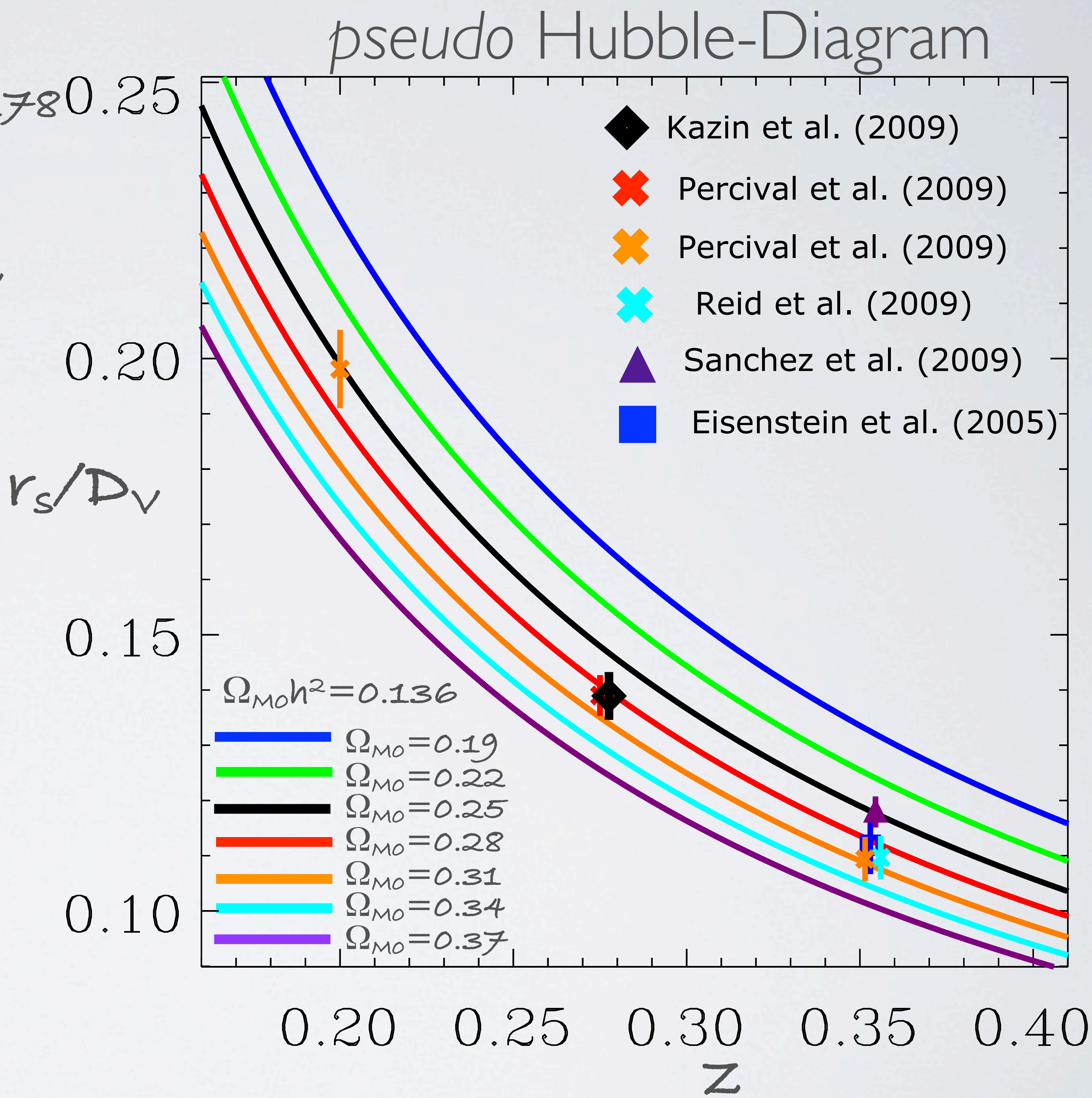

* Method:

$$(D_V/r_s)^{real}=(D_V/r_s)^{fiducial}(s_p^{\ fiducial}/s_p^{\ SDSS})$$

Baryonic Acoustic Feature in SDSS LRGs
Monopole as a Standard Ruler

- Peak position yields
  $r_s/D_V = 0.1389 \pm 0.043^* @\langle z \rangle = 0.278$
- Applying $r_s = 153.3$ Mpc (WMAP5; Komatsu et al.)
  we obtain:
  $D_V(\langle z \rangle = 0.278) = 1103 \pm 43$ Mpc
- Consistent with
  $\Omega_{M0} = [0.25\text{-}0.34]$,
  $h = [0.63\text{-}0.73]$

pseudo Hubble-Diagram

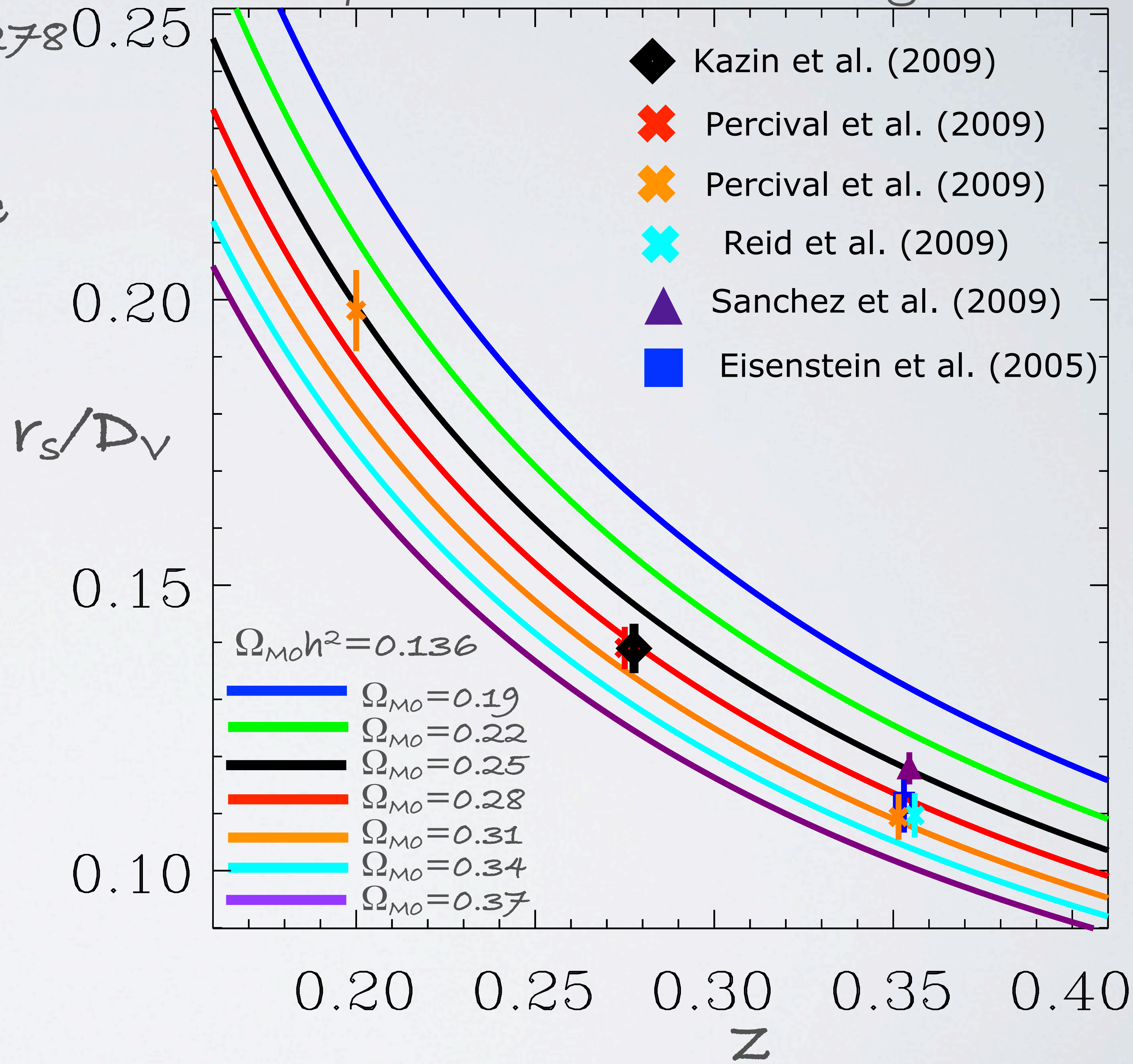

- Comparisons with other studies of a similar sample show that r_s/D_V is not prone to data analysis systematics

Kazin et al. 2009
ApJ 710 (2010) 1444-1461

* Method:

$$(D_V/r_s)^{real} = (D_V/r_s)^{fiducial}(s_p^{\ fiducial}/s_p^{\ SDSS})$$

Clustering as Function of Polar Angle

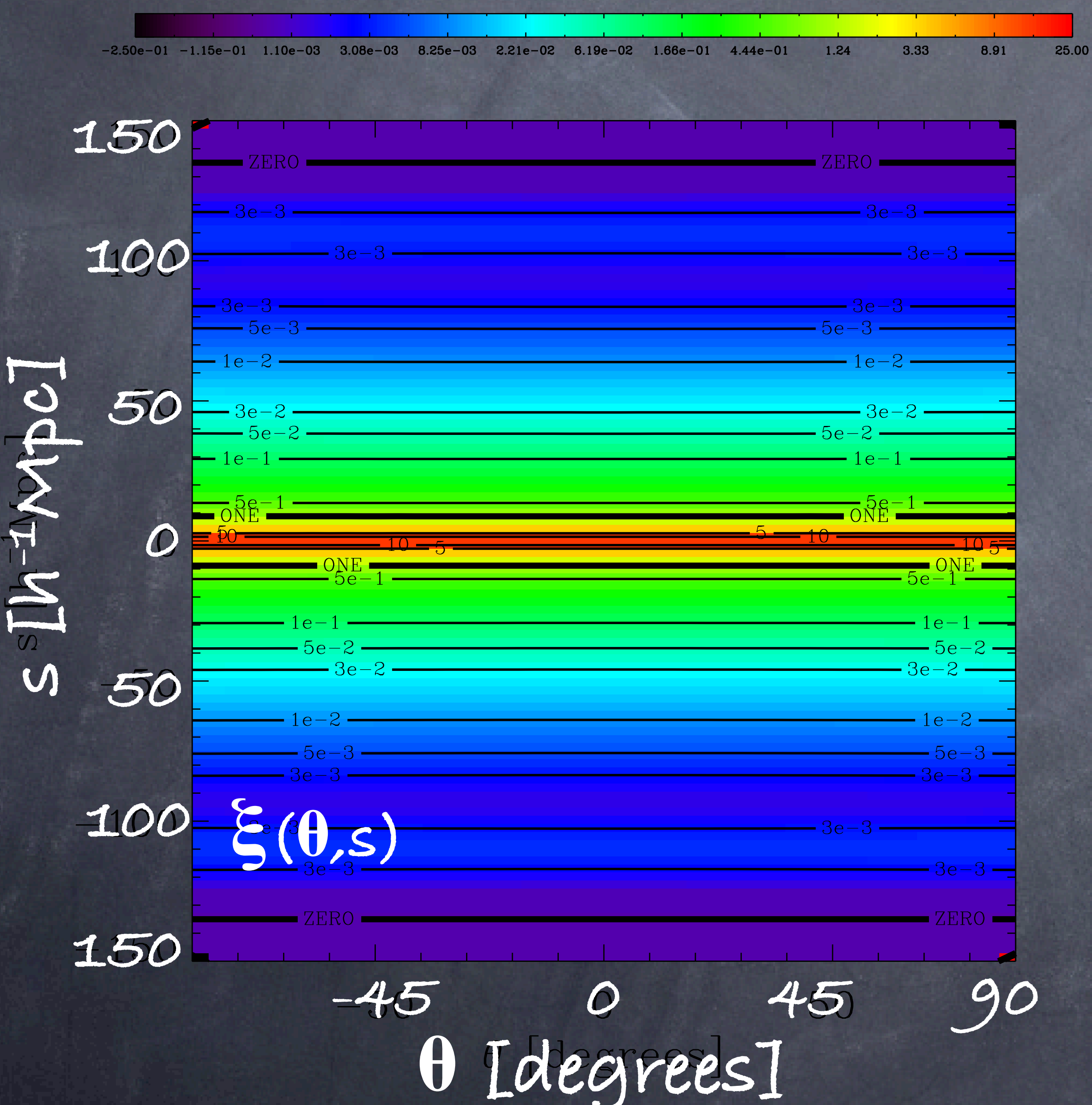

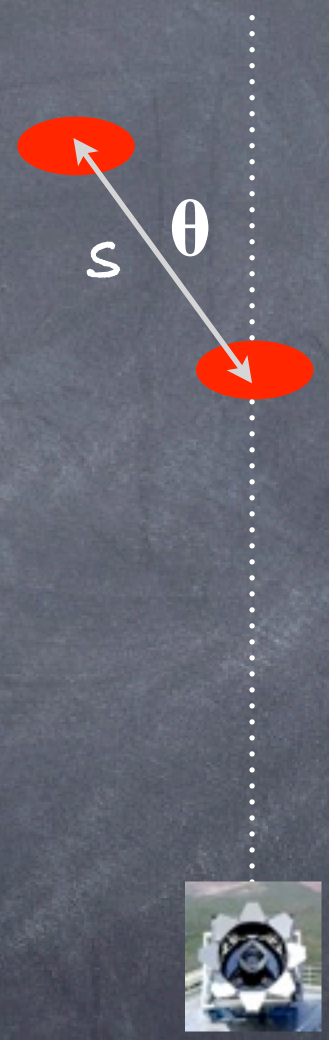

Clustering as Function of Polar Angle

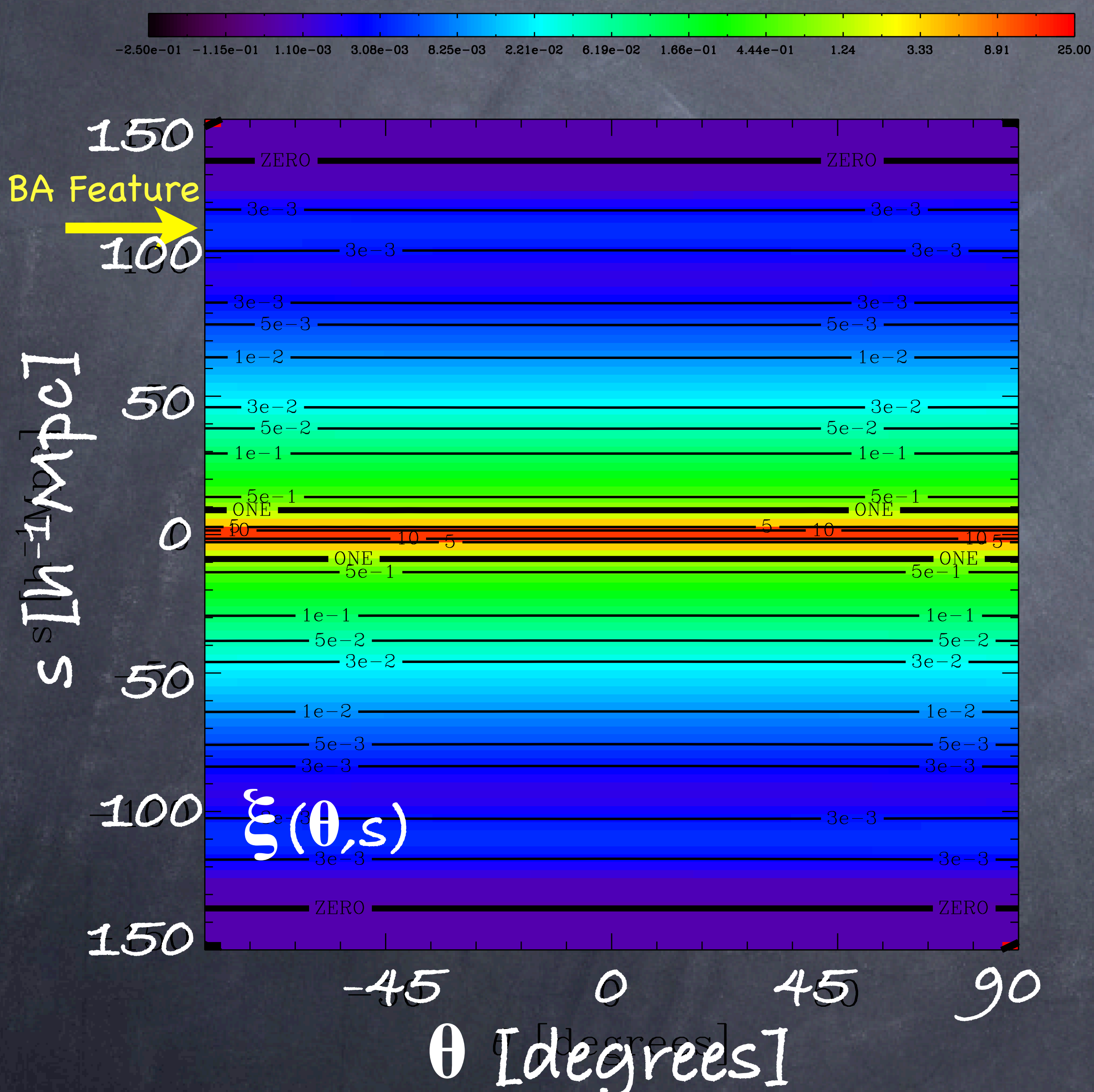

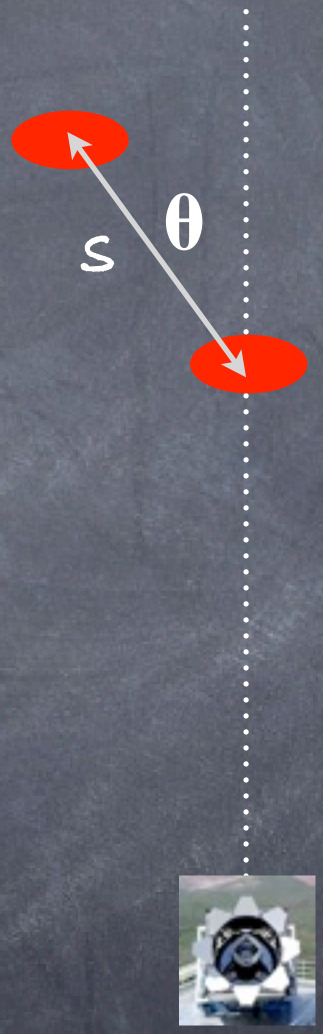

Clustering as Function of Polar Angle

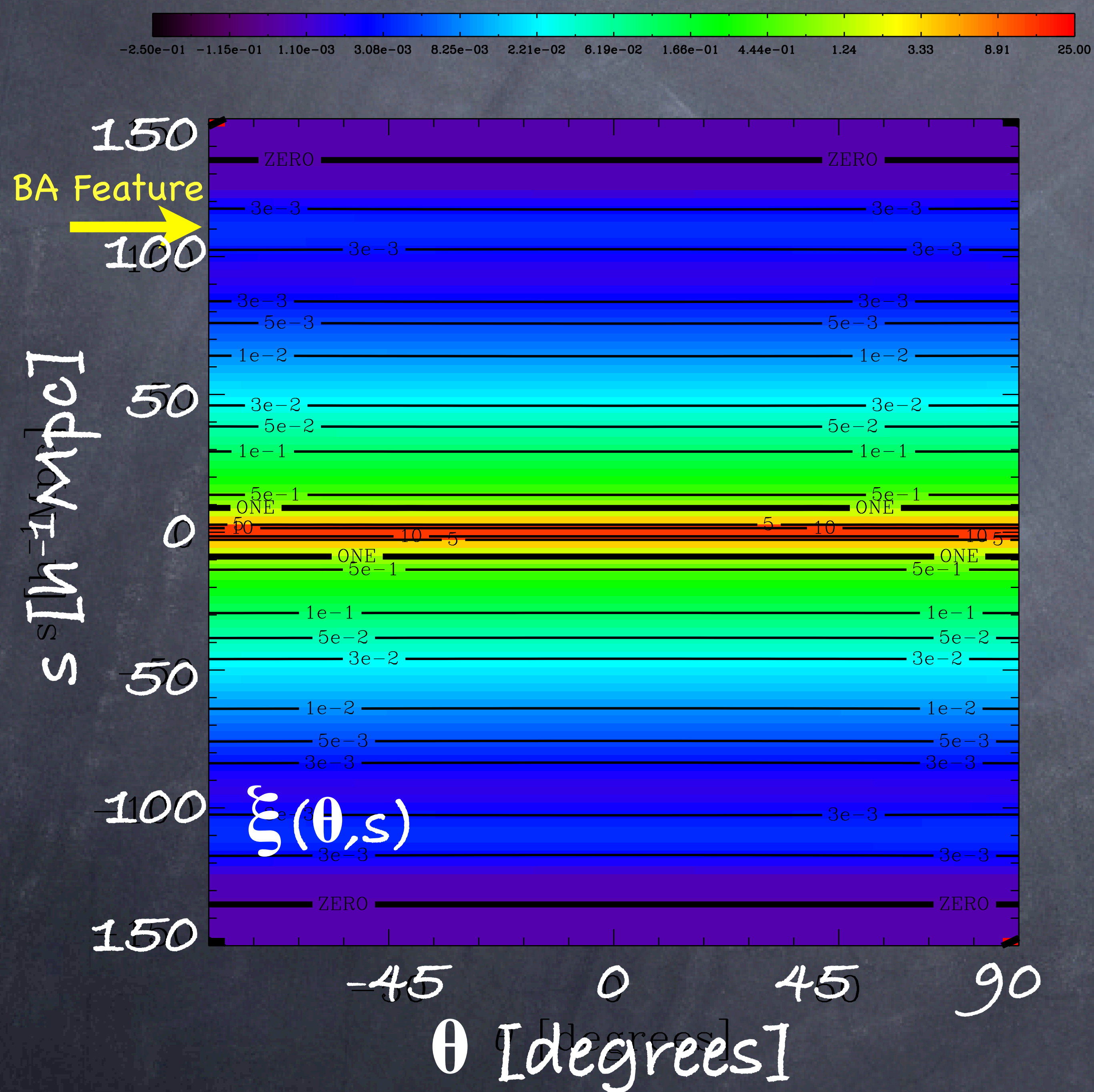

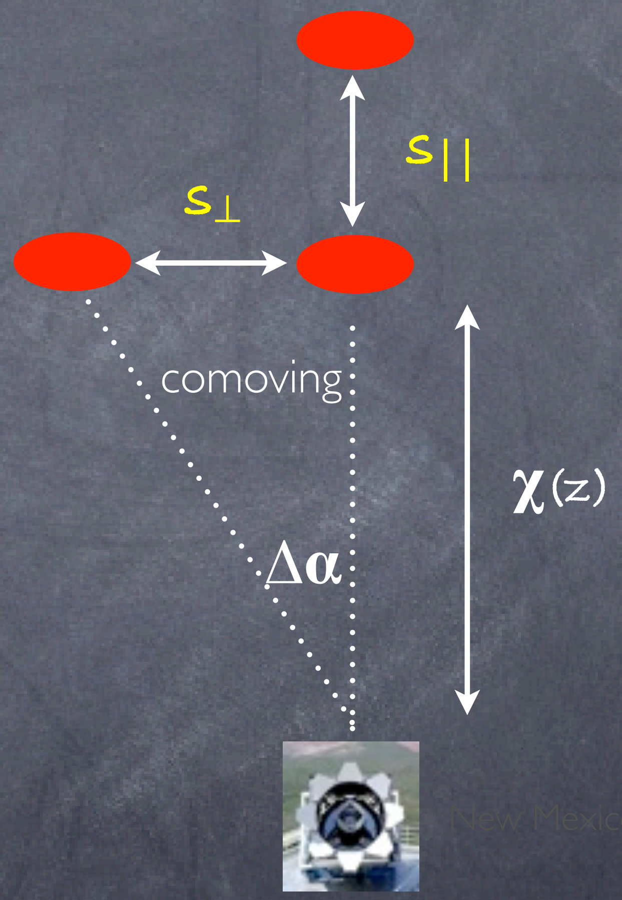

Clustering as Function of Polar Angle

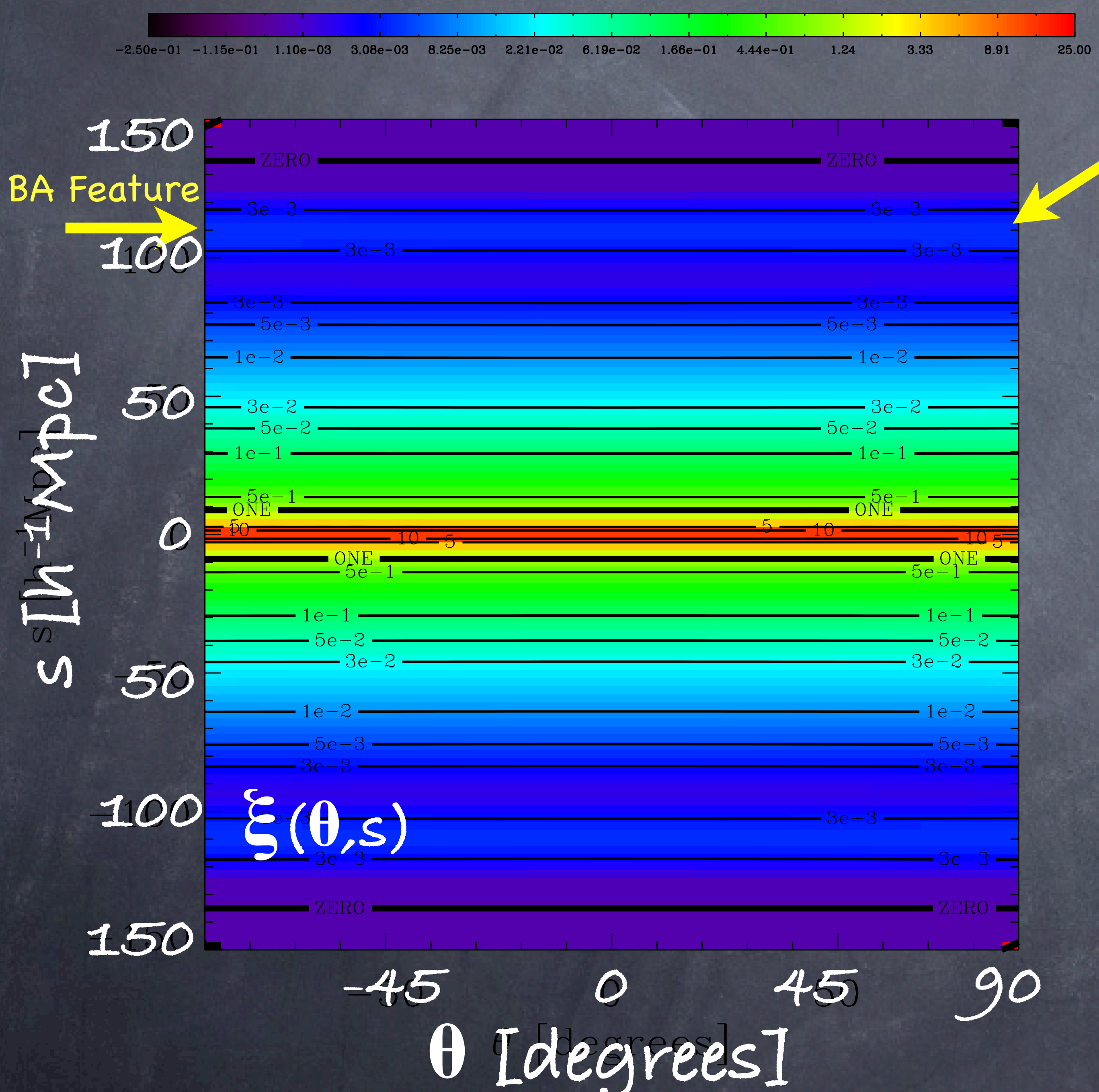

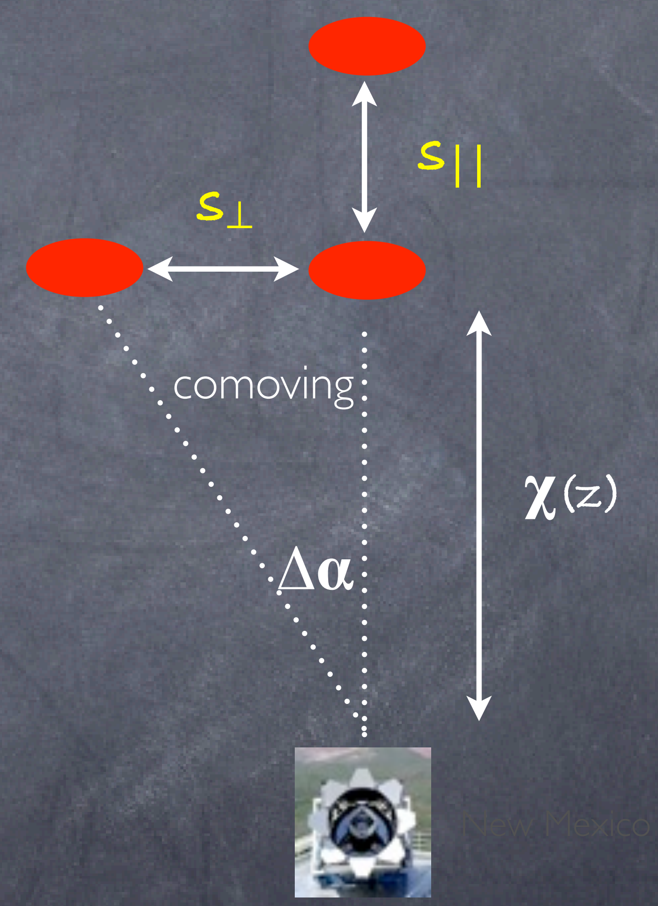

Clustering as Function of Polar Angle

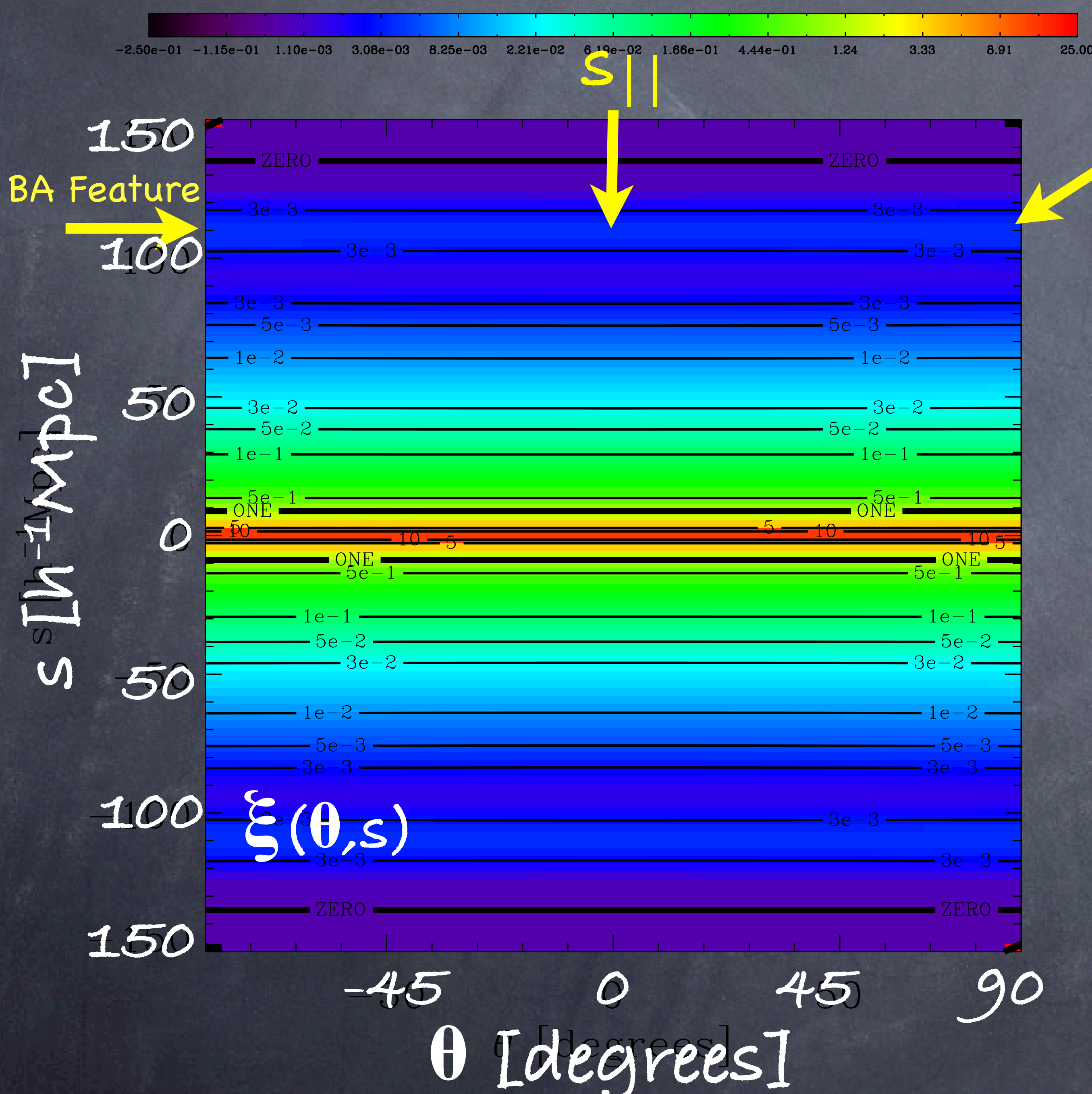

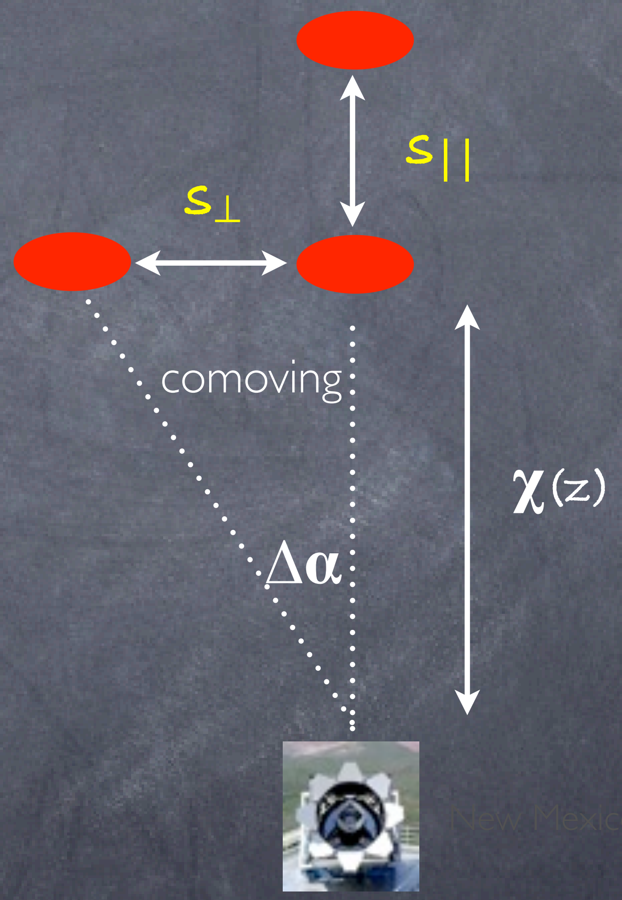

Redshift Distortions

Velocity-Dispersion Effect
(aka Finger of God)
effects small scales ~ few Mpc

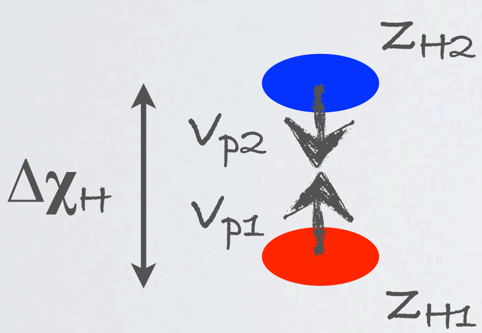

Real Comoving Space

Redshift Space

Redshift Distortions

Velocity-Dispersion Effect
(aka Finger of God)
effects small scales ~ few Mpc

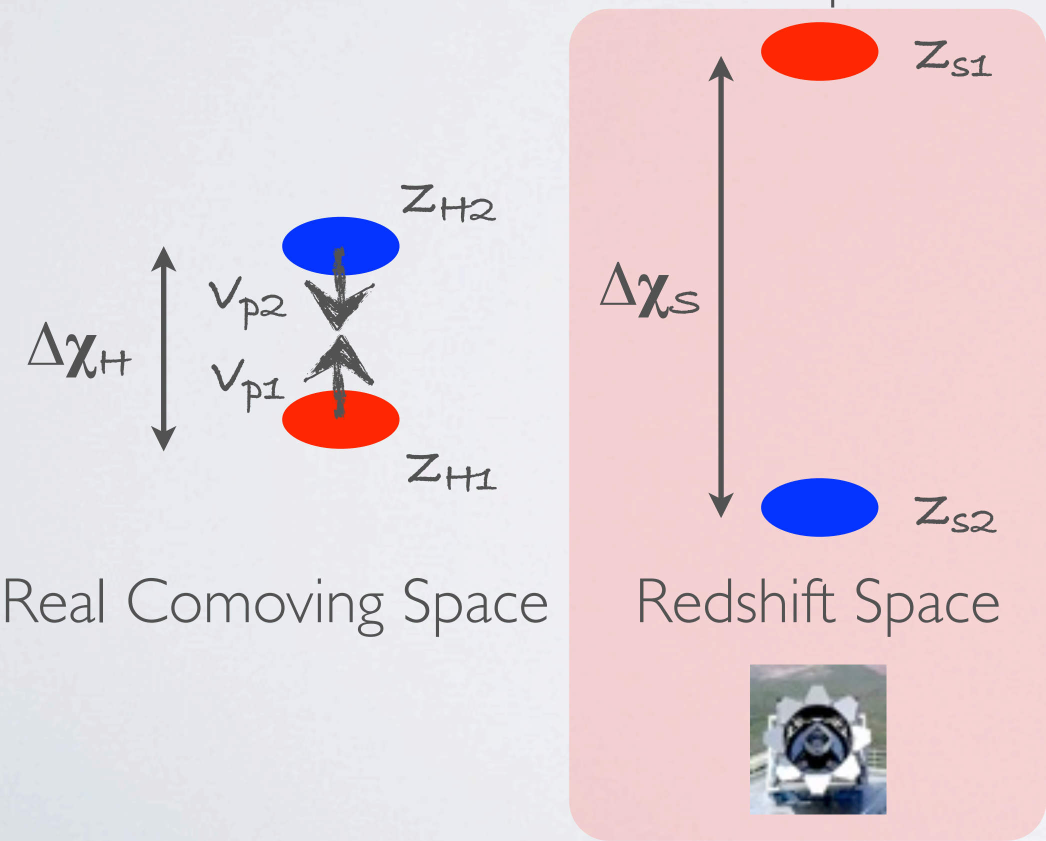

Redshift Distortions

Velocity-Dispersion Effect
(aka Finger of God)
effects small scales ~ few Mpc

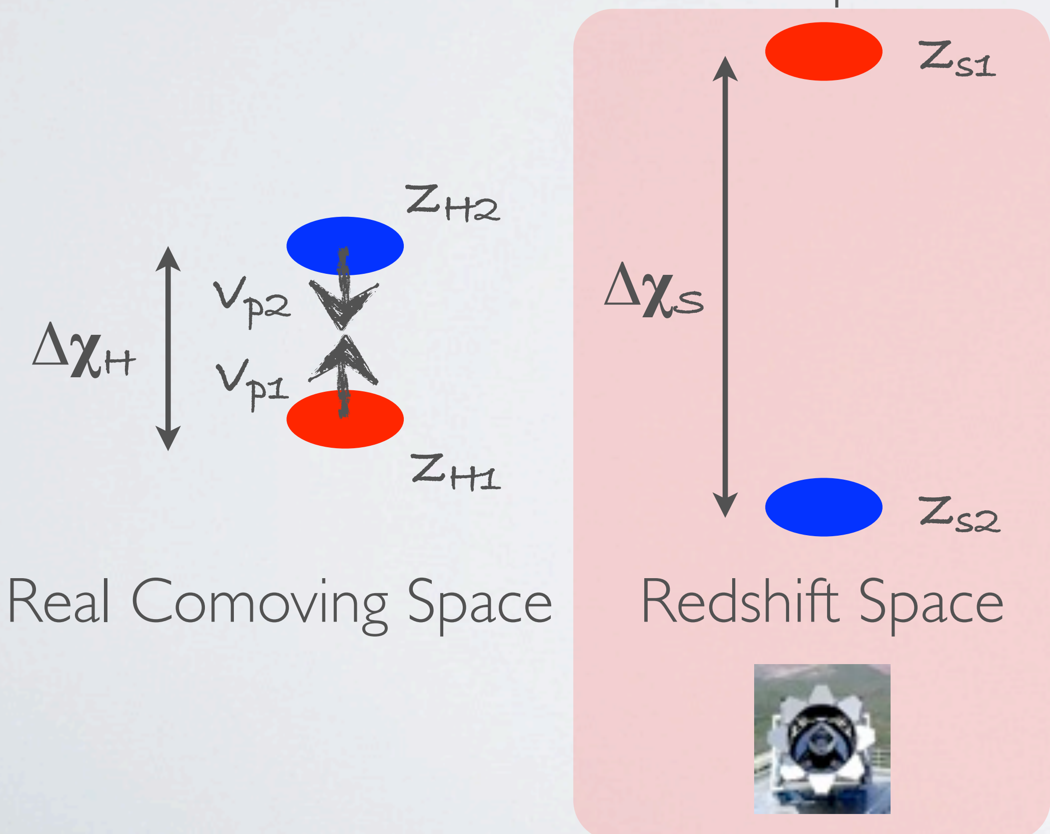

Squashing Effect
effects large scales ~10'sMpc

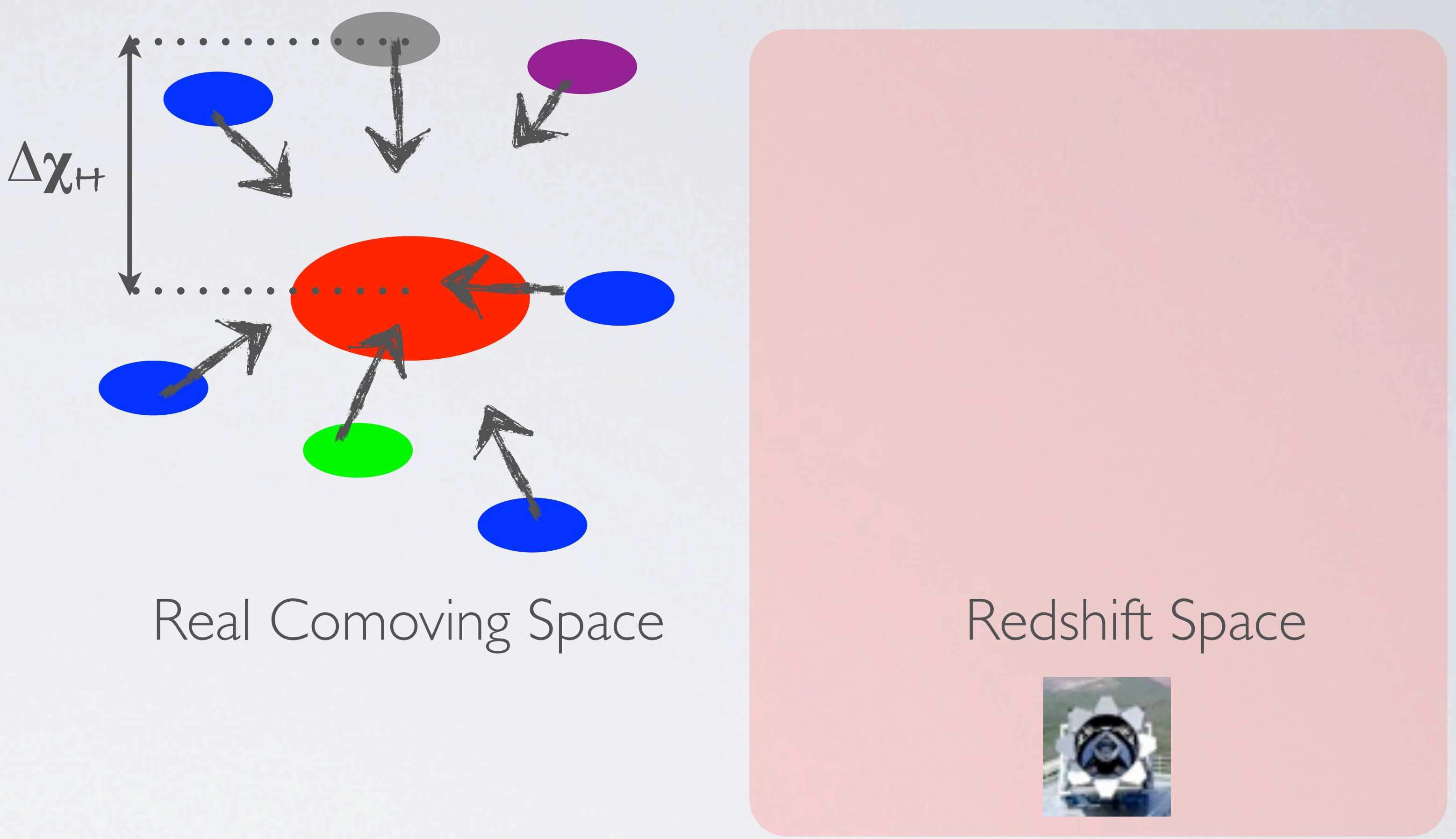

Redshift Distortions

Squashing Effect
effects large scales ~10'sMpc

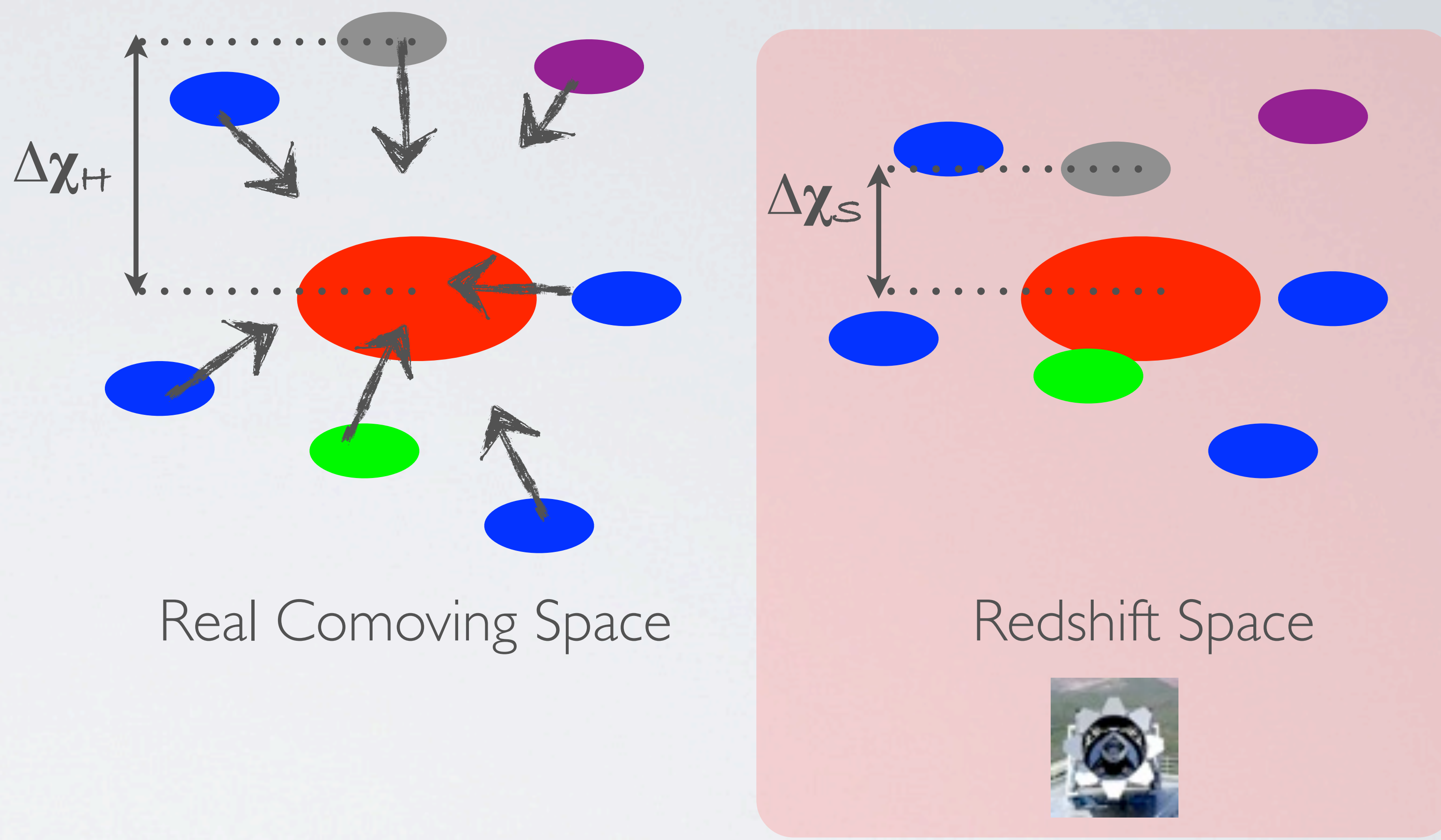

Velocity-Dispersion Effect
(aka Finger of God)
effects small scales ~ few Mpc

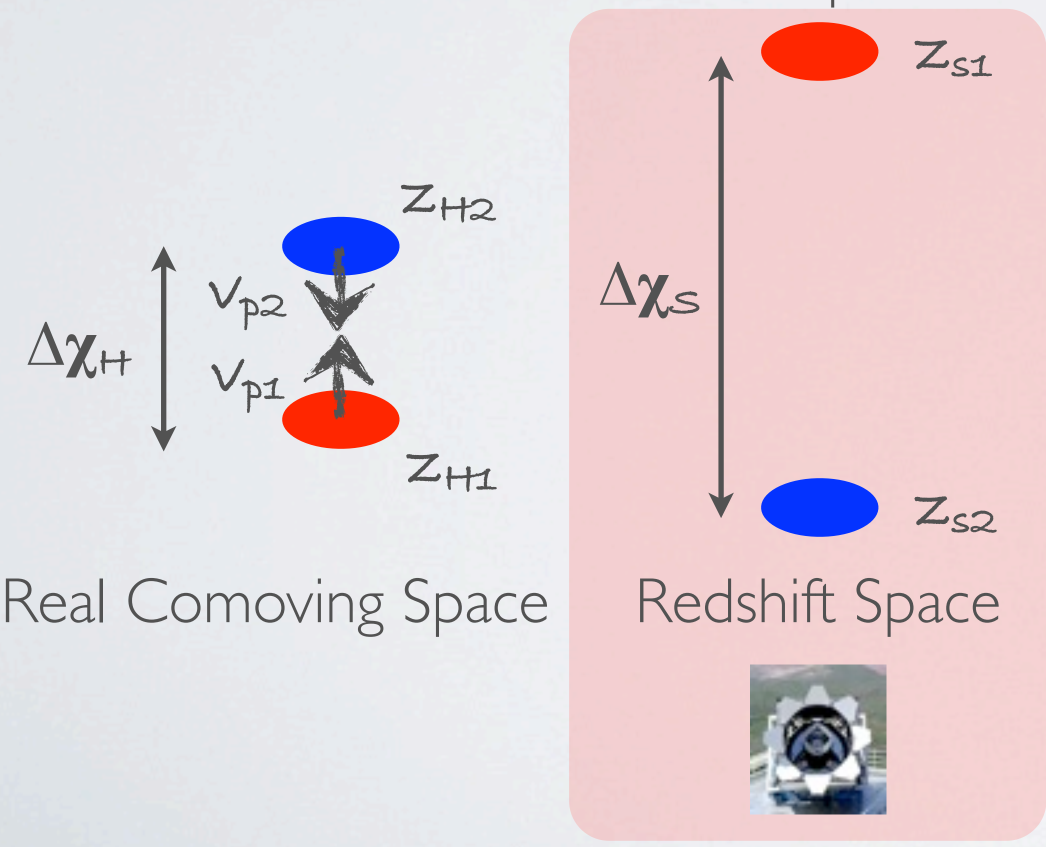

Clustering as Function of Polar Angle

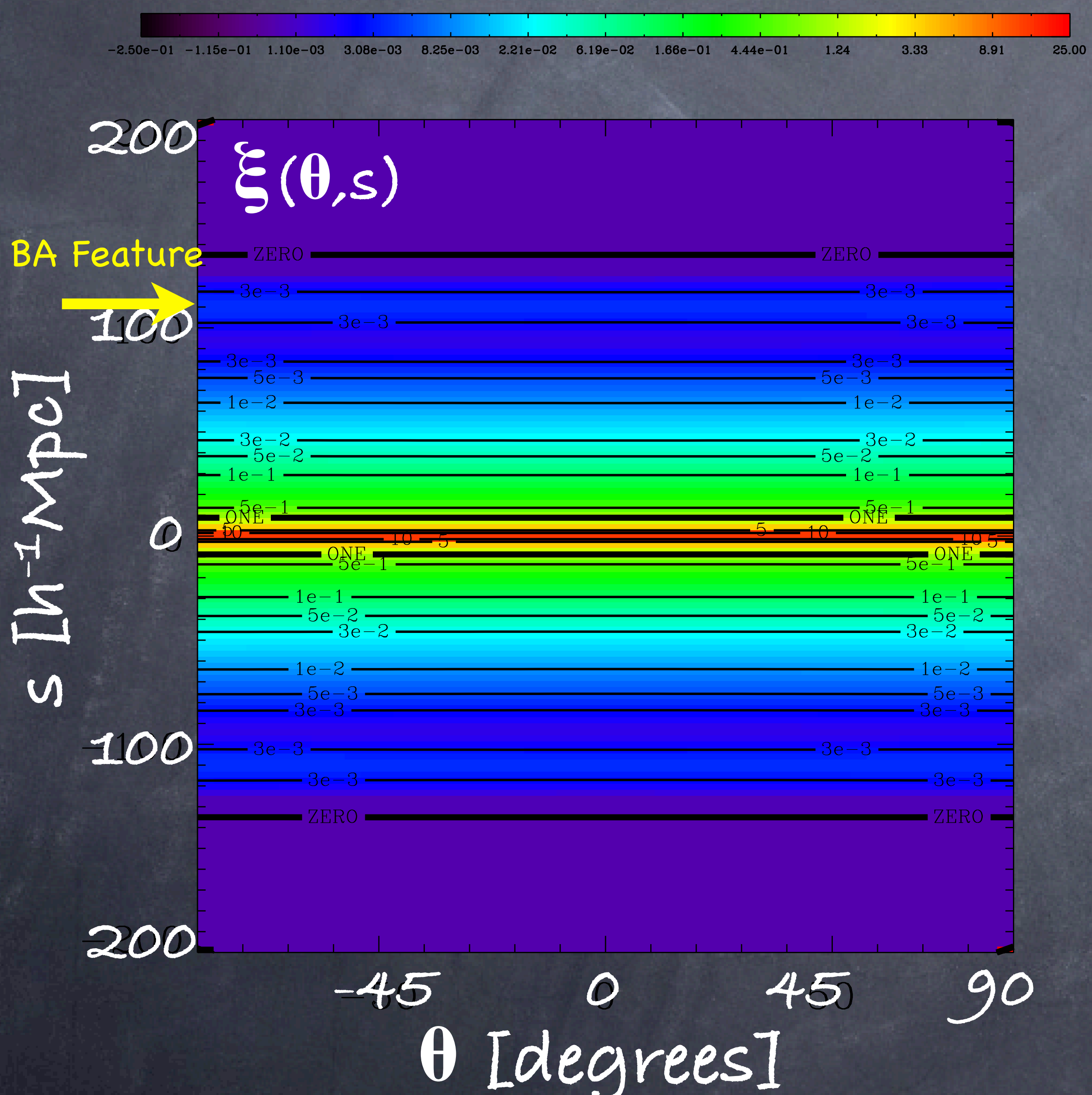

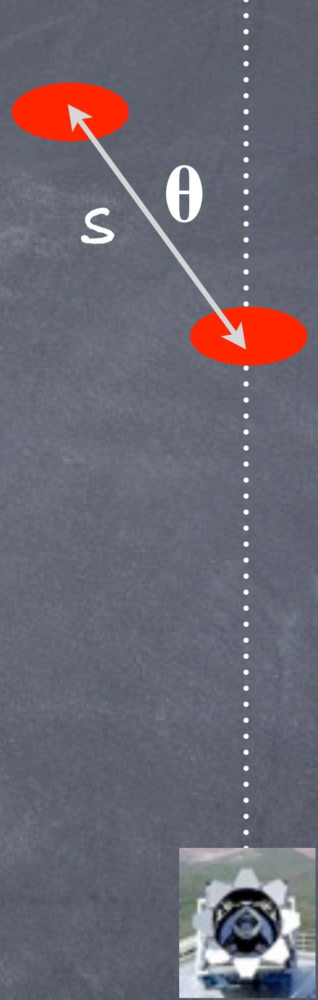

Clustering as Function of Polar Angle

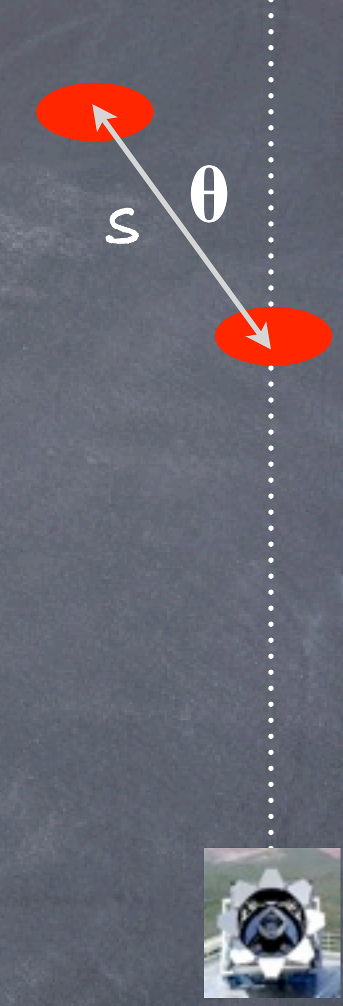

no dynamical distortions
(linear theory)

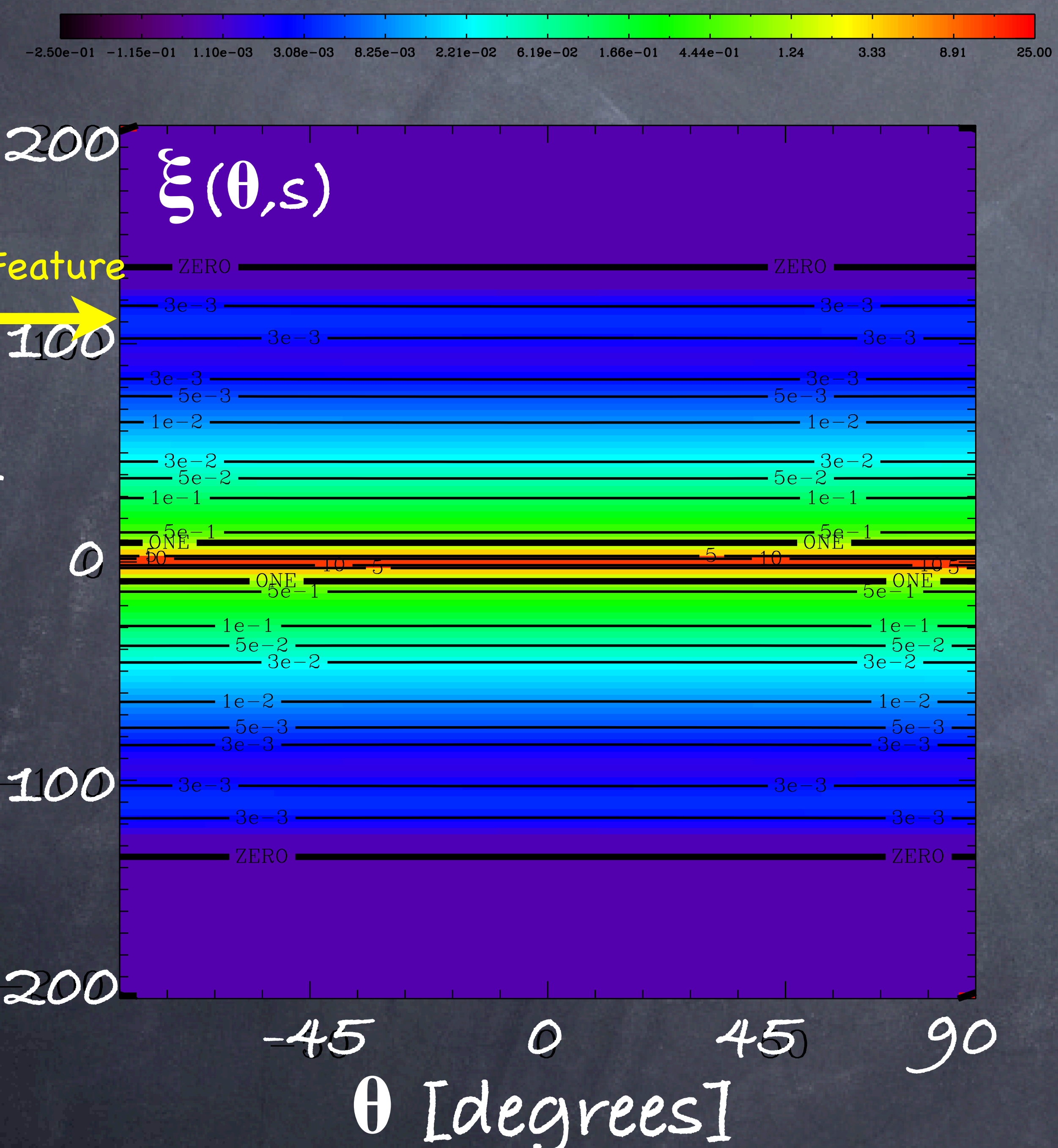

Clustering as Function of Polar Angle with Squashing Effect

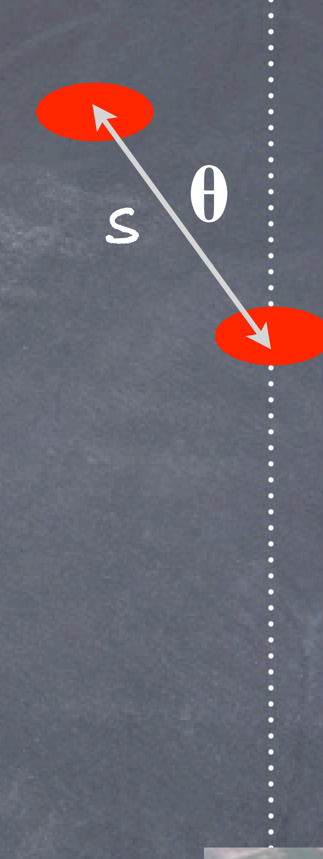

no dynamical distortions
(linear theory)

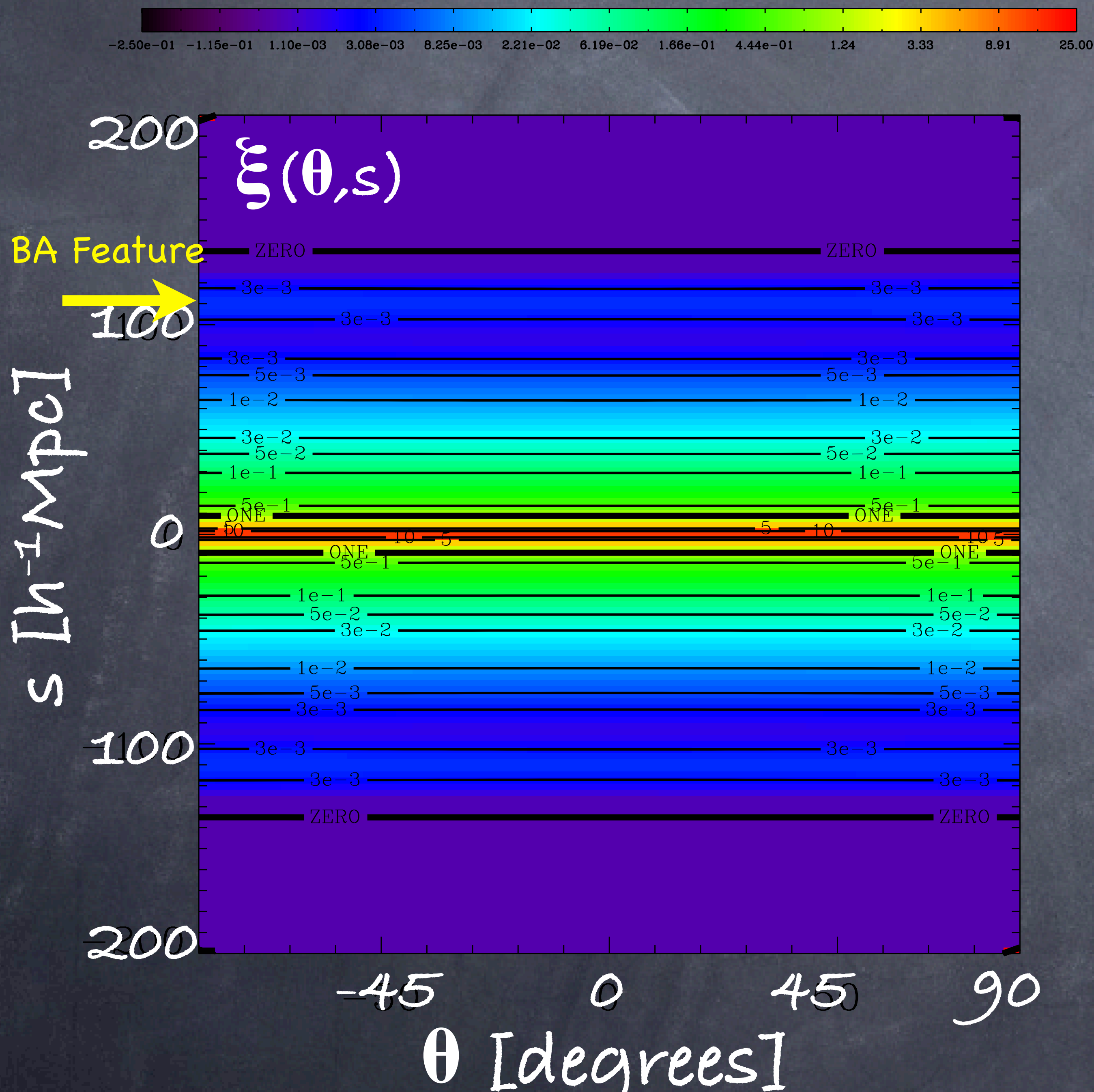

Clustering as Function of Polar Angle with Squashing Effect

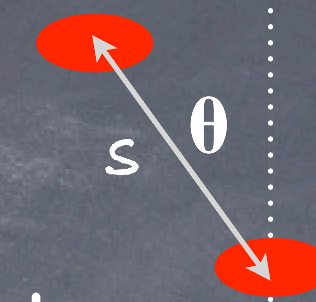

no dynamical distortions
(linear theory)

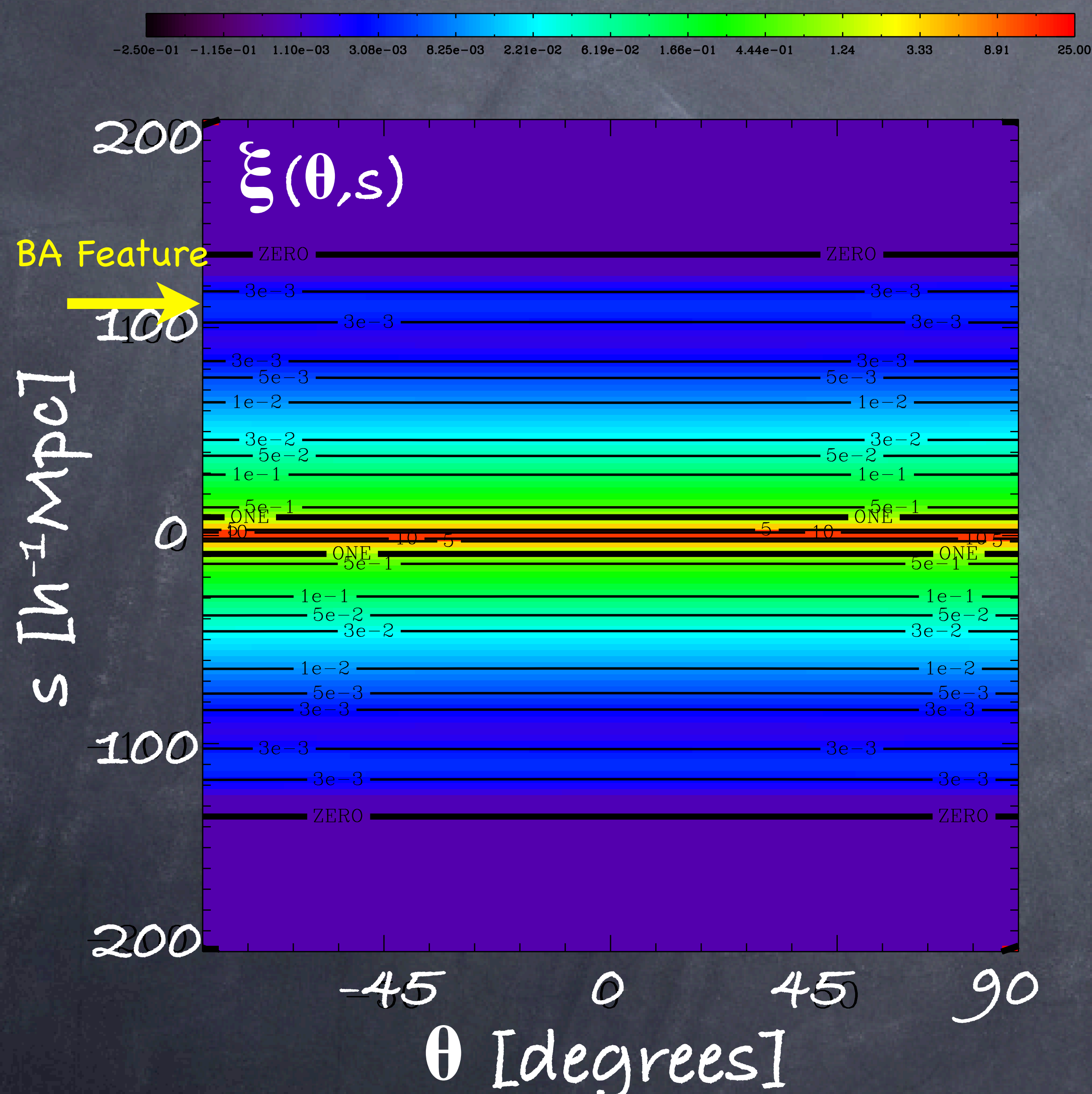

squashing effect only
(linear theory; Matsubara 2004)

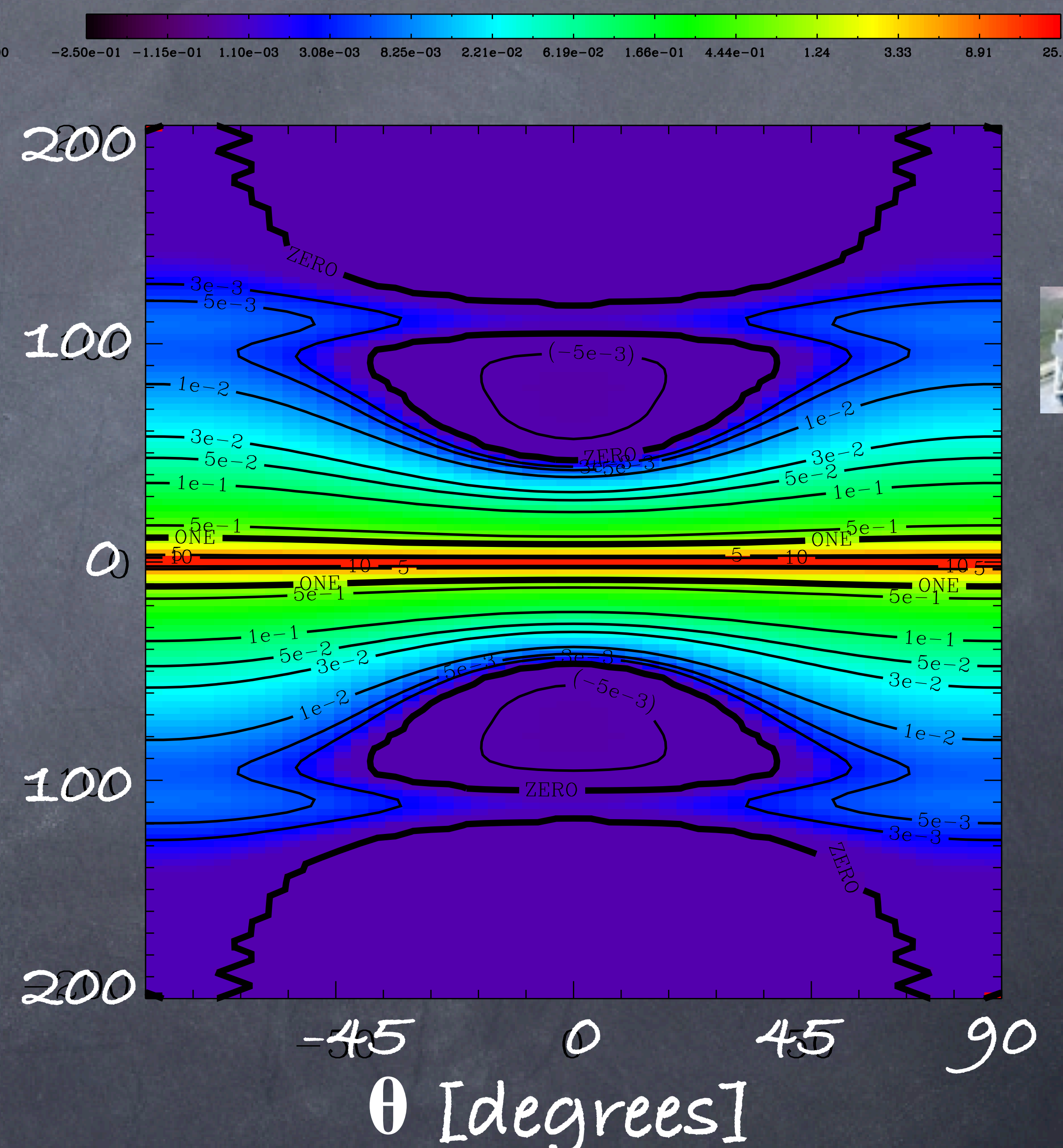

Clustering as Function of Polar Angle with Squashing Effect

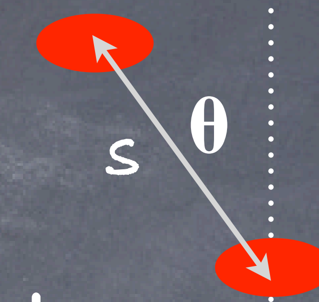

redshift distortions
(non linear theory; LasDamas mocks)

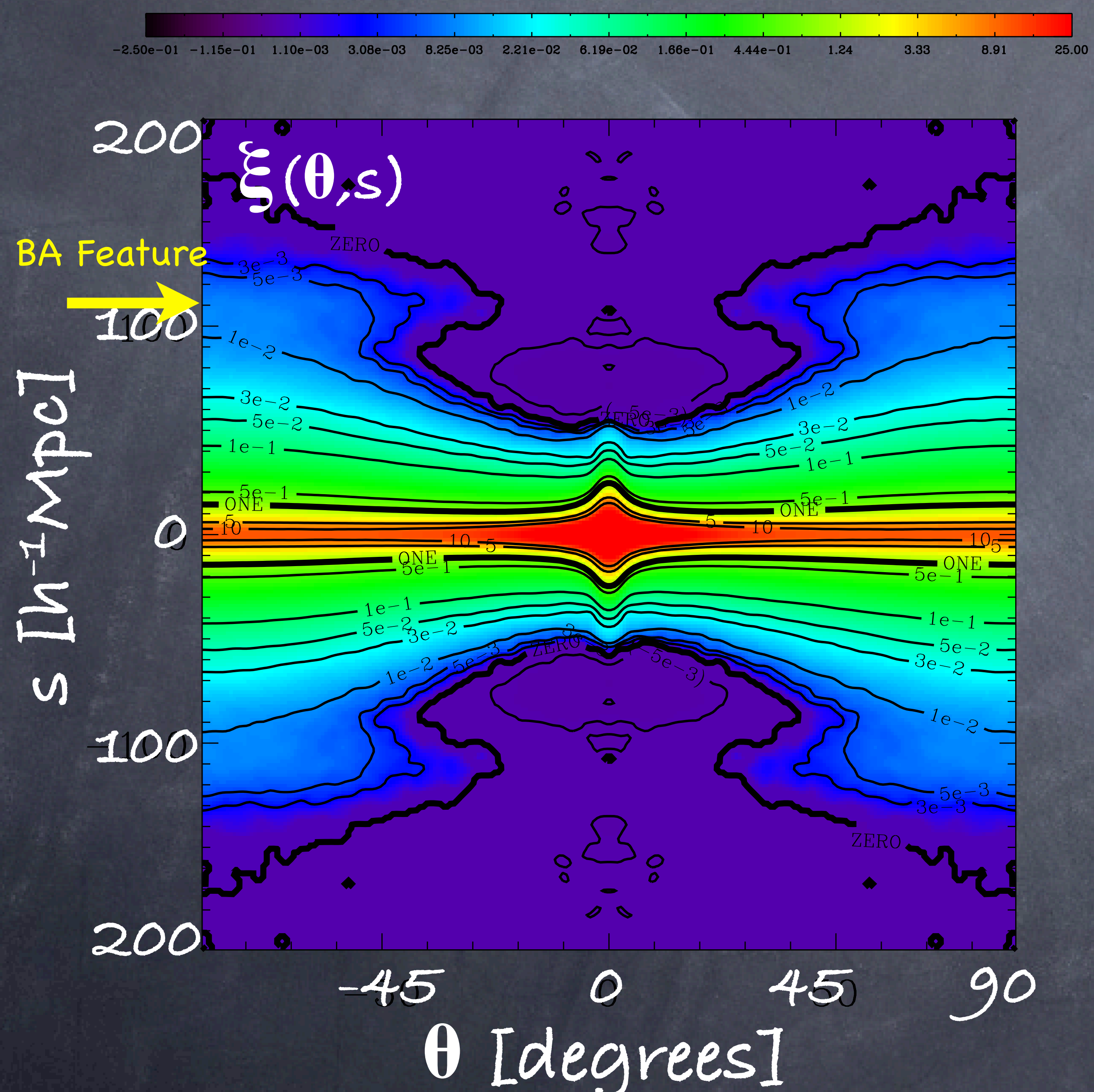

squashing effect only
(linear theory; Matsubara 2004)

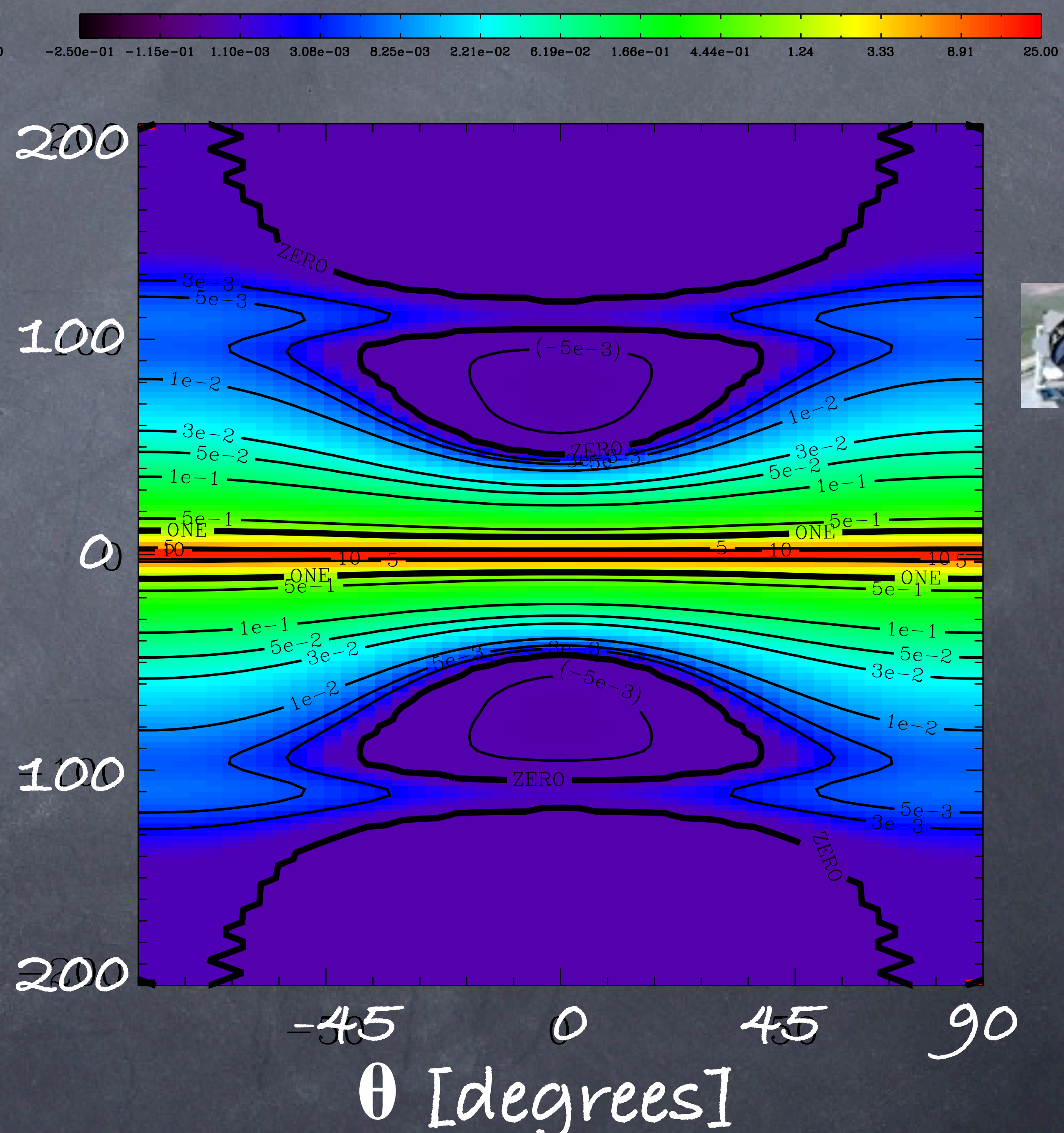

Baryonic Acoustic Feature in SDSS LRGs
Line of Sight Detection?

redshift distortions
(non linear theory; LasDamas mocks)

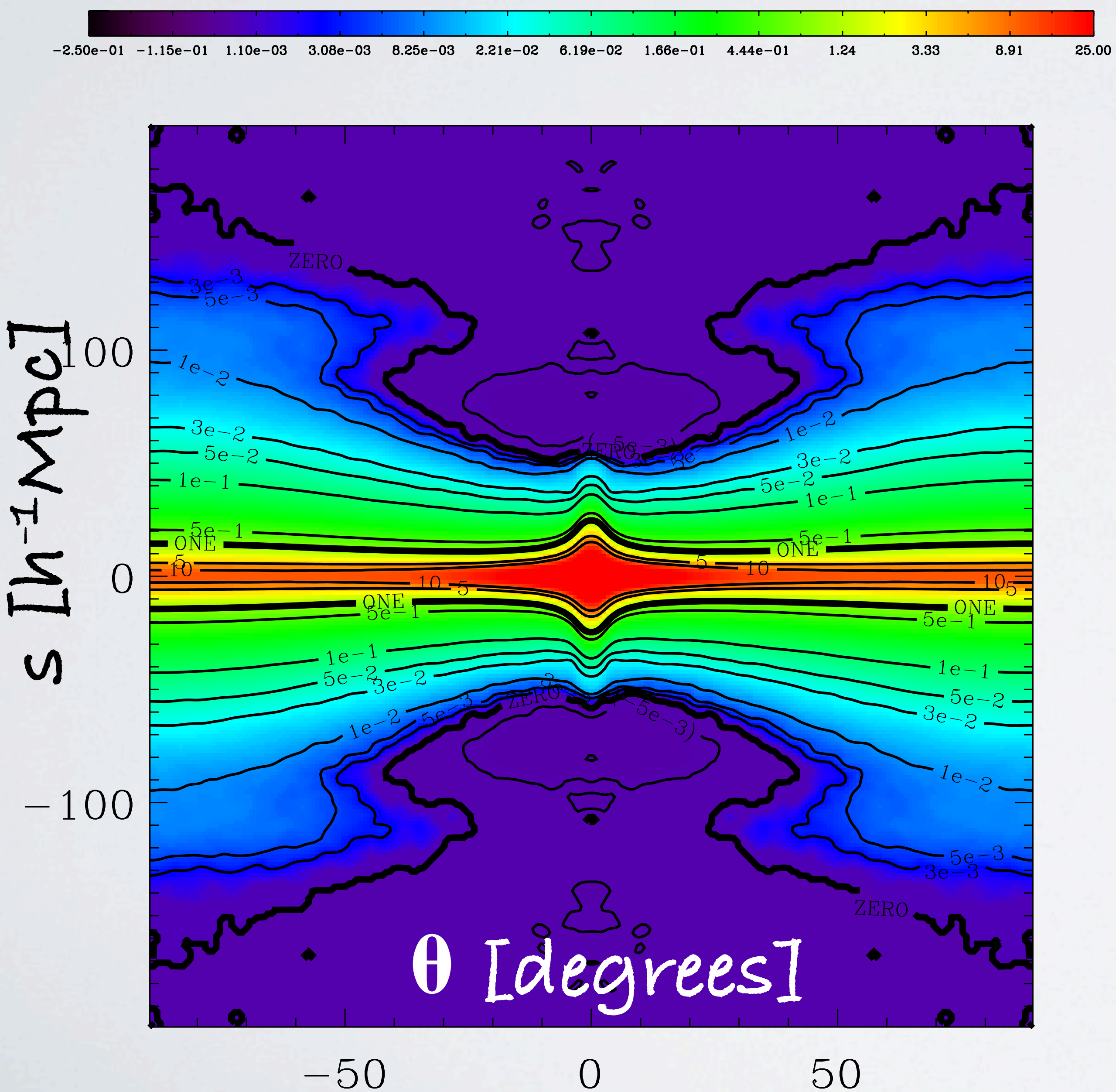

SDSS-II Results

Kazin et al. (in prep.)

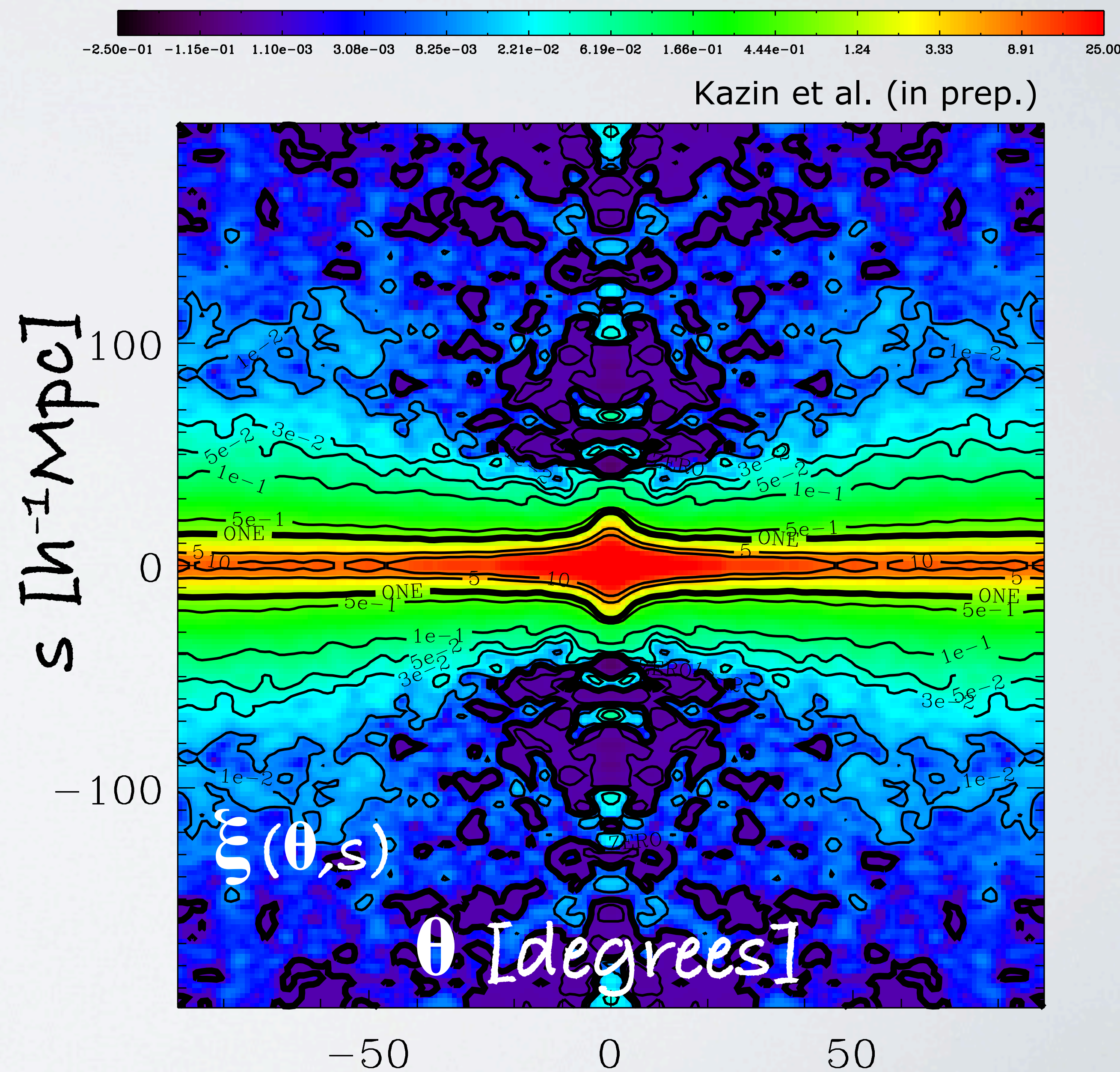

Baryonic Acoustic Feature in SDSS LRGs Line of Sight Detection?

From Gaztañaga et al. (2008)

ABSTRACT

We study the clustering of LRG galaxies in the latest spectroscopic SDSS data releases, DR6 and DR7, which sample over 1 $\mathrm{Gpc}^3/\mathrm{h}^3$ to z=0.47. The 2-point correlation function $\xi(\sigma,\pi)$ is estimated as a function of perpendicular σ and line-of-sight π (radial) directions. We find a significant detection of a peak at $r \simeq 110$Mpc/h, which shows as a circular ring in the $\sigma-\pi$ plane. There is also significant evidence for a peak along the radial direction whose shape is consistent with its originating from the recombination-epoch baryon acoustic oscillations (BAO). A $\xi(\sigma,\pi)$ model with no radial BAO peak is disfavored at 3.2σ, whereas a model with no magnification bias is disfavored at 2σ. The radial data enable, for the first time, a direct measurement of the Hubble parameter $H(z)$ as a function of redshift. This is independent from earlier BAO measurements which used the spherically averaged (monopole) correlation to constrain an integral of $H(z)$. Using the BAO peak position as a standard ruler in the radial

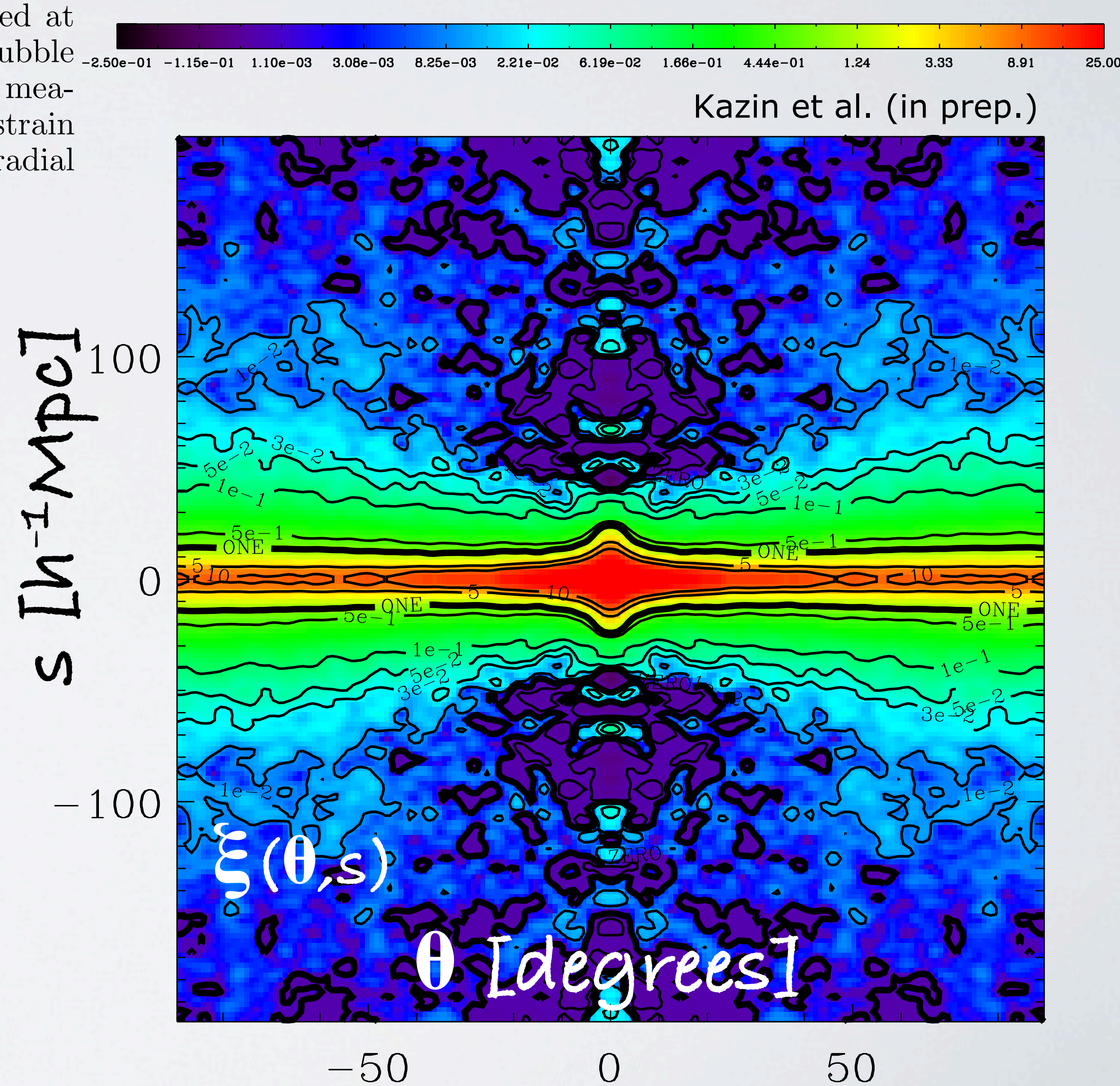

Baryonic Acoustic Feature in SDSS LRGs
Line of Sight Detection?

From Gaztañaga et al. (2008)

ABSTRACT

We study the clustering of LRG galaxies in the latest spectroscopic SDSS data releases, DR6 and DR7, which sample over 1 $\mathrm{Gpc}^3/\mathrm{h}^3$ to z=0.47. The 2-point correlation function $\xi(\sigma, \pi)$ is estimated as a function of perpendicular σ and line-of-sight π (radial) directions. We find a significant detection of a peak at $r \simeq 110$Mpc/h, which shows as a circular ring in the $\sigma - \pi$ plane. There is also significant evidence for a peak along the radial direction whose shape is consistent with its originating from the recombination-epoch baryon acoustic oscillations (BAO). A $\xi(\sigma, \pi)$ model with no radial BAO peak is disfavored at 3.2σ, whereas a model with no magnification bias is disfavored at 2σ. The radial data enable, for the first time, a direct measurement of the Hubble parameter $H(z)$ as a function of redshift. This is independent from earlier BAO measurements which used the spherically averaged (monopole) correlation to constrain an integral of $H(z)$. Using the BAO peak position as a standard ruler in the radial

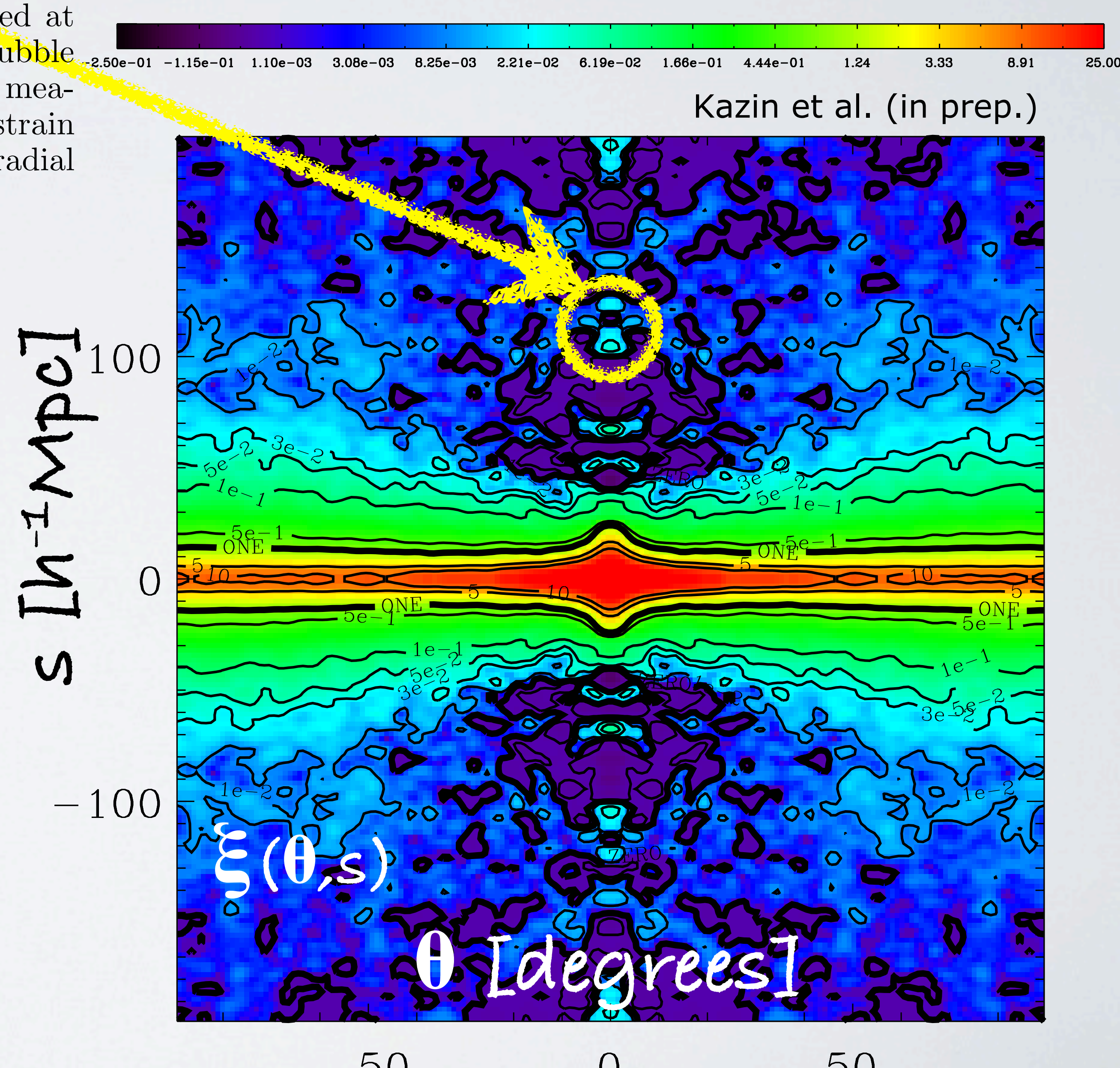

Kazin et al. (in prep.)

Baryonic Acoustic Feature in SDSS LRGs
Line of Sight Detection?

From Gaztañaga et al. (2008)

ABSTRACT
We study the clustering of LRG galaxies in the latest spectroscopic SDSS data releases, DR6 and DR7, which sample over 1 $\mathrm{Gpc}^3/\mathrm{h}^3$ to z=0.47. The 2-point correlation function $\xi(\sigma, \pi)$ is estimated as a function of perpendicular σ and line-of-sight π (radial) directions. We find a significant detection of a peak at $r \simeq 110$Mpc/h, which shows as a circular ring in the $\sigma - \pi$ plane. There is also significant evidence for a peak along the radial direction whose shape is consistent with its originating from the recombination-epoch baryon acoustic oscillations (BAO). A $\xi(\sigma, \pi)$ model with no radial BAO peak is disfavored at 3.2σ, whereas a model with no magnification bias is disfavored at 2σ. The radial data enable, for the first time, a direct measurement of the Hubble parameter $H(z)$ as a function of redshift. This is independent from earlier BAO measurements which used the spherically averaged (monopole) correlation to constrain an integral of $H(z)$. Using the BAO peak position as a standard ruler in the radial

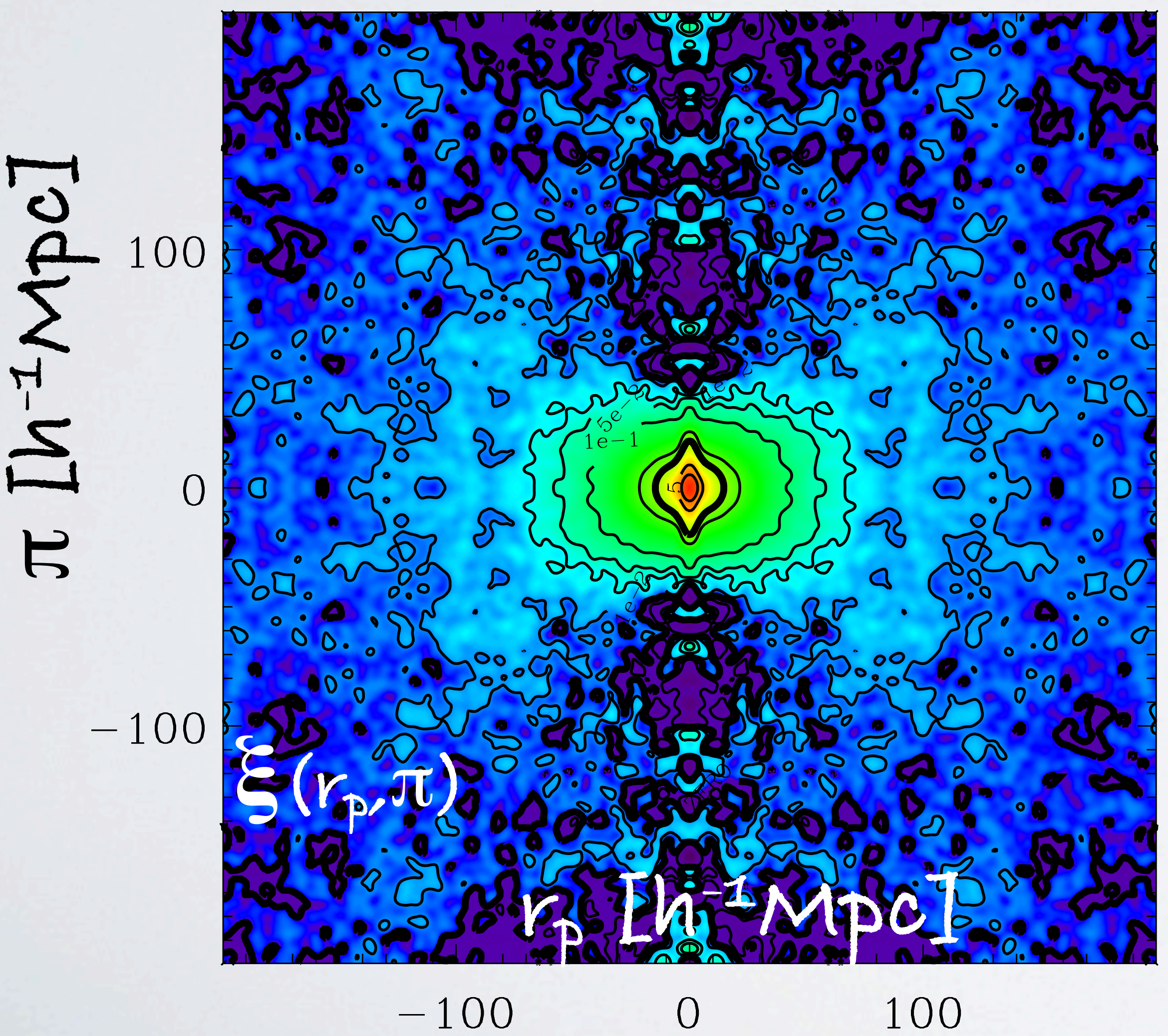

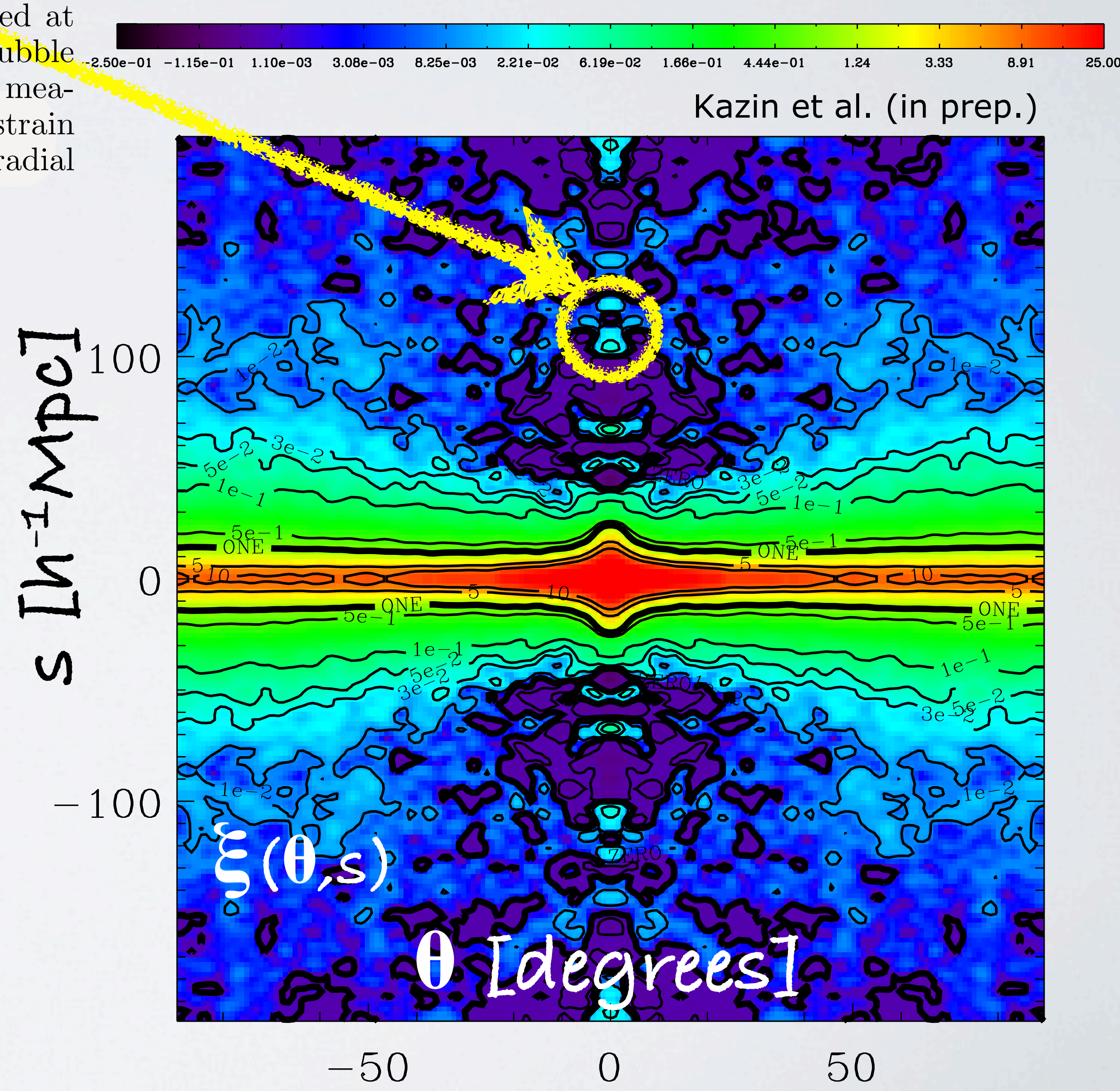

Baryonic Acoustic Feature in SDSS LRGs
Line of Sight Detection?

From Gaztañaga et al. (2008)

ABSTRACT

We study the clustering of LRG galaxies in the latest spectroscopic SDSS data releases, DR6 and DR7, which sample over 1 Gpc^3/h^3 to z=0.47. The 2-point correlation function $\xi(\sigma, \pi)$ is estimated as a function of perpendicular σ and line-of-sight π (radial) directions. We find a significant detection of a peak at $r \simeq 110$Mpc/h, which shows as a circular ring in the $\sigma - \pi$ plane. There is also significant evidence for a peak along the radial direction whose shape is consistent with its originating from the recombination-epoch baryon acoustic oscillations (BAO). A $\xi(\sigma, \pi)$ model with no radial BAO peak is disfavored at 3.2σ, whereas a model with no magnification bias is disfavored at 2σ. The radial data enable, for the first time, a direct measurement of the Hubble parameter $H(z)$ as a function of redshift. This is independent from earlier BAO measurements which used the spherically averaged (monopole) correlation to constrain an integral of $H(z)$. Using the BAO peak position as a standard ruler in the radial

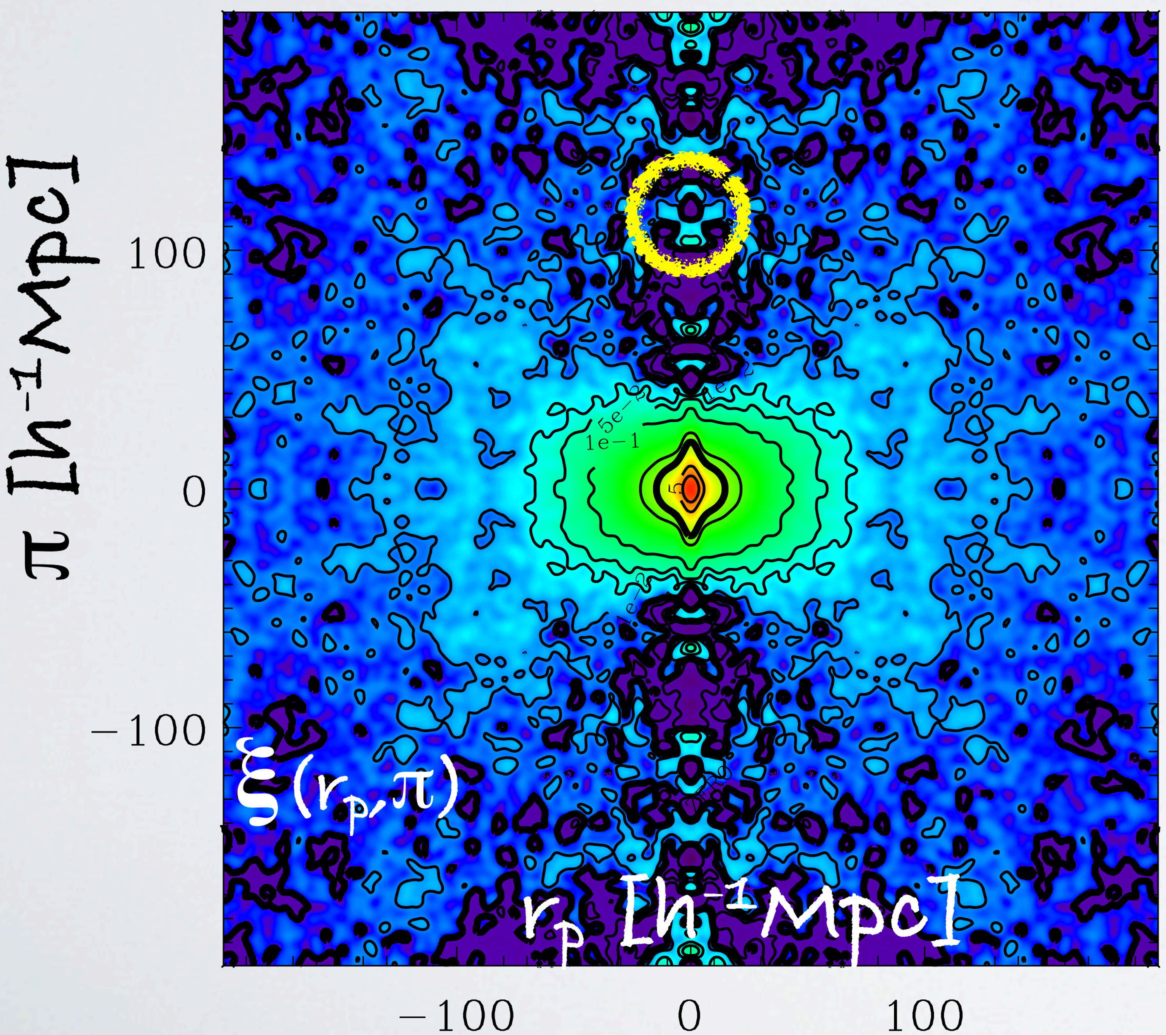

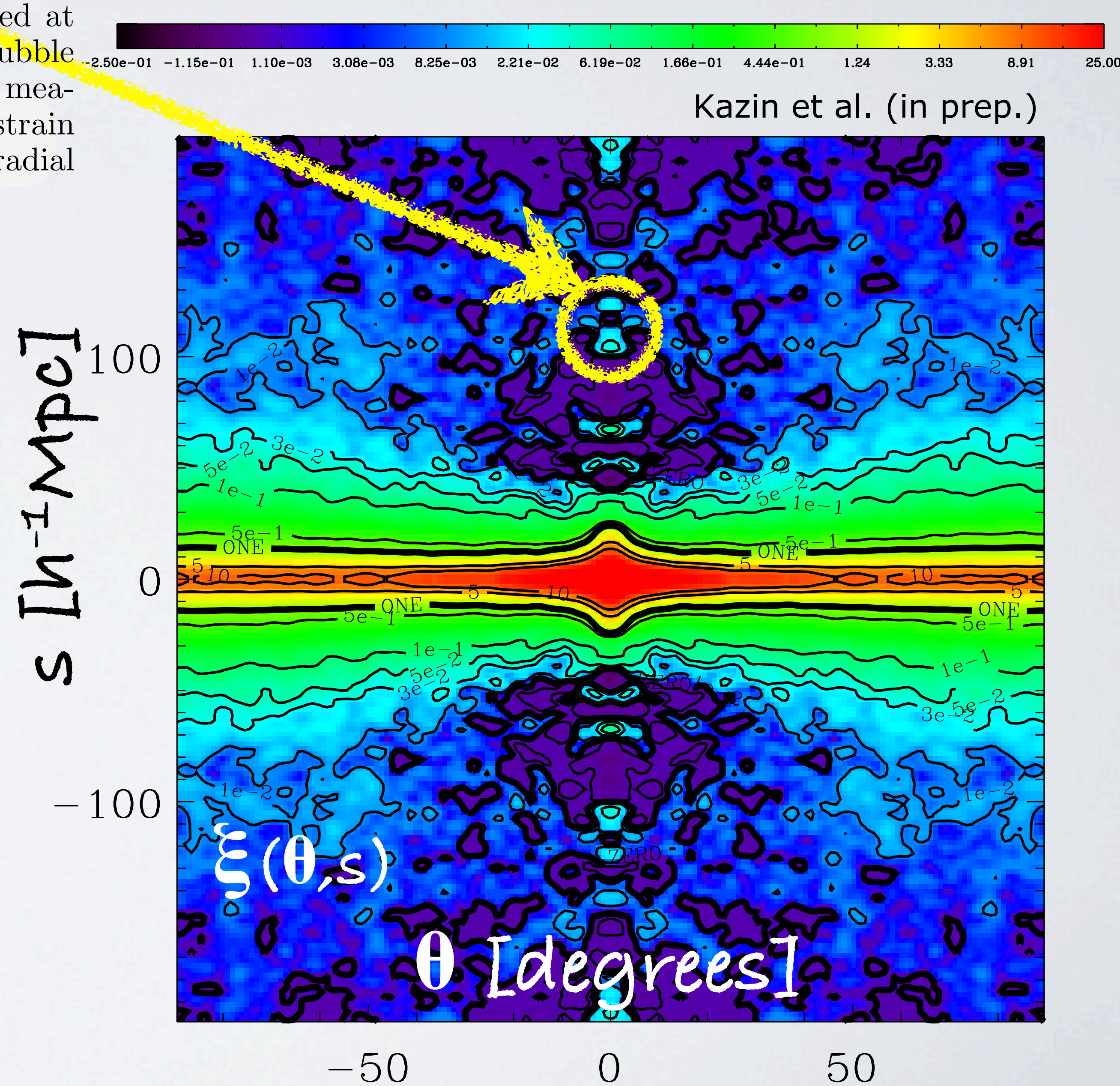

Kazin et al. (in prep.)

Baryonic Acoustic Feature in SDSS LRGs Line of Sight Detection?

From Gaztañaga et al. (2008)

ABSTRACT

We study the clustering of LRG galaxies in the latest spectroscopic SDSS data releases, DR6 and DR7, which sample over 1 $\mathrm{Gpc}^3/\mathrm{h}^3$ to z=0.47. The 2-point correlation function $\xi(\sigma, \pi)$ is estimated as a function of perpendicular σ and line-of-sight π (radial) directions. We find a significant detection of a peak at $r \simeq 110\mathrm{Mpc/h}$, which shows as a circular ring in the $\sigma - \pi$ plane. There is also significant evidence for a peak along the radial direction whose shape is consistent with its originating from the recombination-epoch baryon acoustic oscillations (BAO). A $\xi(\sigma, \pi)$ model with no radial BAO peak is disfavored at 3.2σ, whereas a model with no magnification bias is disfavored at 2σ. The radial data enable, for the first time, a direct measurement of the Hubble parameter $H(z)$ as a function of redshift. This is independent from earlier BAO measurements which used the spherically averaged (monopole) correlation to constrain an integral of $H(z)$. Using the BAO peak position as a standard ruler in the radial

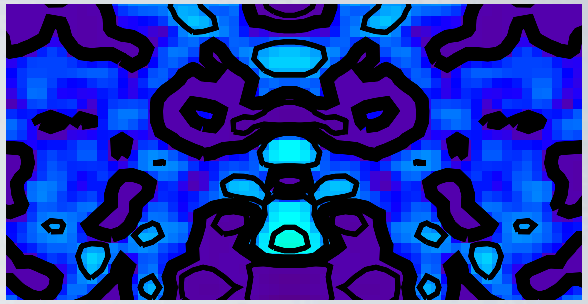

Full LRG sample

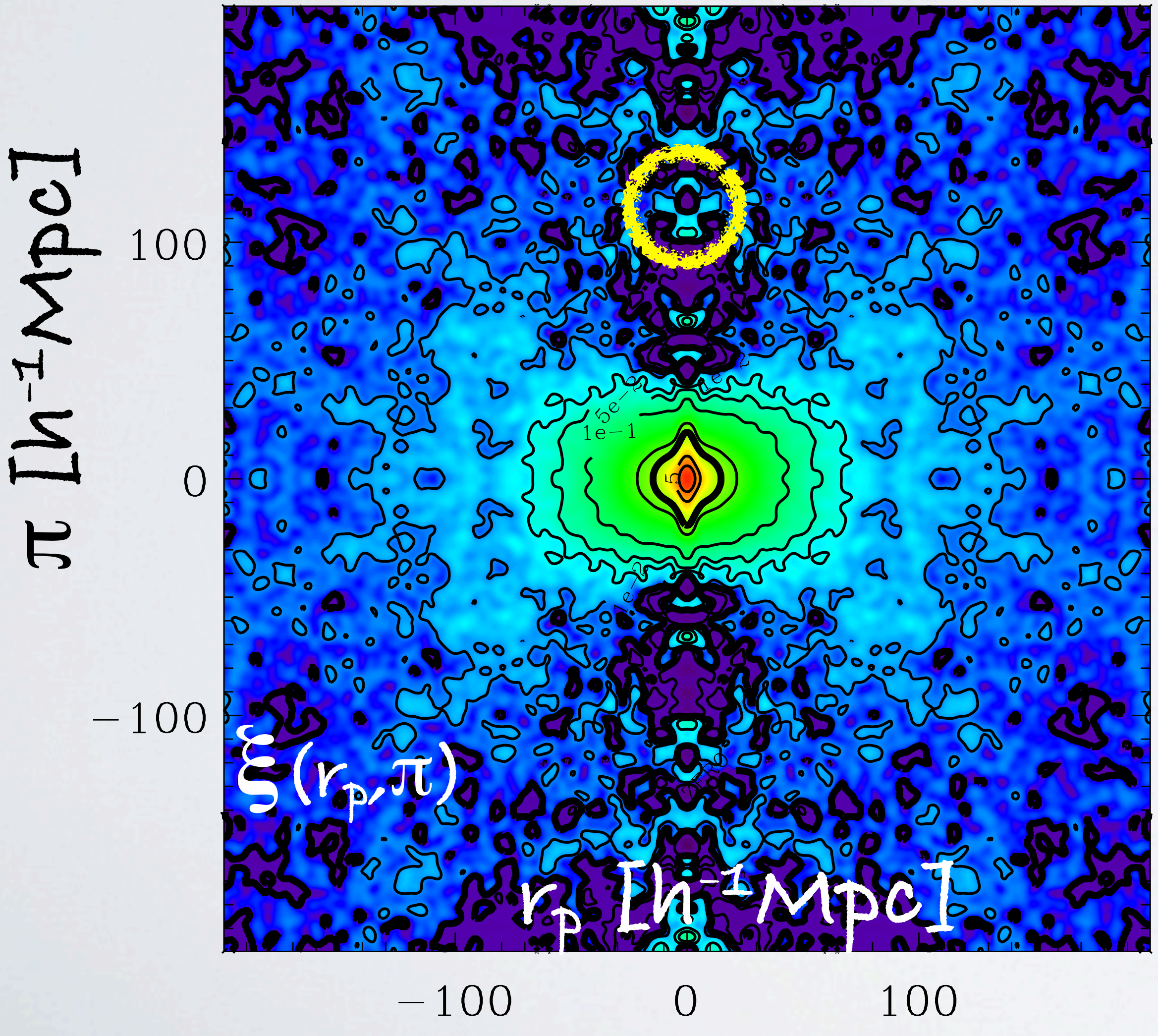

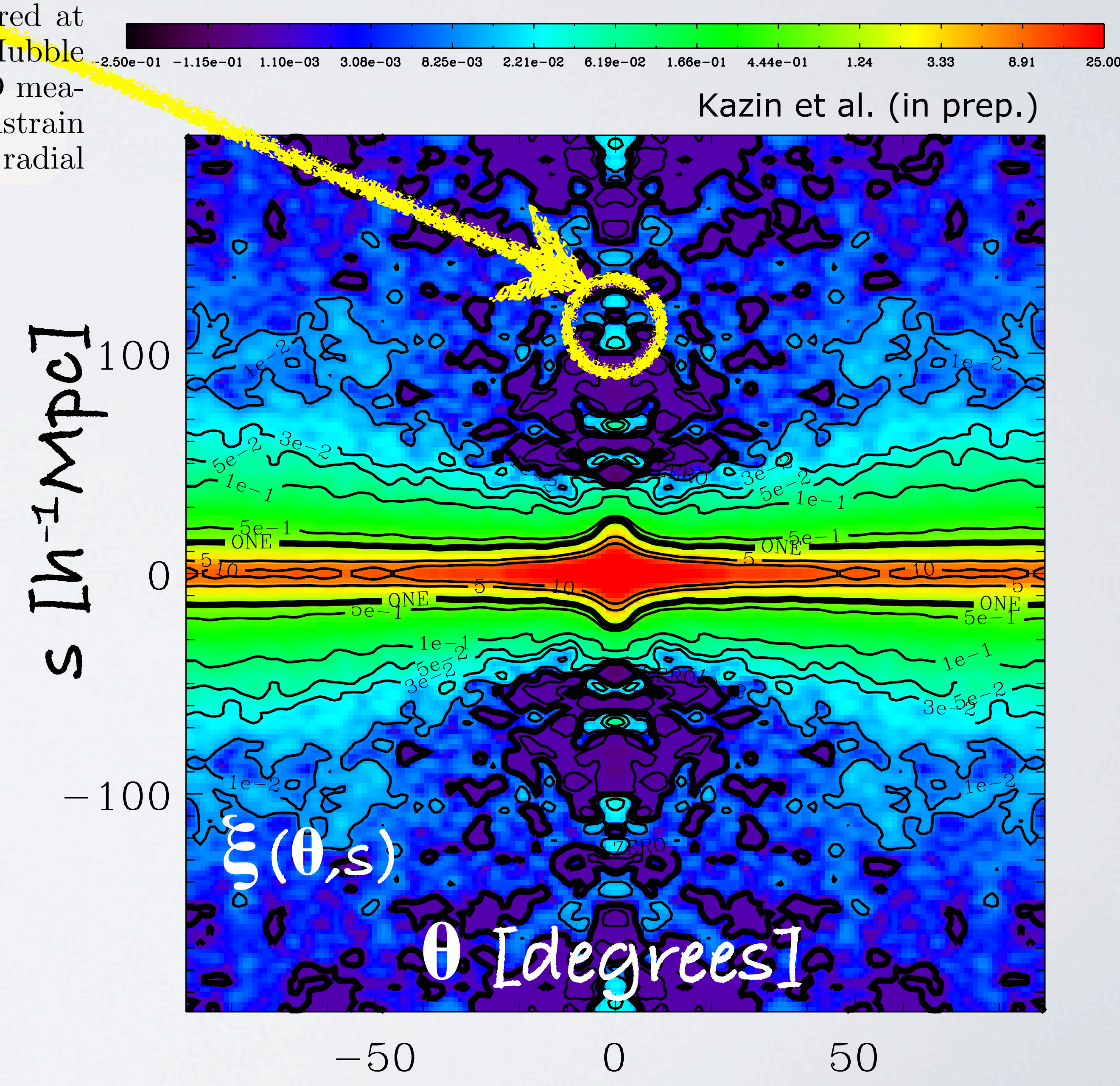

Baryonic Acoustic Feature in SDSS LRGs
Line of Sight Detection?

From Gaztañaga et al. (2008)

ABSTRACT
We study the clustering of LRG galaxies in the latest spectroscopic SDSS data releases, DR6 and DR7, which sample over 1 Gpc^3/h^3 to z=0.47. The 2-point correlation function $\xi(\sigma,\pi)$ is estimated as a function of perpendicular σ and line-of-sight π (radial) directions. We find a significant detection of a peak at $r \simeq 110$Mpc/h, which shows as a circular ring in the $\sigma-\pi$ plane. There is also significant evidence for a peak along the radial direction whose shape is consistent with its originating from the recombination-epoch baryon acoustic oscillations (BAO). A $\xi(\sigma,\pi)$ model with no radial BAO peak is disfavored at 3.2σ, whereas a model with no magnification bias is disfavored at 2σ. The radial data enable, for the first time, a direct measurement of the Hubble parameter $H(z)$ as a function of redshift. This is independent from earlier BAO measurements which used the spherically averaged (monopole) correlation to constrain an integral of $H(z)$. Using the BAO peak position as a standard ruler in the radial

Volume Limited sample

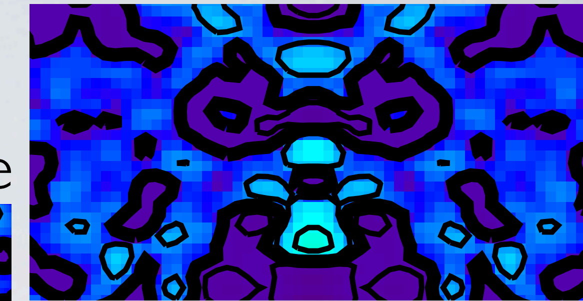

Full LRG sample

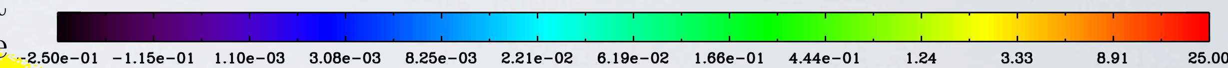

Kazin et al. (in prep.)

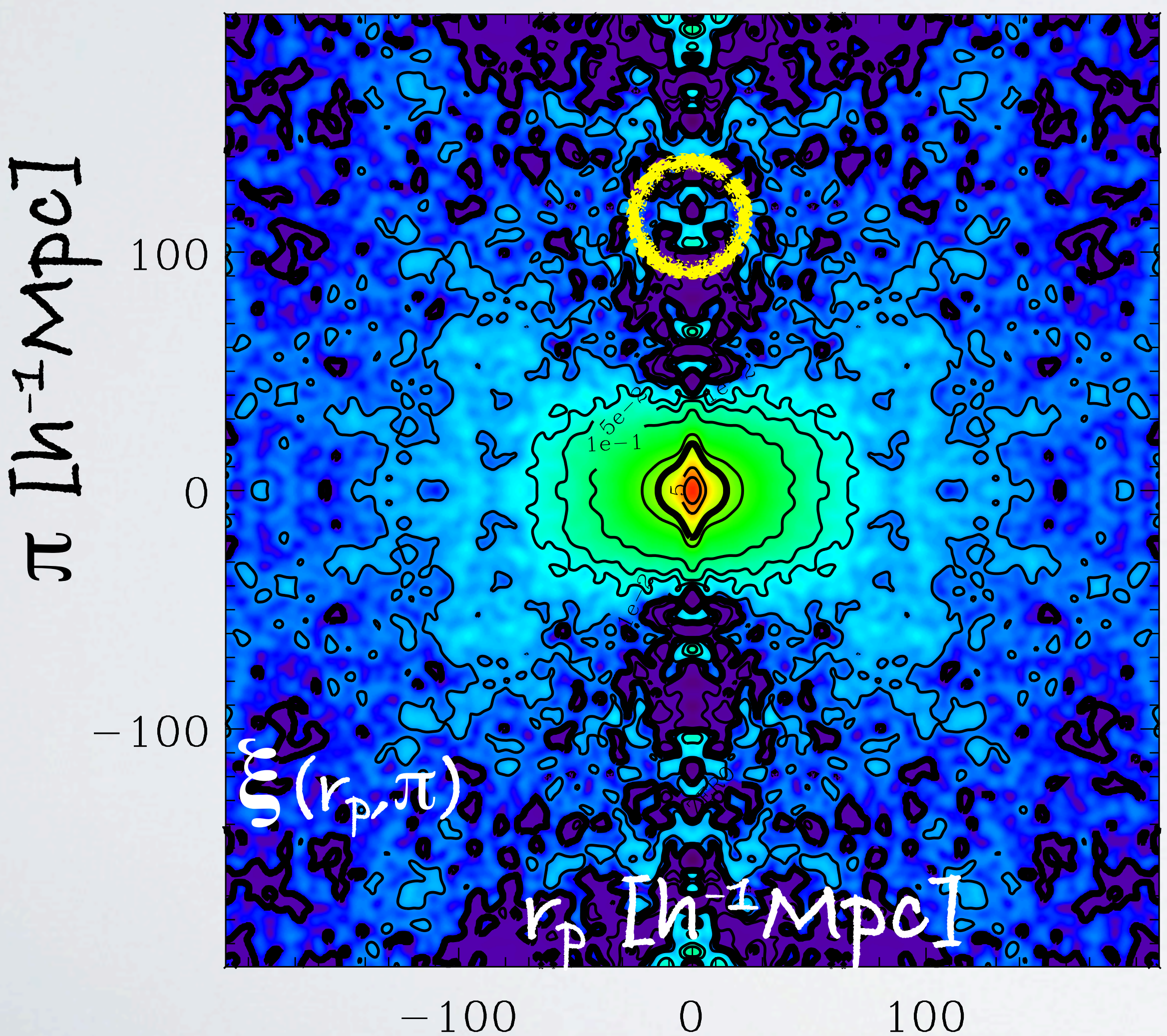

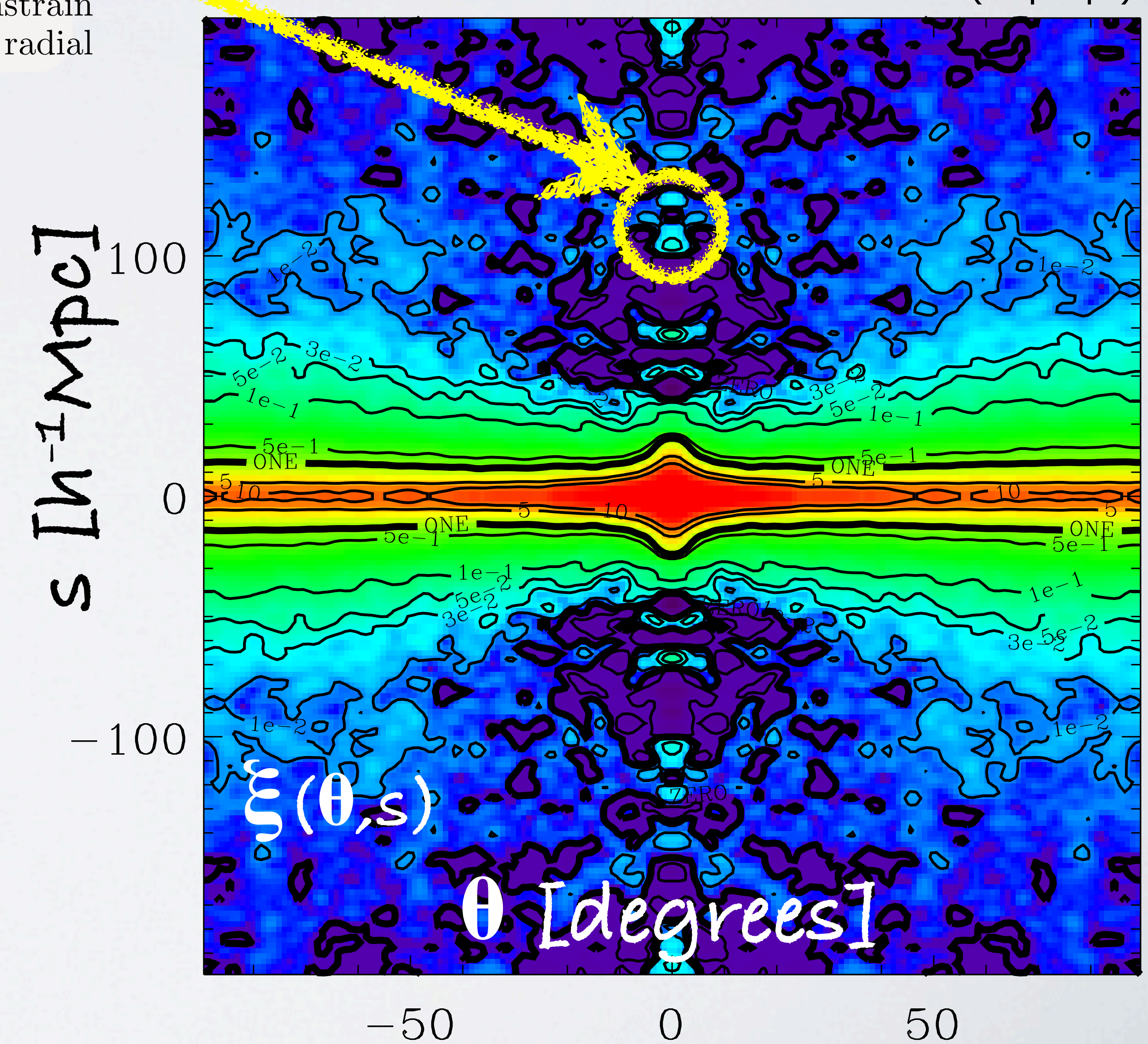

Baryonic Acoustic Feature in SDSS LRGs
Line of Sight Detection?

$\xi(\theta<3°, s)$ Volume Limited sample

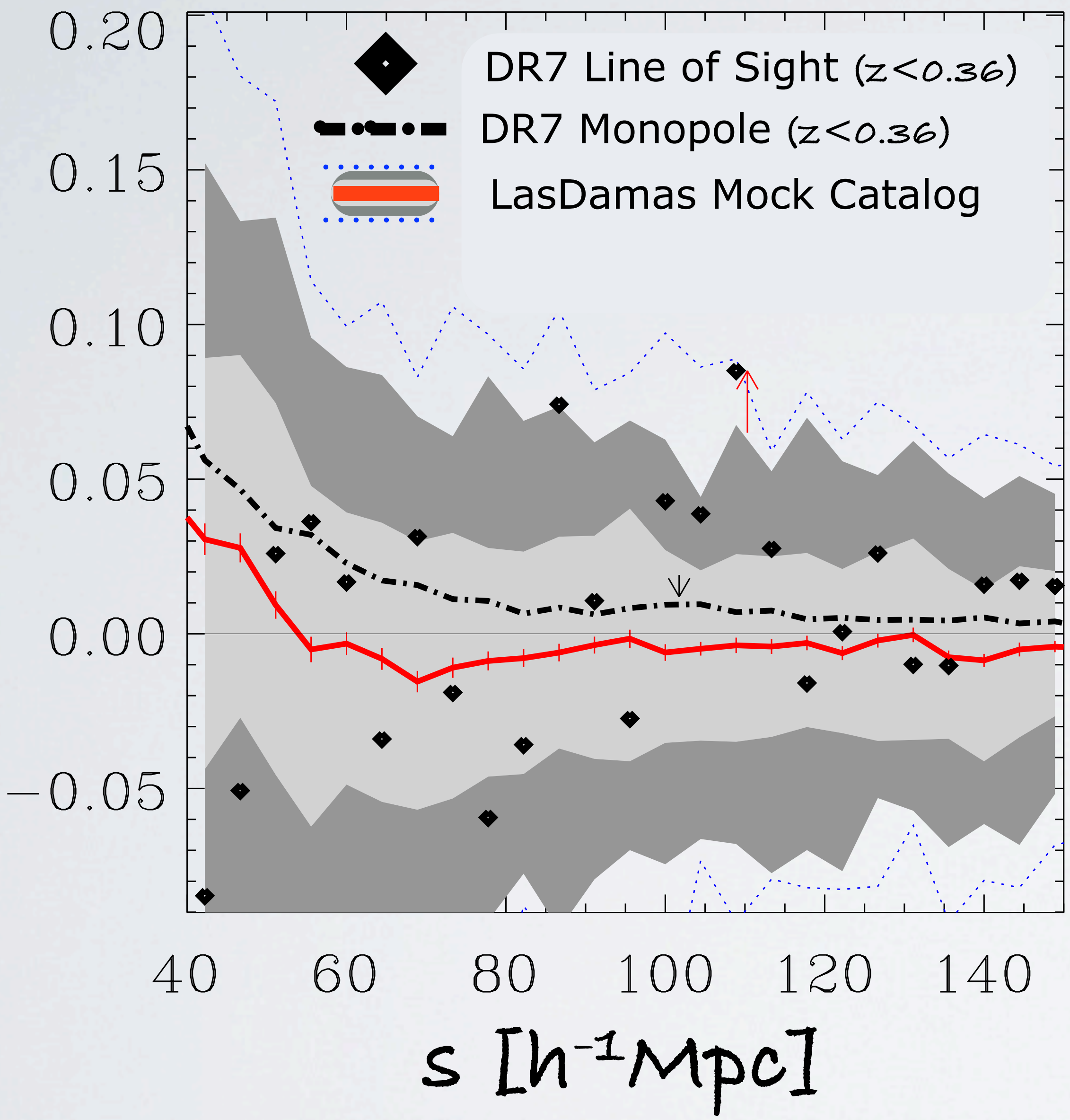

Baryonic Acoustic Feature in SDSS LRGs
Line of Sight Detection?

$\xi(\theta<3^\circ, s)$ Volume Limited sample

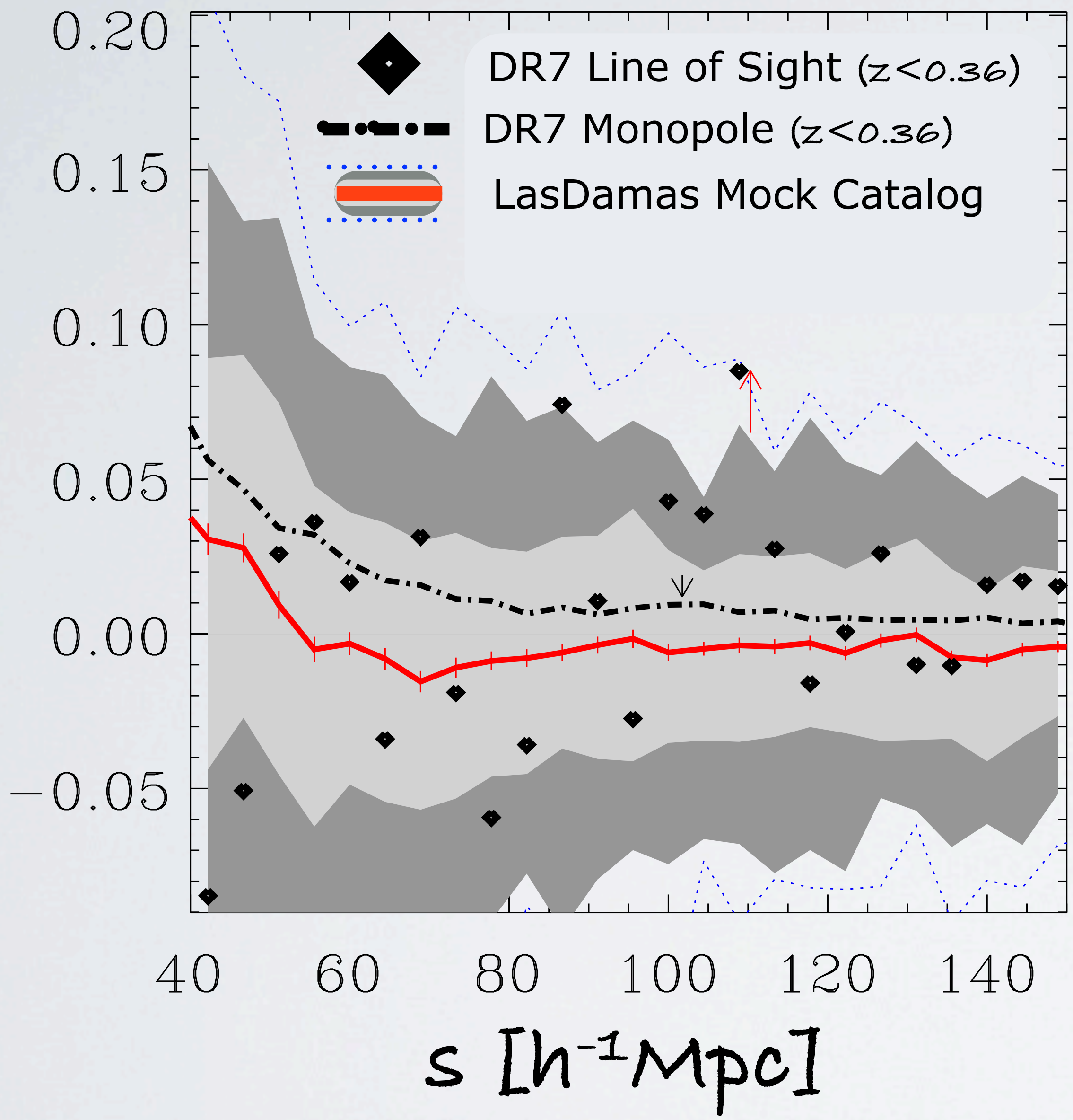

- SDSS-II does not contain enough modes to measure the line of sight BA feature at $\theta<3^\circ$
- The strong signal at 110 h^{-1}Mpc, although unlikely, is consistent with being noise

Baryonic Acoustic Feature in BOSS LRGs in Line of Sight and Transverse Directions

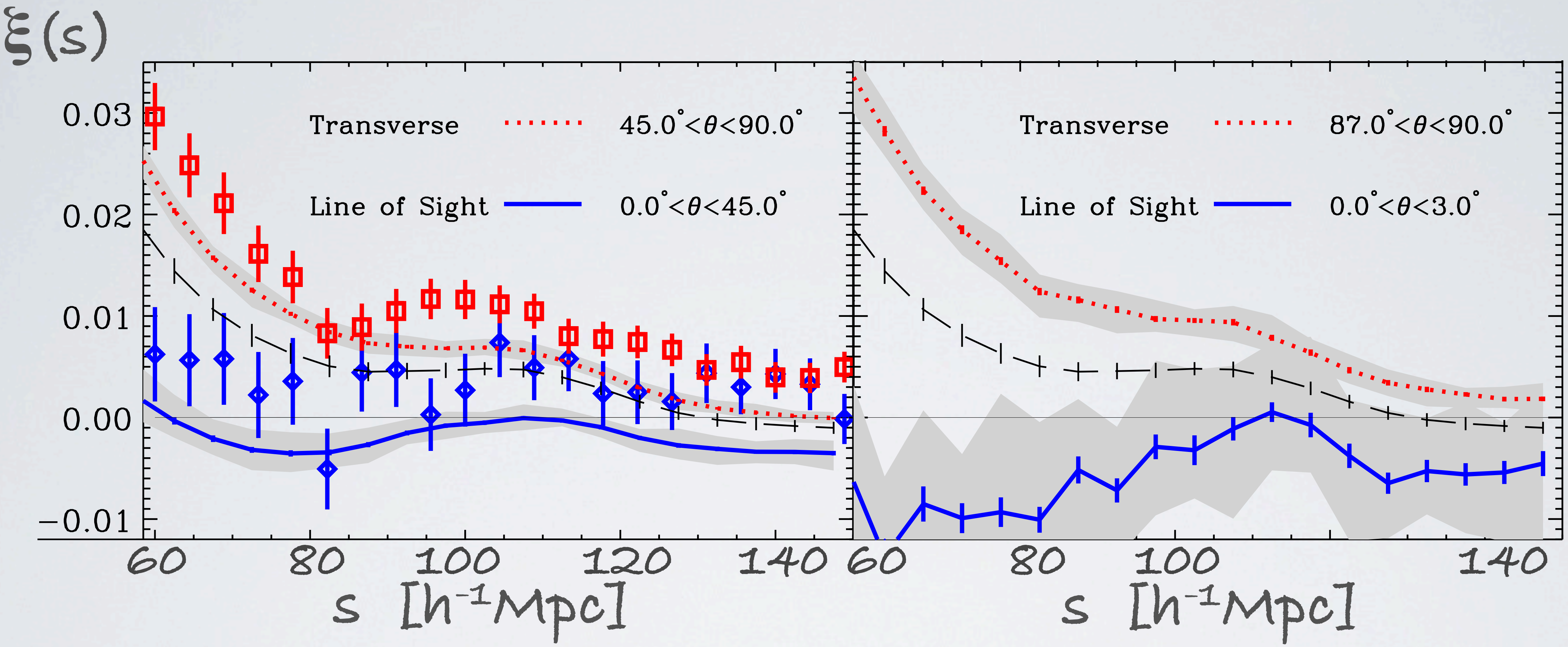

Baryonic Acoustic Feature in BOSS LRGs in Line of Sight and Transverse Directions

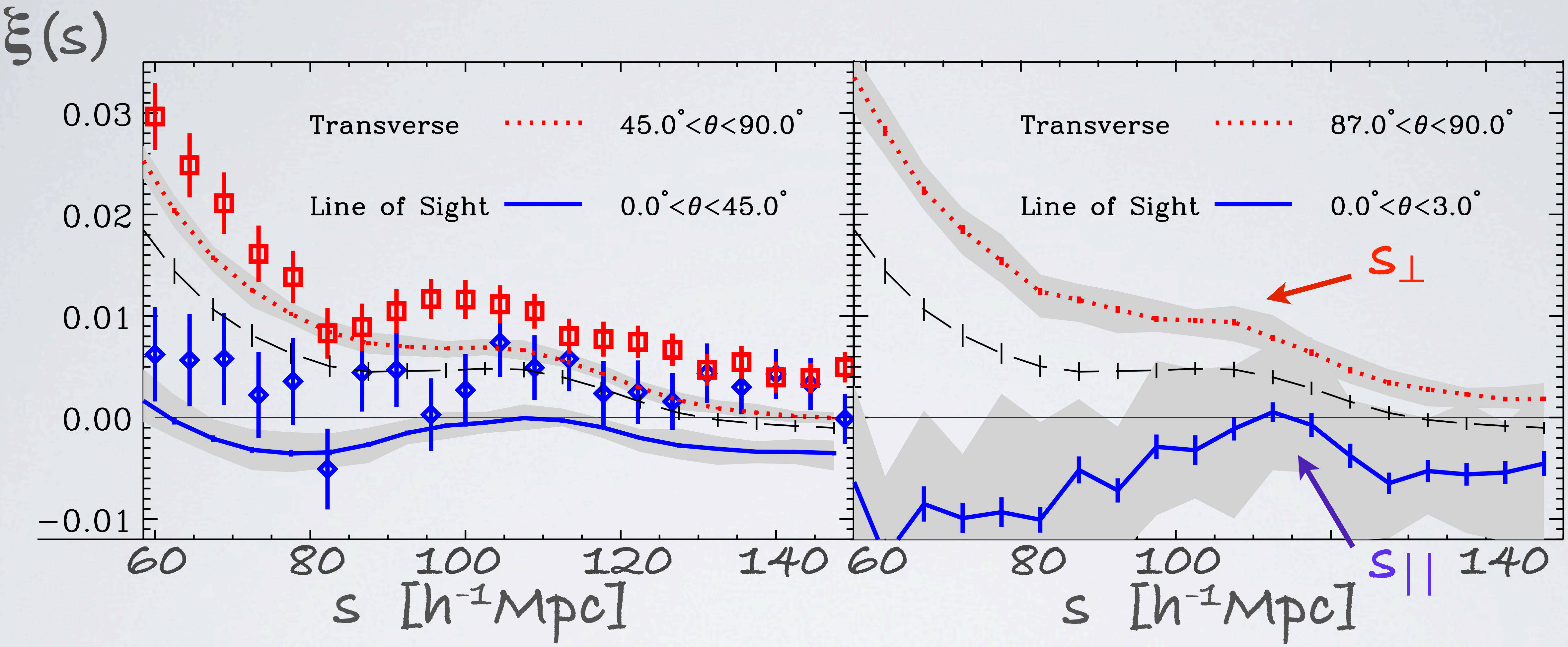

$$\int dz'/H(z') = s_\perp / \Delta\alpha / c$$
$$H(\langle z \rangle) \sim c\Delta z / s_{||}$$

Baryonic Acoustic Feature in BOSS LRGs in Line of Sight and Transverse Directions

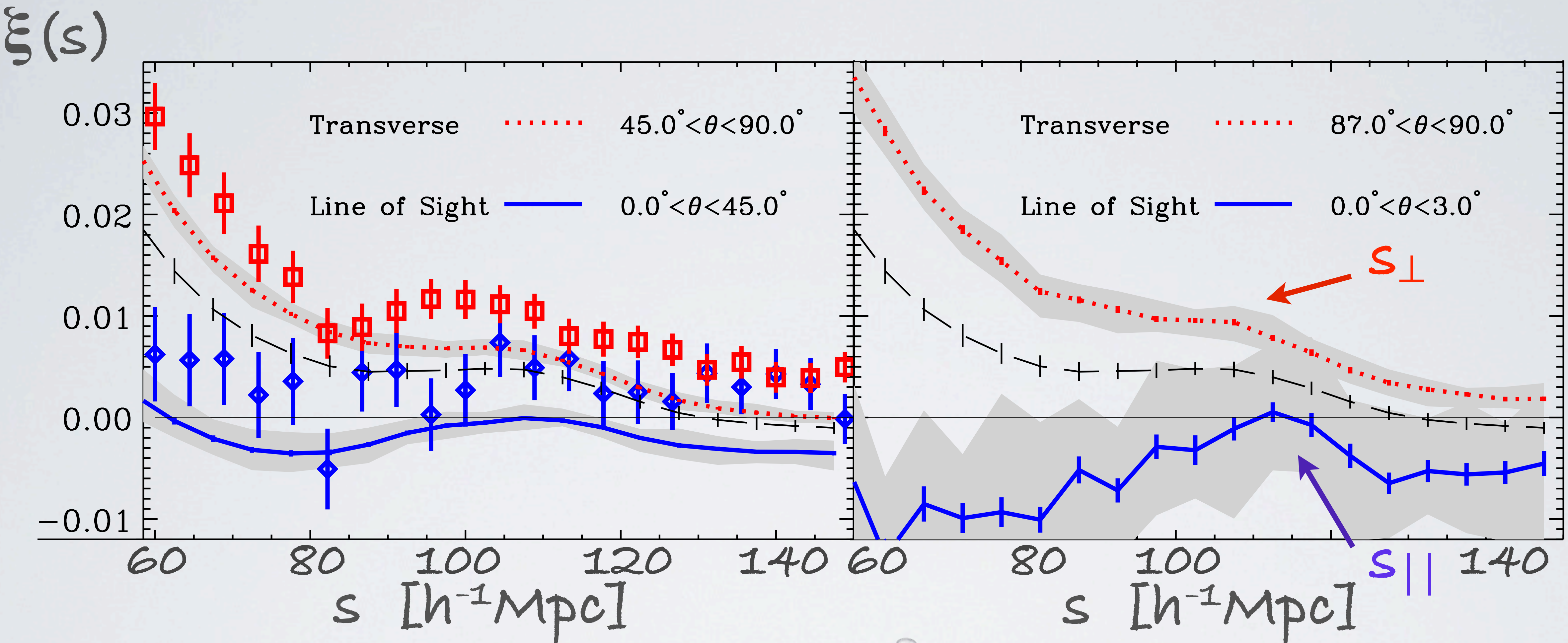

- The strong SDSS-II signal at 110 h^{-1}Mpc is predicted to be ruled out by BOSS
- BOSS *does contain* enough modes to measure the line of sight BA feature, although for r_p<5.5 h^{-1}Mpc the signal is noisy.

$$\int dz'/H(z') = s_\perp / \Delta\alpha / c$$

$$H(\langle z \rangle) \sim c\Delta z / s_{||}$$

Baryonic Acoustic Feature in BOSS LRGs in Line of Sight and Transverse Directions

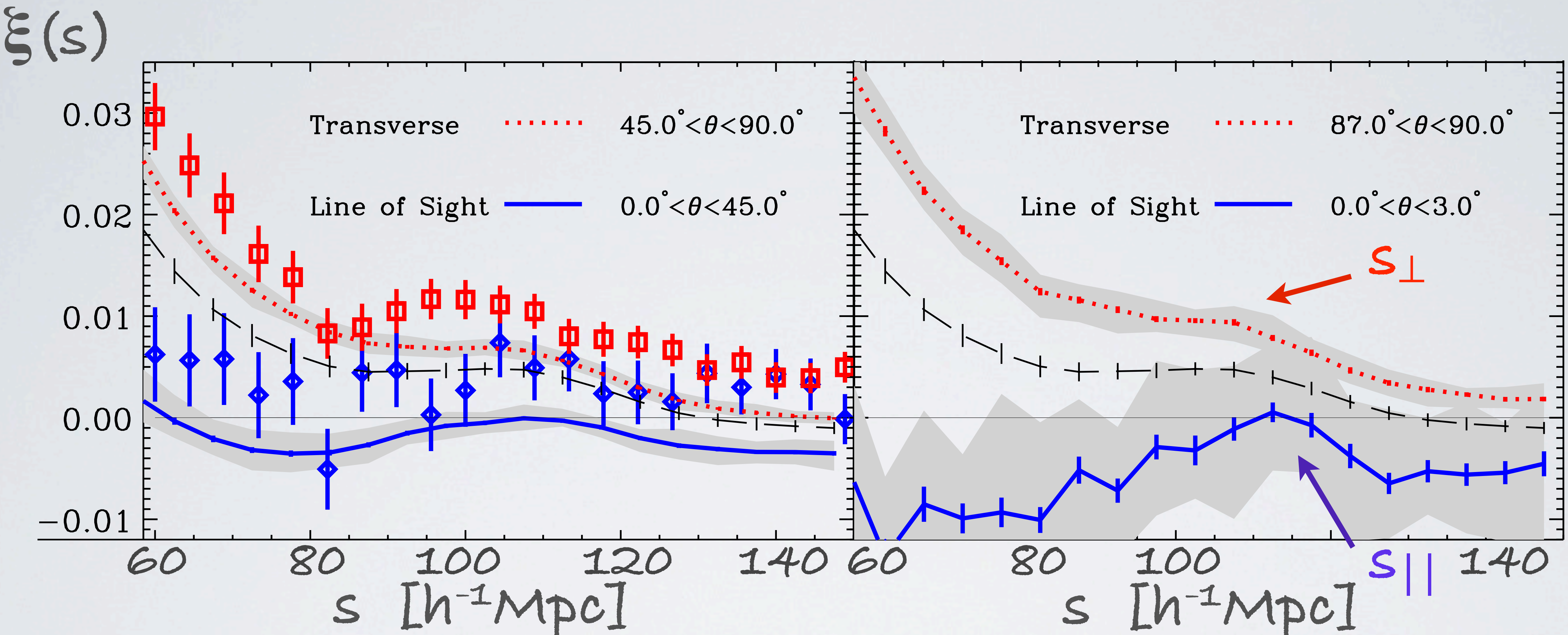

- The expected separation btw line-of-sight and transverse signals for large $\Delta\theta$ raise optimism for disentangling $H(\langle z\rangle)$ and $D_A(\langle z\rangle)$

- The strong SDSS-II signal at 110 h^{-1}Mpc is predicted to be ruled out by BOSS

- BOSS *does contain* enough modes to measure the line of sight BA feature, although for $r_p<5.5$ h^{-1}Mpc the signal is noisy.

$$\int dz'/H(z') = s_\perp / \Delta\alpha / c$$
$$H(\langle z\rangle) \sim c\Delta z / s_{||}$$

Baryonic Acoustic Feature in BOSS LRGs in Line of Sight and Transverse Directions

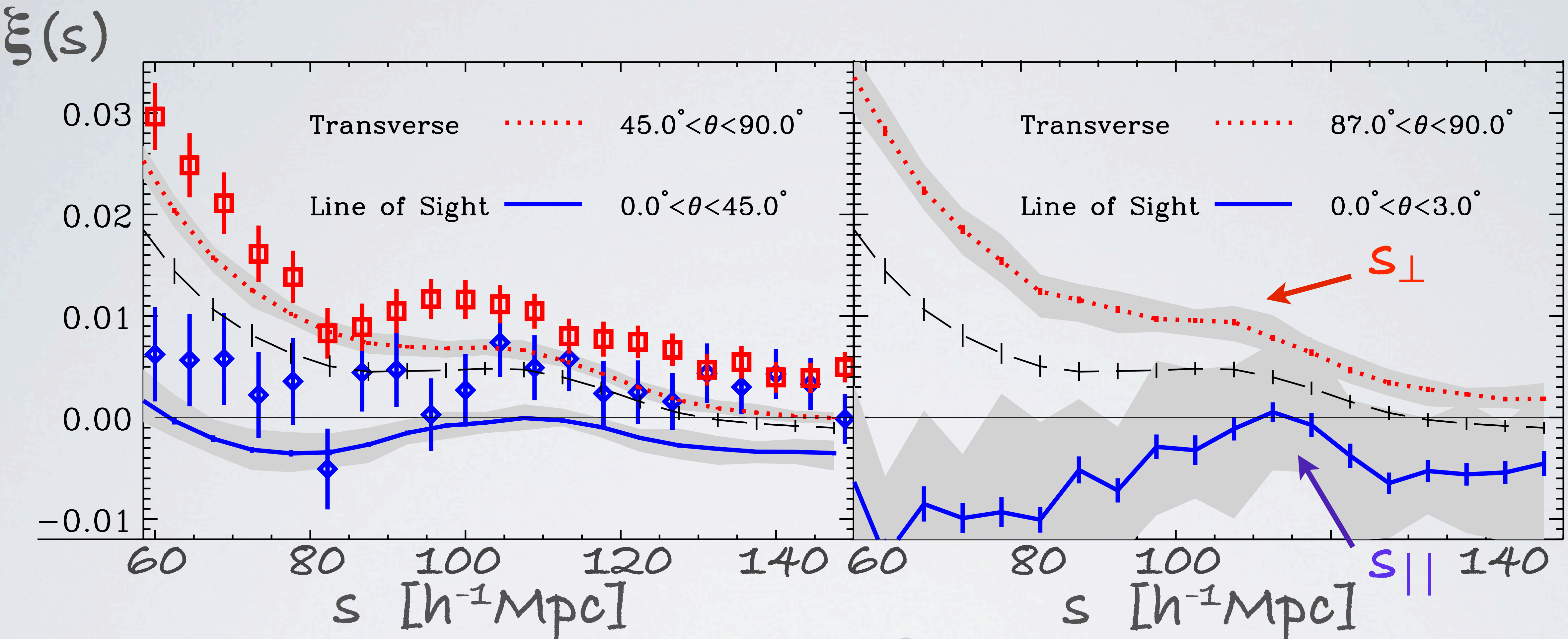

- The expected separation btw line-of-sight and transverse signals for large $\Delta\theta$ raise optimism for disentangling $H(\langle z\rangle)$ and $D_A(\langle z\rangle)$

- The strong SDSS-II signal at 110 h^{-1}Mpc is predicted to be ruled out by BOSS

- BOSS *does contain* enough modes to measure the line of sight BA feature, although for $r_p<5.5$ h^{-1}Mpc the signal is noisy.

$$\int dz'/H(z') = s_\perp / \Delta\alpha / c$$
$$H(\langle z\rangle) \sim c\Delta z / s_{||}$$

Kazin et al. coming very soon...

Today I will discuss:

- ☐ Introduction 13 minutes
  - ☑ Quantifying Clustering
  - ☑ LRGs- Why (should) we like these galaxies so much?
  - ☑ The Sloan Digital Sky Survey
- ☑ Baryonic Acoustic Feature 30 minutes
- ☐ Introduction to Redshift Distortions 2 minutes
- ☐ Redshift Distortions in Clustering 5 minutes

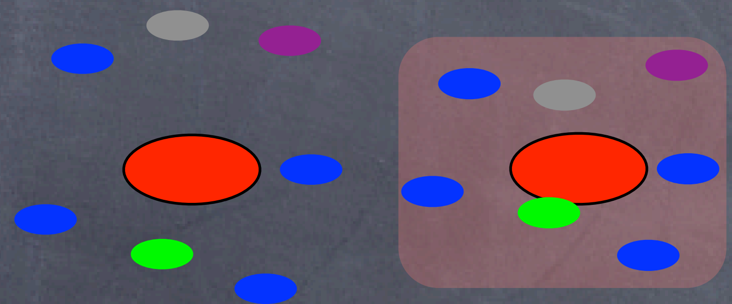

Quantifying the Squashing Effect

Kaiser 1987: conservation of number of objects when going from real-space to z-space

$$n(s)\,d^3s = n(r)\,d^3r$$

where

$\mu \equiv \cos(\theta)$

$f \equiv d\ln(D_1)/d\ln(a)$

$$P^{(S)}(k,\mu) = (1 + f\mu^2)^2\, P(k)$$

z-space matter — real space matter

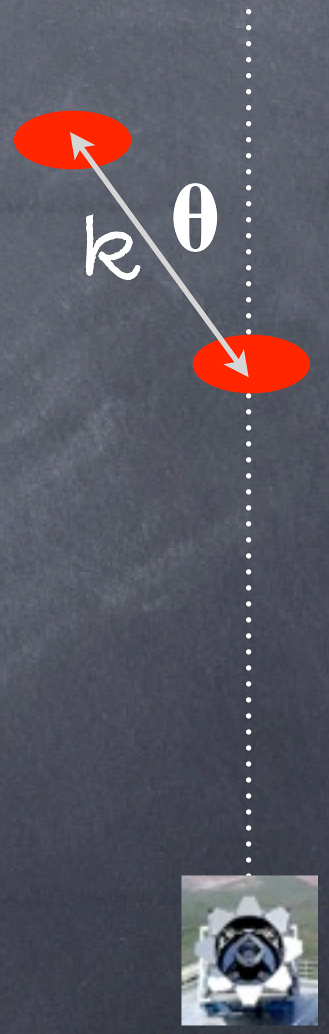

and

overdensity $\delta(a) \approx D_1 \delta_{initial}$ D_1 – linear growth factor

$a = 1/(1+z)$ expansion factor

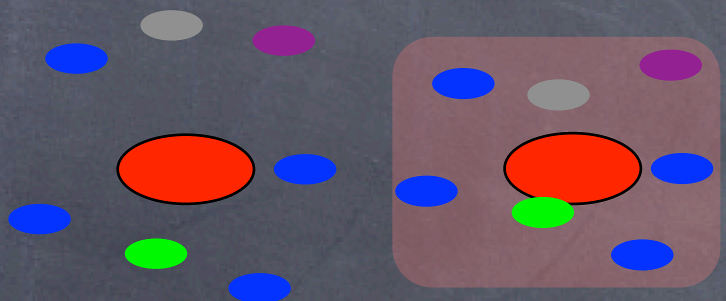

Quantifying the Squashing Effect

Kaiser 1987: conservation of number of objects when going from real-space to z-space

$$n(s)\,d^3s = n(r)\,d^3r$$

$$P^{(S)}(k,\mu) = (1 + f\mu^2)^2 P(k)$$

z-space matter — real space matter

where

$\mu \equiv \cos(\theta)$

$f \equiv d\ln(D_1)/d\ln(a)$

and

overdensity $\delta(a) \approx D_1 \delta_{initial}$ D_1–linear growth factor

$a = 1/(1+z)$ expansion factor

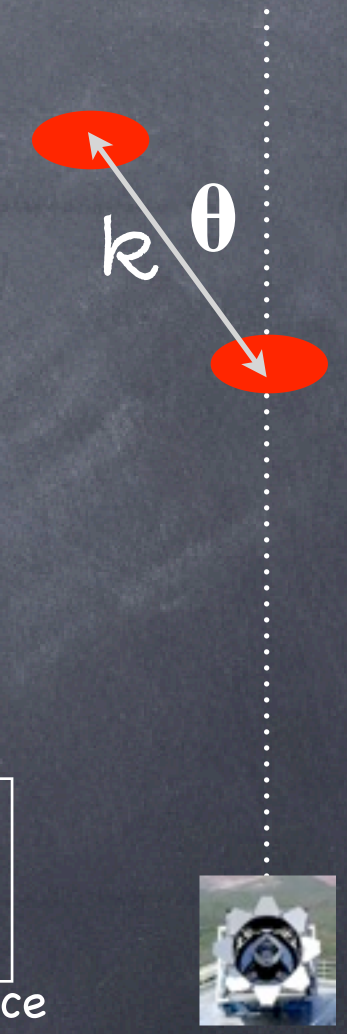

$$P^{(S)}_{gal}(k,\mu) = (1 + \beta\mu^2)^2 P_{gal}(k)$$

z-space tracer — real space tracer

$$= (b + f\mu^2)^2 P(k)$$

real space matter

$\beta \equiv f/b_1$

where

$\delta_{gal} \approx b_1 \delta$

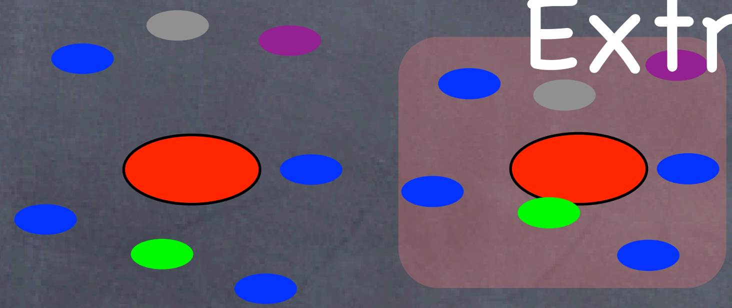

Extracting information from the Squashing Effect

growth index

ΛCDM: $\gamma \sim 0.56$

DGP: $\gamma \sim 0.68$

Kaiser 1987: $\beta \equiv f(z)/b_1 \approx \Omega_M^{\gamma}(z)/b_1$

So: $\beta \leftrightarrow \Omega_M$

Or: $\beta \leftrightarrow$ gravity (through γ; Linder 2005)

Or: $\beta \leftrightarrow$ break (bias)σ_8 degeneracy

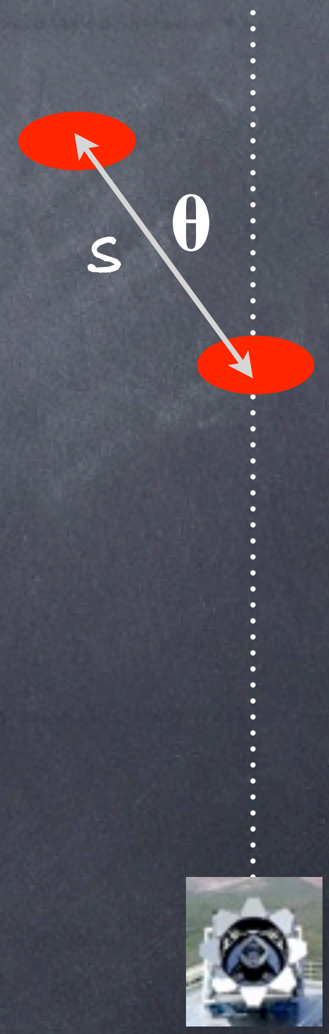

Extracting information from the Squashing Effect

Kaiser 1987: $\beta \equiv f(z)/b_1 \approx \Omega_M^{\gamma}(z)/b_1$

growth index

ΛCDM: $\gamma \sim 0.56$

DGP: $\gamma \sim 0.68$

So: $\beta \leftrightarrow \Omega_M$

Or: $\beta \leftrightarrow$ gravity (through γ; Linder 2005)

Or: $\beta \leftrightarrow$ break (bias) σ_8 degeneracy

Quadrupole Test: No dependence on scale!

quadrupole/monopole

$$Q \equiv P_2(k)/P_0(k) = (4/3\beta + 4/7\beta^2)/(1 + 2/3\beta + 1/5\beta^2)$$

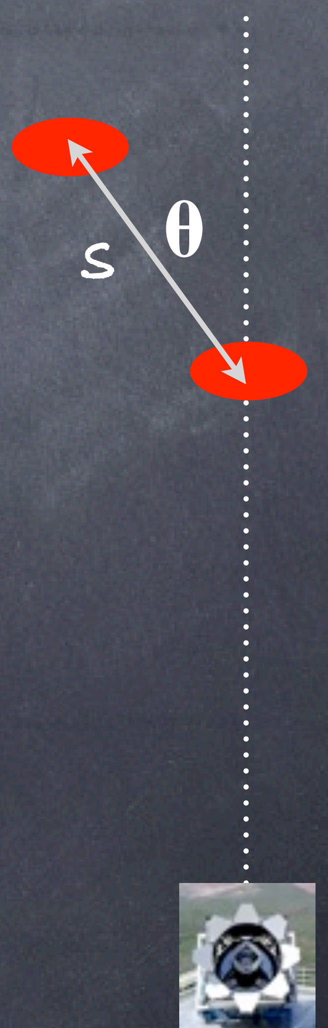

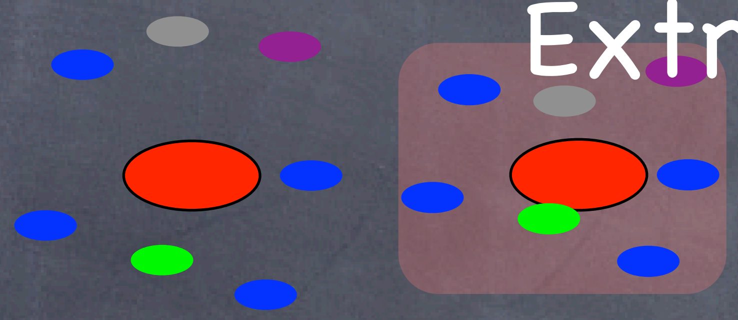

Extracting information from the Squashing Effect

growth index

Kaiser 1987: $\beta \equiv f(z)/b_1 \approx \Omega_M^{\gamma}(z)/b_1$

ΛCDM: $\gamma \sim 0.56$

DGP: $\gamma \sim 0.68$

So: $\beta \leftrightarrow \Omega_M$

Or: $\beta \leftrightarrow$ gravity (through γ; Linder 2005)

Or: $\beta \leftrightarrow$ break (bias) σ_8 degeneracy

Quadrupole Test: No dependence on scale!

quadrupole/monopole

$$Q \equiv P_2(k)/P_0(k) = (4/3\beta + 4/7\beta^2)/(1 + 2/3\beta + 1/5\beta^2)$$

In configuration space (Hamilton 1992):

$$Q = \xi_2(s)/[\xi_0(s) - \langle \xi_0(s) \rangle] = (4/3\beta + 4/7\beta^2)/(1 + 2/3\beta + 1/5\beta^2)$$

where $\xi_l(s) = (2l+1)/2 \int \xi(\mu', s)\, \mathcal{L}_l(\mu')\, d\mu'$

β through the Quadrupole Test
Non-Linear Theory

$$Q = \xi_2(s)/[\xi_0(s) - \langle \xi_0(s) \rangle] = (4/3\beta + 4/7\beta^2)/(1 + 2/3\beta + 1/5\beta^2)$$

$\xi(\theta, s)$

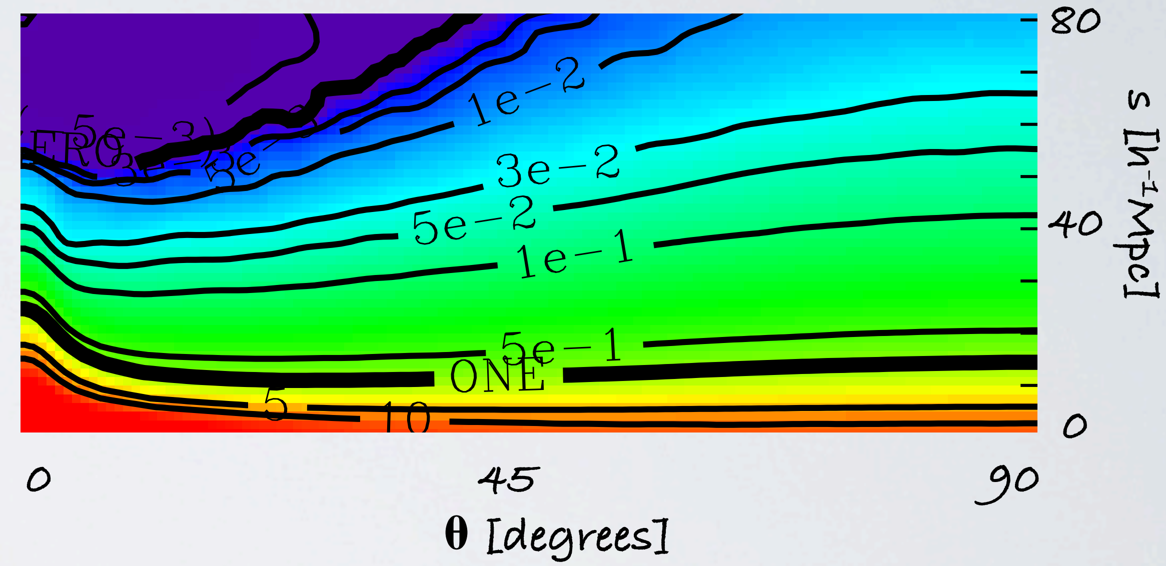

$$\beta \equiv f(z)/b_1 \approx \Omega_M^{\gamma}(z)/b_1$$

β through the Quadrupole Test
Non-Linear Theory

$$Q = \xi_2(s) / [\xi_0(s) - \langle \xi_0(s) \rangle] = (4/3\beta + 4/7\beta^2) / (1 + 2/3\beta + 1/5\beta^2)$$

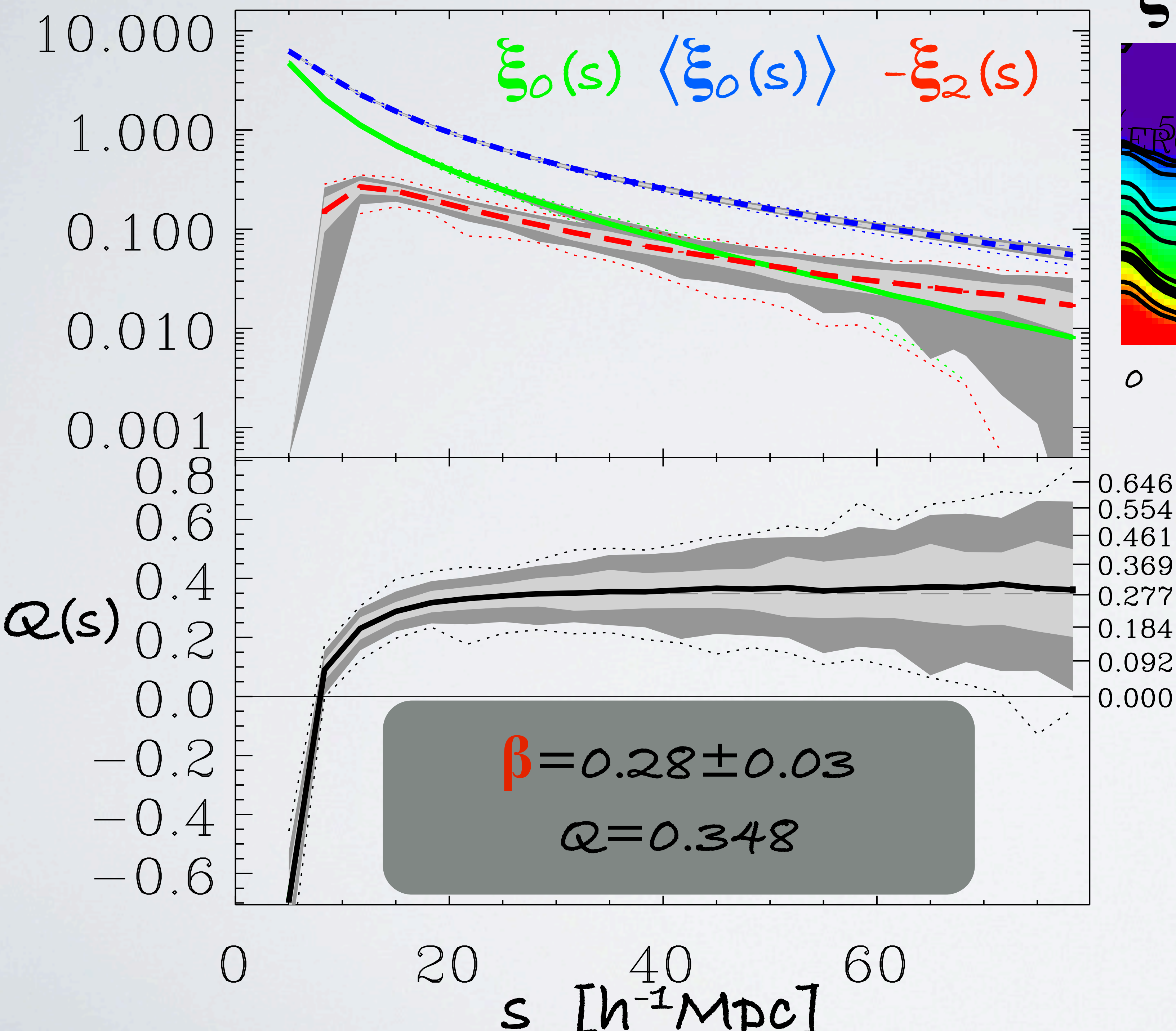

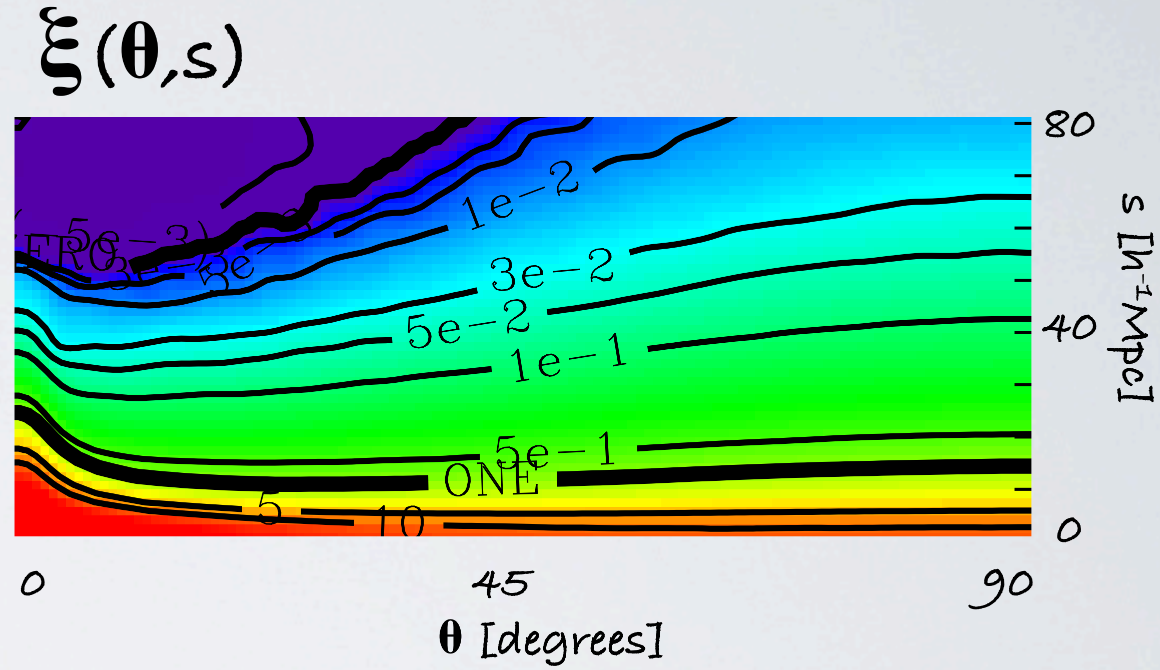

$$\beta \equiv f(z)/b_1 \approx \Omega_M^{\gamma}(z)/b_1$$

β through the Quadrupole Test
SDSS-II Results

$$Q = \xi_2(s) / [\xi_0(s) - \langle \xi_0(s) \rangle] = (4/3\beta + 4/7\beta^2)/(1 + 2/3\beta + 1/5\beta^2)$$

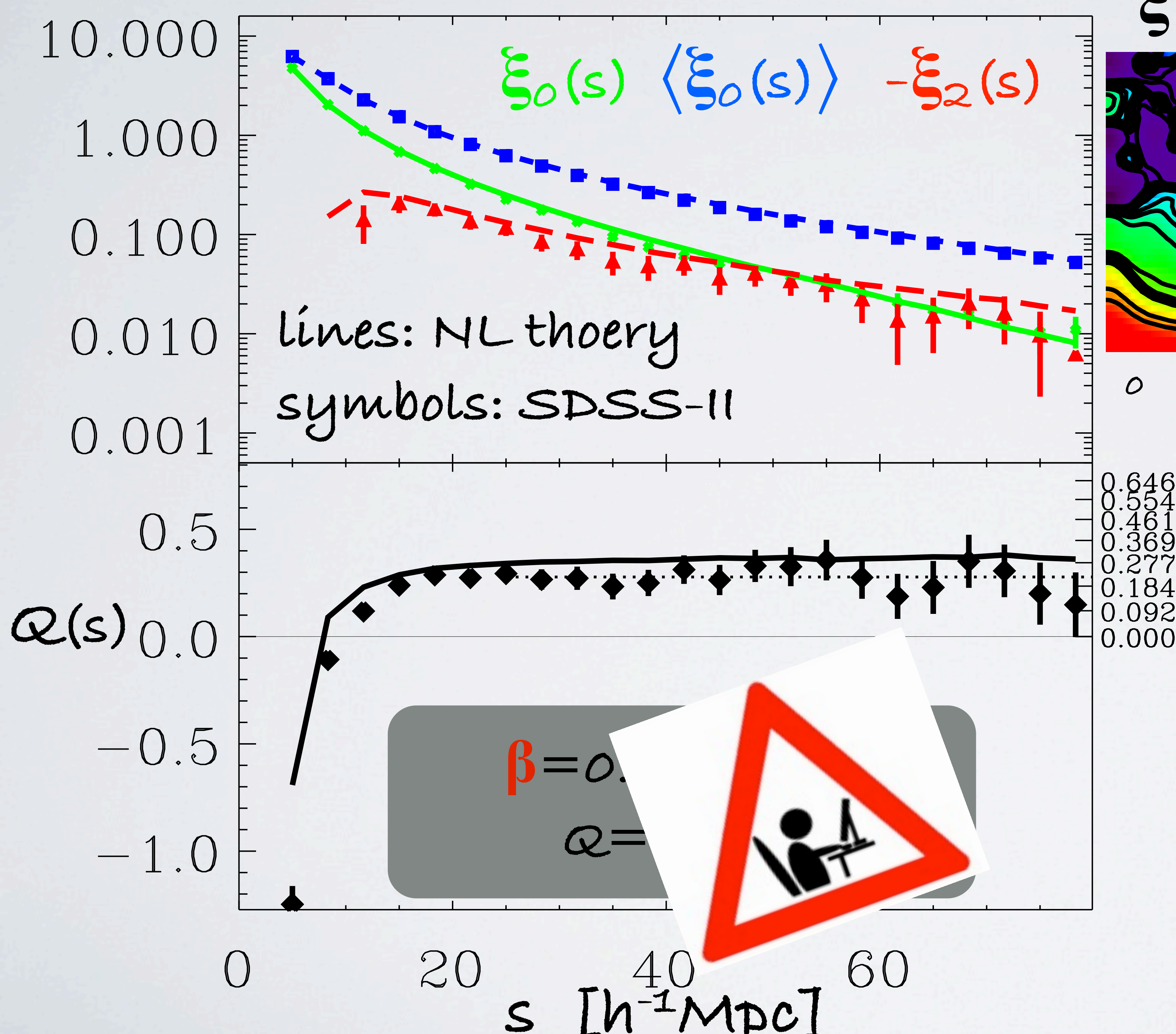

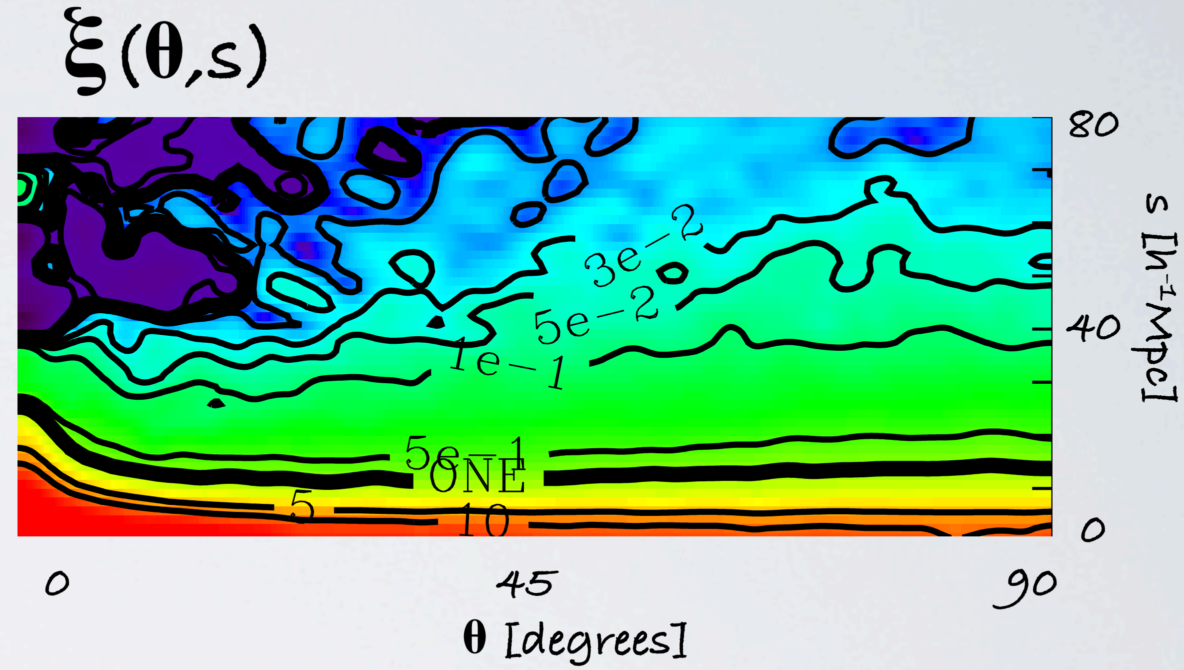

$$\beta \equiv f(z)/b_1 \approx \Omega_M^{\gamma}(z)/b_1$$

Quadrupole Test- Cosmological Significance

$$\beta \equiv f(z)/b_1 \approx \Omega_M^{\gamma}(z)/b_1$$

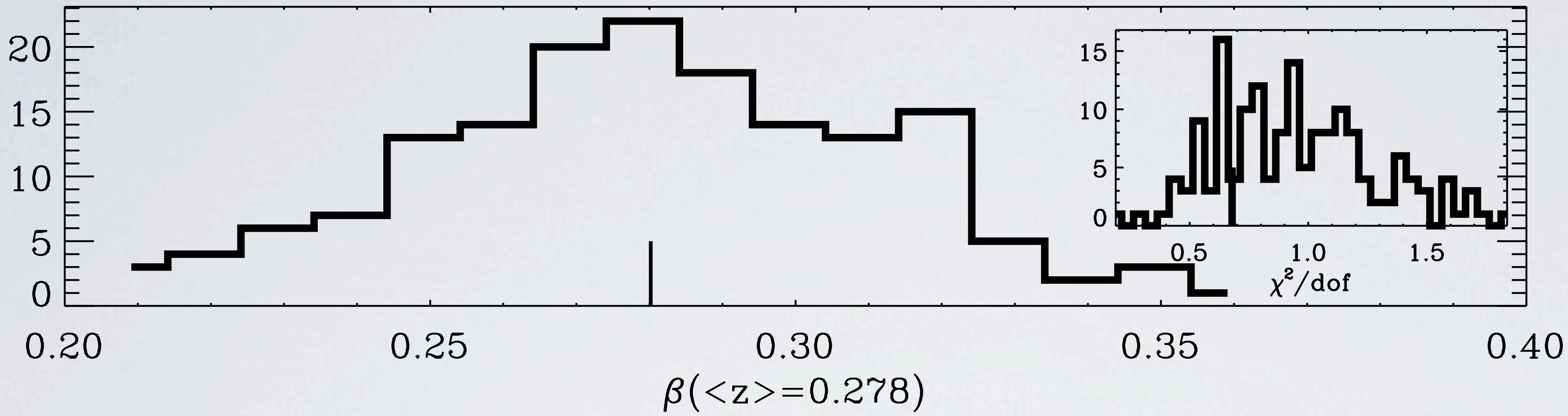

$\sigma_\beta/\beta \sim 10\%$

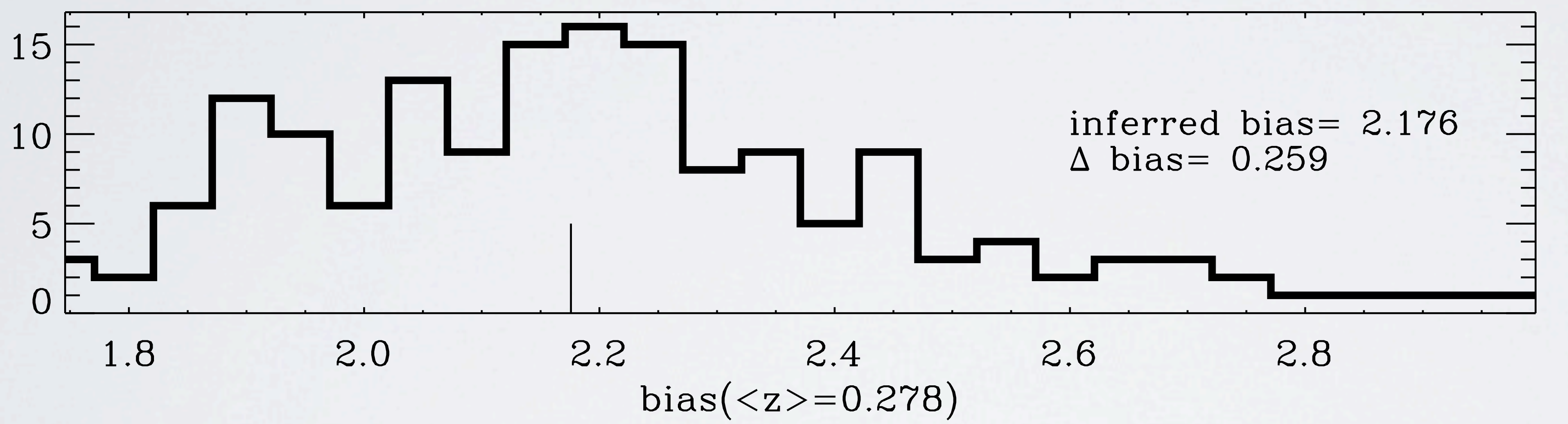

$\sigma_{bias}/bias \sim 10\%$

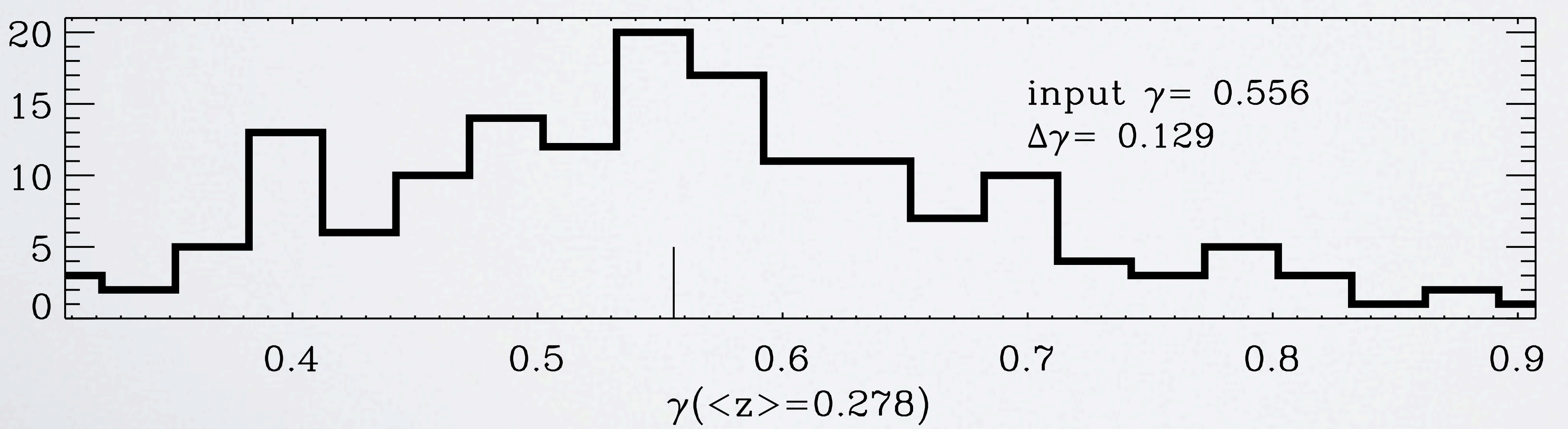

$\sigma_\gamma/\gamma \sim 25\%$

Quadrupole Test- Cosmological Significance

$$\beta \equiv f(z)/b_1 \approx \Omega_M^{\gamma}(z)/b_1$$

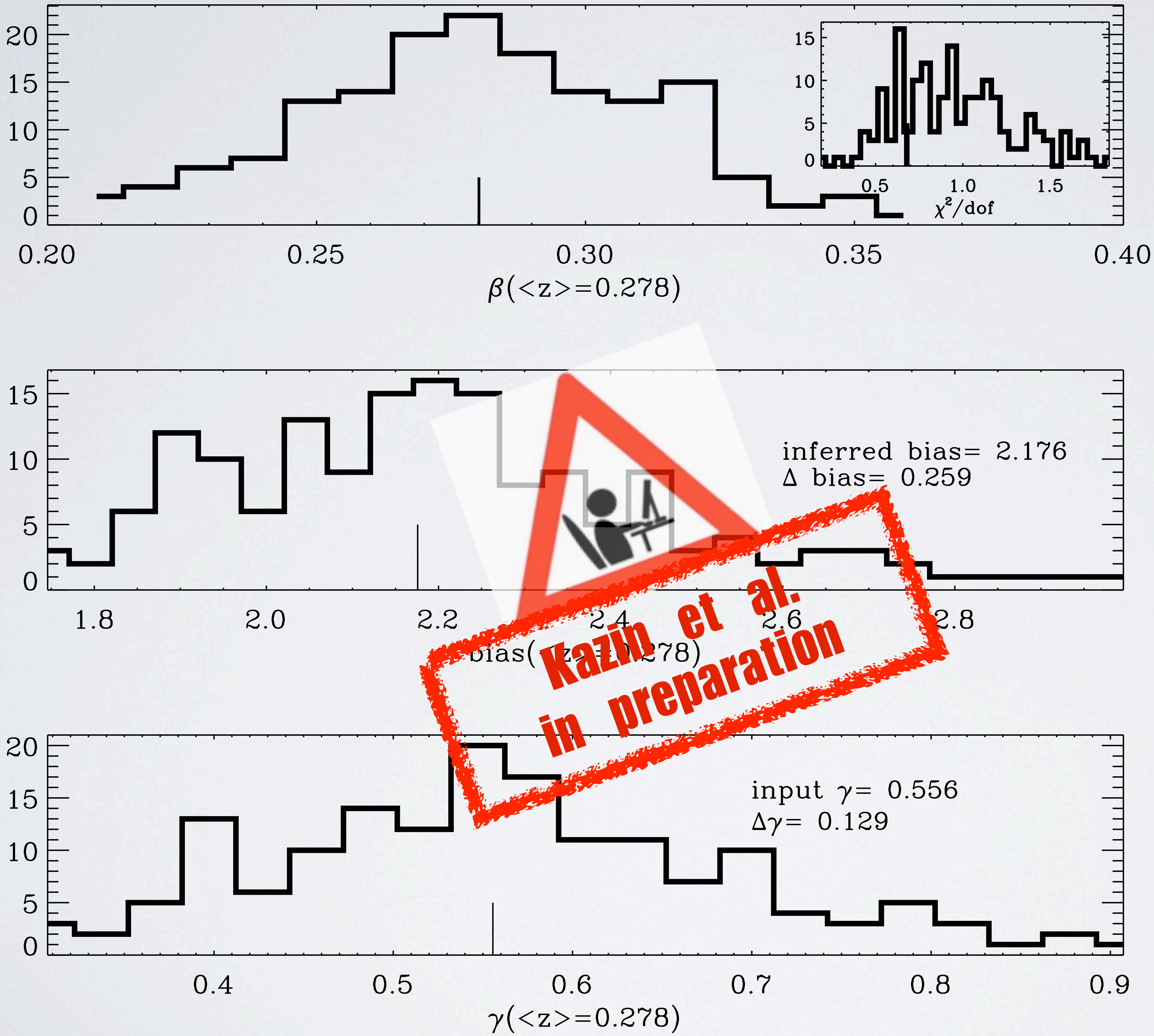

$\sigma_\beta/\beta \sim 10\%$

$\sigma_{bias}/bias \sim 10\%$

$\sigma_\gamma/\gamma \sim 25\%$

β through the Quadrupole Test
Non-Linear Theory

$$Q = \xi_2(s) / [\xi_0(s) - \langle \xi_0(s) \rangle] = (4/3\beta + 4/7\beta^2)/(1 + 2/3\beta + 1/5\beta^2)$$

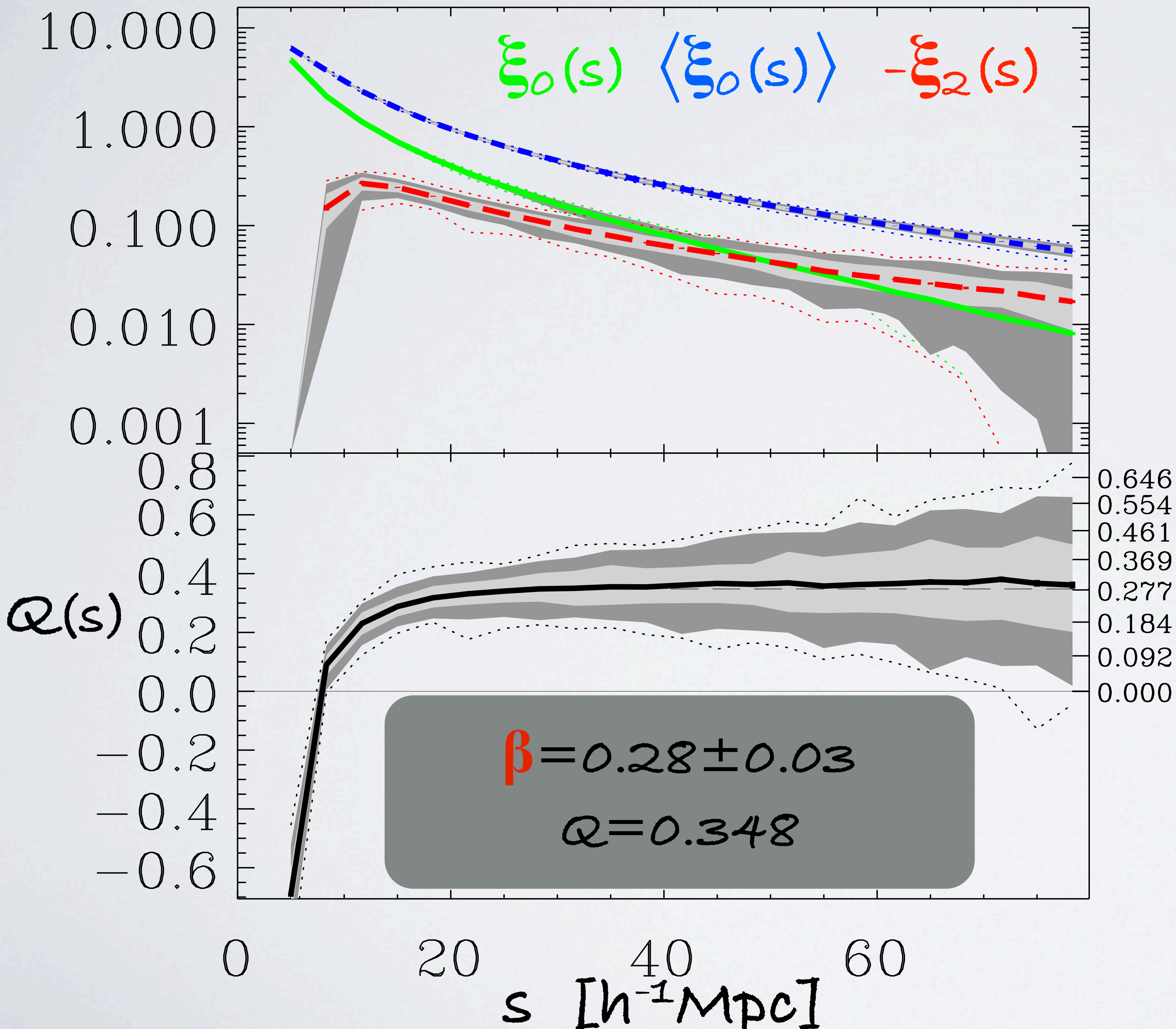

SDSS-II

$\sigma_\beta/\beta \sim 10\%-15\%$

$\beta \equiv f(z)/b_1 \approx \Omega_M^\gamma(z)/b_1$

β through the Quadrupole Test
Non-Linear Theory

$Q = \xi_2(s)/[\xi_0(s) - \langle\xi_0(s)\rangle] = (4/3\beta + 4/7\beta^2)/(1 + 2/3\beta + 1/5\beta^2)$

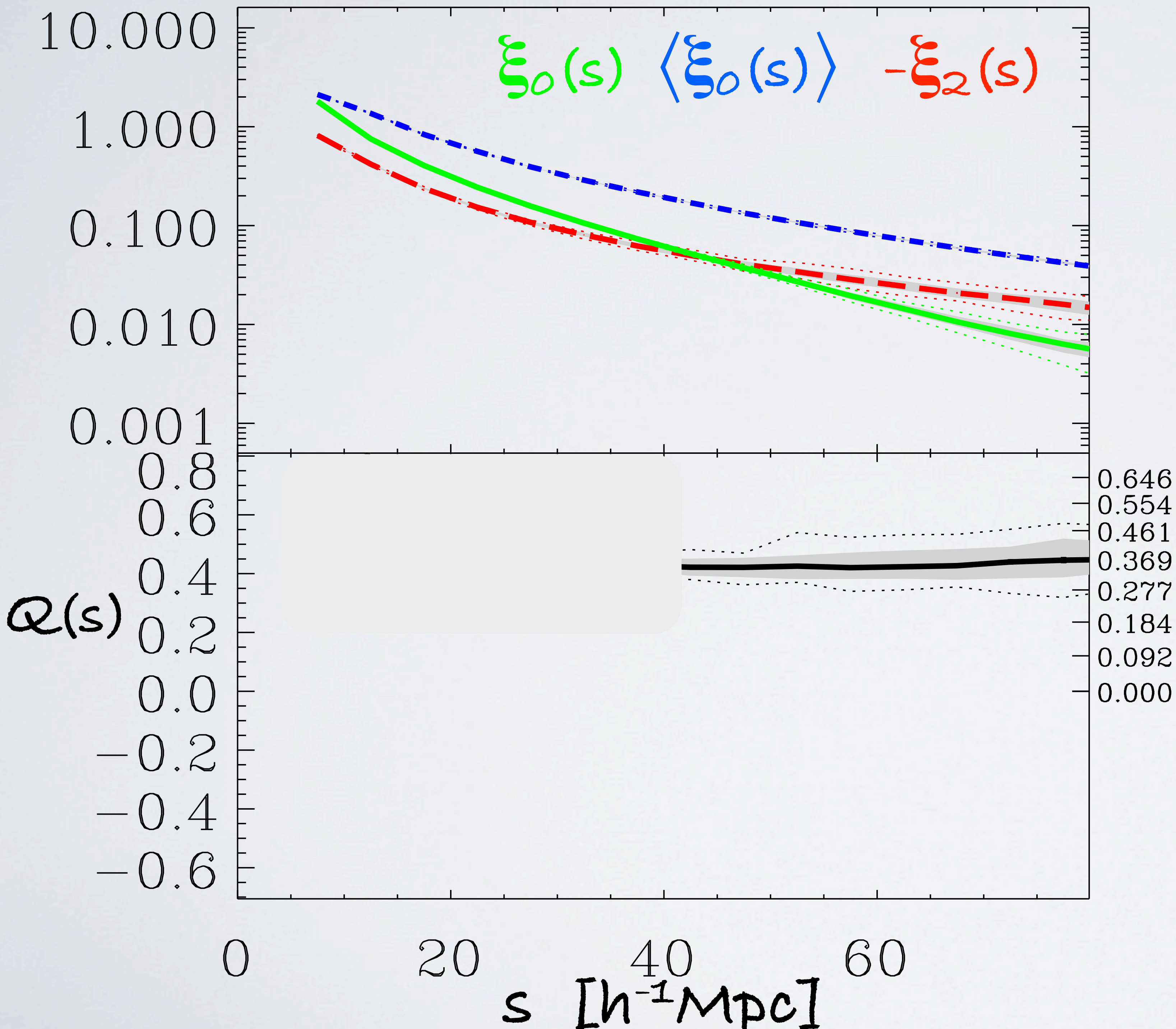

SDSS-III

$\sigma_\beta/\beta \sim 7\%$

$\beta \equiv f(z)/b_1 \approx \Omega_M^\gamma(z)/b_1$

Summary

- ☑ Baryonic Acoustic Feature in SDSS-II ξ Monopole
  - ☑ Apparent in LRG clustering, and consistent with ΛCDM cosmology.
  - ☑ Can be used to measure distance to $z\sim0.28$ at accuracy of 3%
  - ☑ Prediction: Strong signal at $s\sim130\ h^{-1}\mathrm{Mpc}$ will not appear in BOSS
- ☑ Baryonic Acoustic Feature in Line of Sight ξ
  - ☑ Not measurable in SDSS-II due to lack of modes
  - ☑ Will be noisy in BOSS when restricting to thin angular slice ($\theta<3°$)
  - ☑ Using wider wedges- BOSS will be able to be distinguished from transverse signal, enabling disentanglement of $H(z)$ and $D_A(z)$
- ☐ Redshift Distortions in Clustering
  - ☑ Yields $\sigma_\beta/\beta\sim10\%$ @ $z\sim0.28$ (sample variance)
  - ☐ Cosmological constraints

"All astronomers do these days is count photons, galaxies and citations", M.R.B

Summary

- ☑ Baryonic Acoustic Feature in SDSS-II ξ Monopole
  - ☑ Apparent in LRG clustering, and consistent with ΛCDM cosmology.
  - ☑ Can be used to measure distance to $z\sim0.28$ at accuracy of 3%
  - ☑ Prediction: Strong signal at $s\sim130\ h^{-1}\mathrm{Mpc}$ will not appear in BOSS
- ☑ Baryonic Acoustic Feature in Line of Sight ξ
  - ☑ Not measurable in SDSS-II due to lack of modes
  - ☑ Will be noisy in BOSS when restricting to thin angular slice ($\theta<3°$)
  - ☑ Using wider wedges- BOSS will be able to be distinguished from transverse signal, enabling disentanglement of $H(z)$ and $D_A(z)$
- ☐ Redshift Distortions in Clustering
  - ☑ Yields $\sigma_\beta/\beta\sim10\%$ @ $z\sim0.28$ (sample variance)
  - ☐ Cosmological constraints

"All astronomers do these days is count photons, galaxies and citations", M.R.B

ξ, c_{ij} results as well as LRG sample may be obtained here!
http://cosmo.nyu.edu/~eak306/LSS.html

Summary

- ☑ Baryonic Acoustic Feature in SDSS-II ξ Monopole
  - ☑ Apparent in LRG clustering, and consistent with ΛCDM cosmology.
  - ☑ Can be used to measure distance to $z\sim0.28$ at accuracy of 3%
  - ☑ Prediction: Strong signal at $s\sim130\ h^{-1}\mathrm{Mpc}$ will not appear in BOSS
- ☑ Baryonic Acoustic Feature in Line of Sight ξ
  - ☑ Not measurable in SDSS-II due to lack of modes
  - ☑ Will be noisy in BOSS when restricting to thin angular slice ($\theta<3°$)
  - ☑ Using wider wedges- BOSS will be able to be distinguished from transverse signal, enabling disentanglement of $H(z)$ and $D_A(z)$
- ☐ Redshift Distortions in Clustering
  - ☑ Yields $\sigma_\beta/\beta\sim10\%$ @ $z\sim0.28$ (sample variance)
  - ☐ Cosmological constraints

Thank You!

"All astronomers do these days is count photons, galaxies and citations", M.R.B

ξ, c_{ij} results as well as LRG sample may be obtained here!

http://cosmo.nyu.edu/~eak306/LSS.html

Luminous Red Galaxies

Eisenstein et al. (2001)

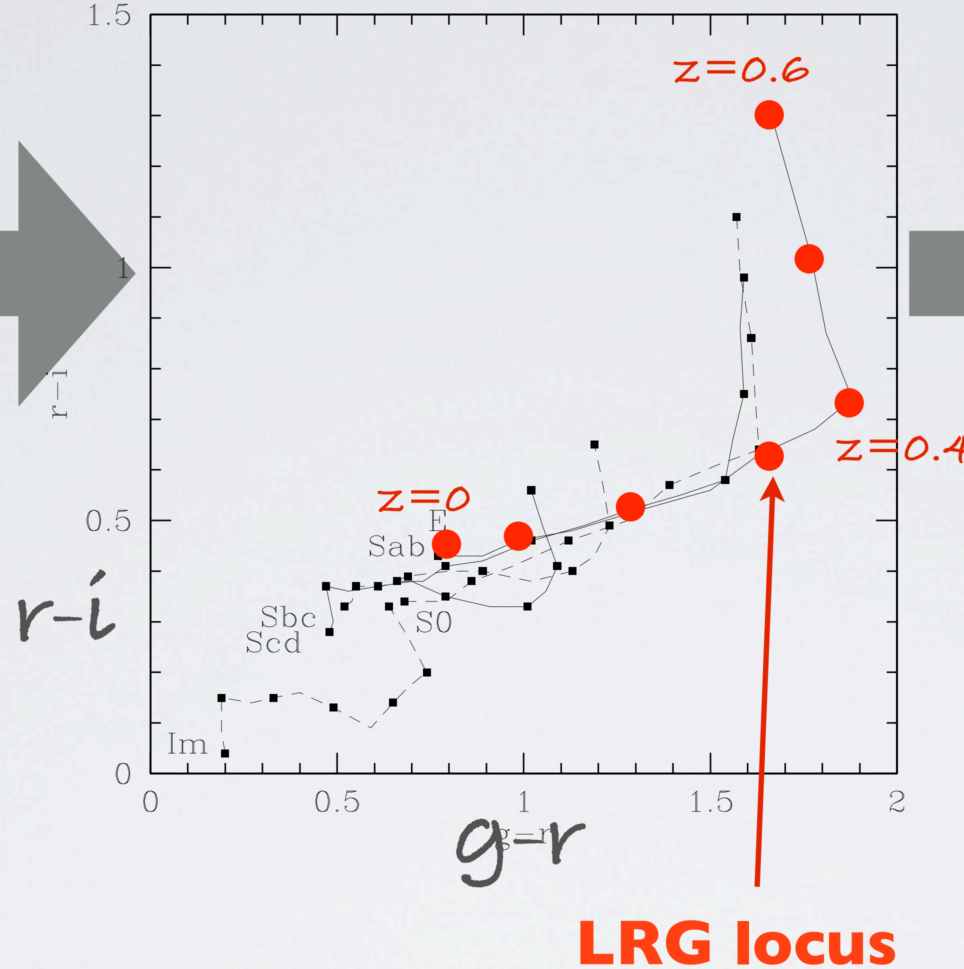

Padmanabhan et al. (2007)

based on Bruzual&Charlot (2003) model

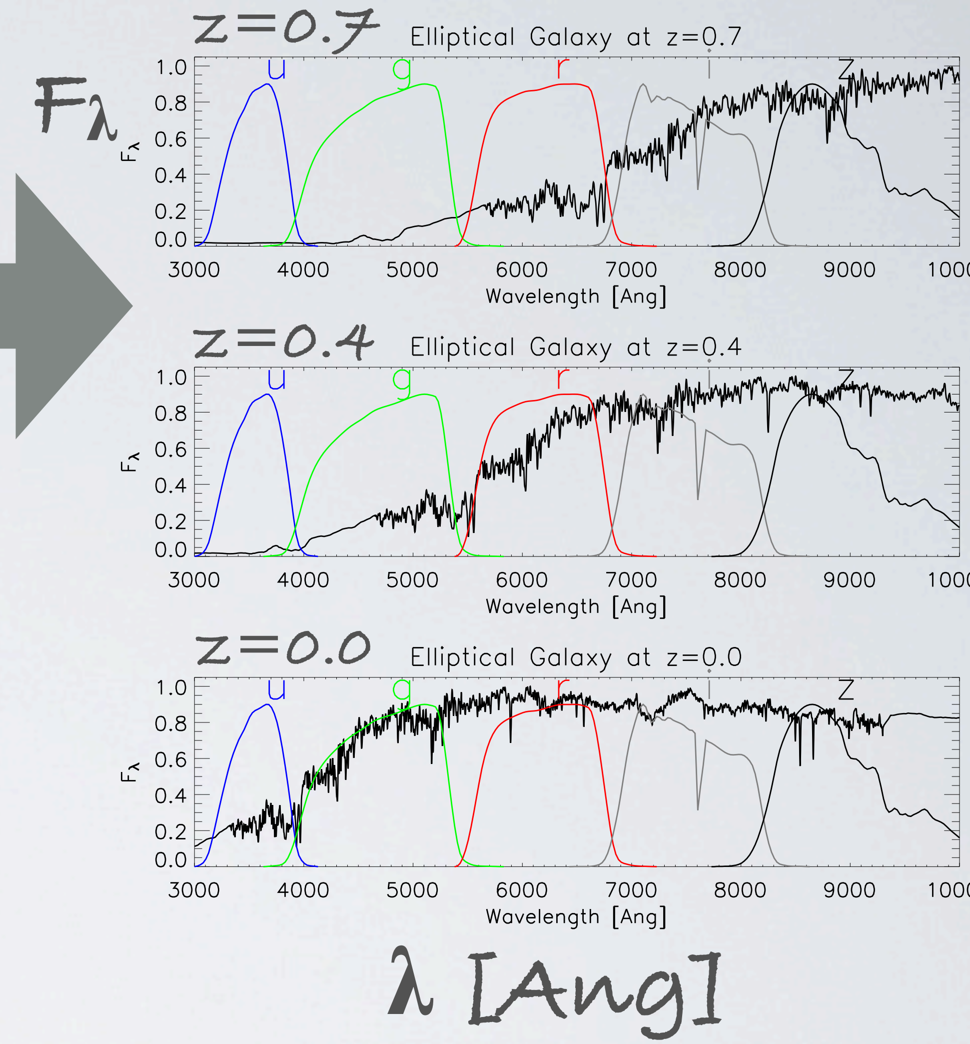

- Luminous ➢ Enable large volume limited samples
- Not too rare $n(z) \sim 3 \cdot 10^{-4}\ (h\mathrm{Mpc}^{-1})^3$
- Trace Matter well, "*bias*" (*clustering gain*) $b_{Lin} \sim 2$
- Easy to identify by color cuts, spectra

$$\delta_{gal} \approx b_{Lin}\,\delta$$

Some Cosmography

Hubble Equation; assumptions: low z's $v_H << c$

$$cz = v_H = H_0 d = H_0 \chi / (1+z)$$

Comoving distances generalized

$$\chi(z) = c\int_0^z dz'/H(z')$$

Assuming flat ΛCDM

expansion rate

$$H(z) = H_0\{\Omega_M (1+z)^3 + \Omega_\Lambda f(z)\}^{0.5}$$

where

$$f(z) \equiv \exp[3\int_0^z dz'(1+w(z'))/(1+z')]$$

equation of state $w \equiv P_\Lambda / \rho_\Lambda$

Some Cosmography

↑ more

$$\chi(z) = c\int_0^z dz'/H(z')$$ comoving distance

$$D_A = \frac{\sin\{\sqrt{(-\Omega_K)}\,\chi\}}{(1+z)\sqrt{(-\Omega_K)}}$$ angular distance (not comoving!)

$\Omega_K > 0$ open universe
$\Omega_K < 0$ closed

$$\approx \frac{\chi}{(1+z)}$$

assuming flat universe $\Omega_K \Rightarrow 0$

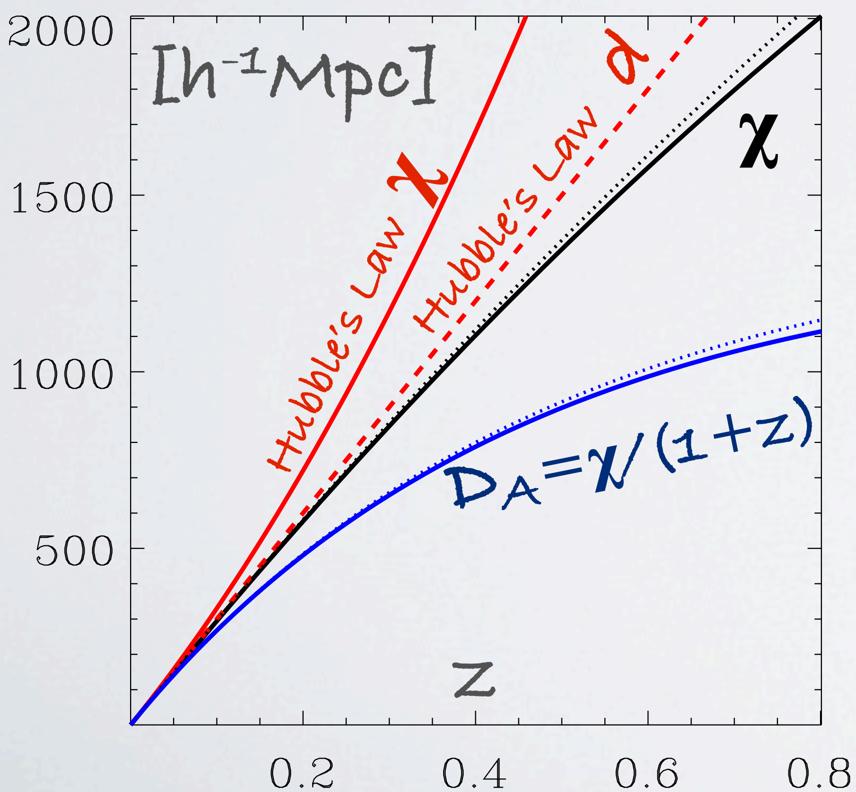

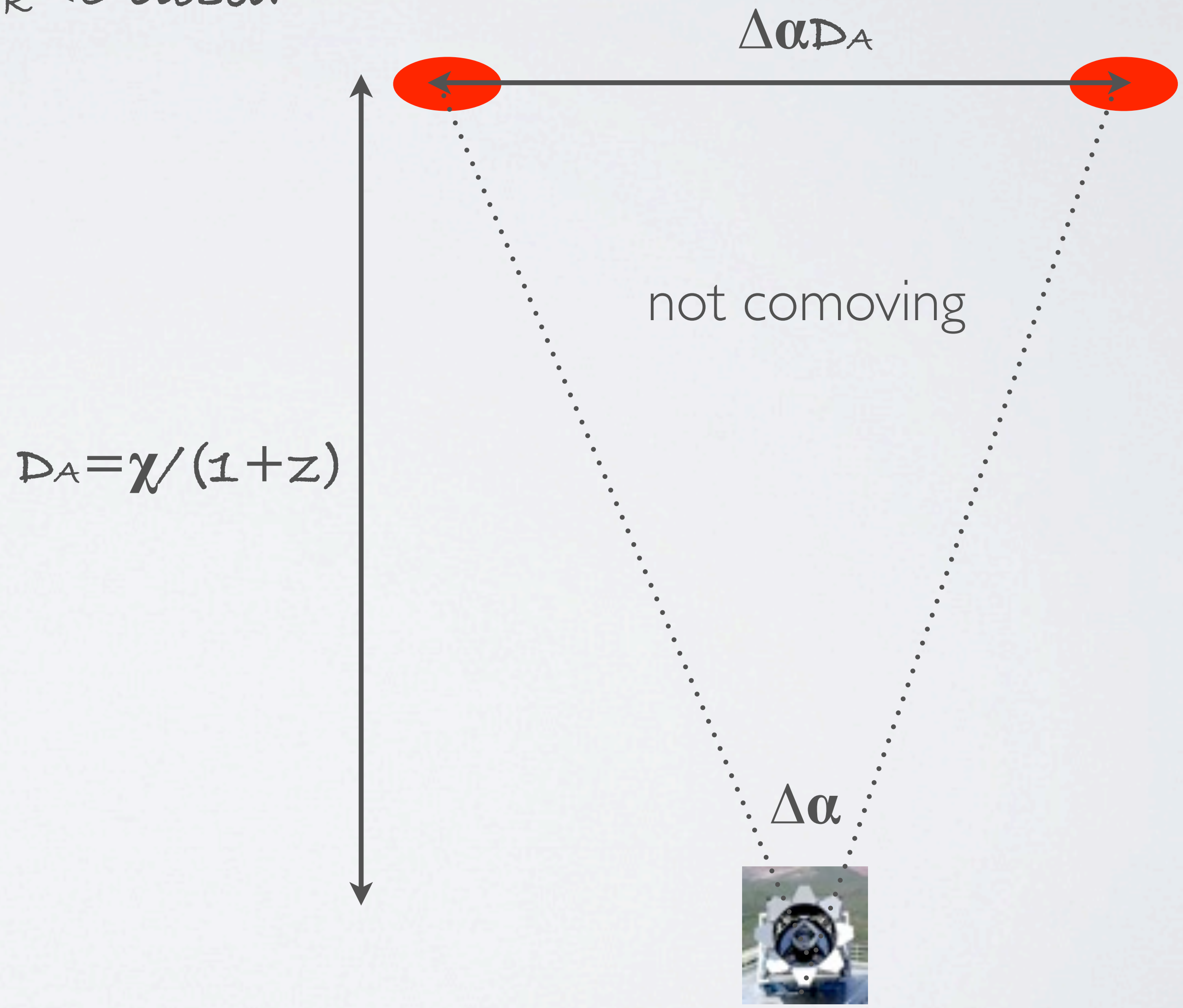

Redshift Distortions

Dark Matter Simulation

Benítez et al. (2008)

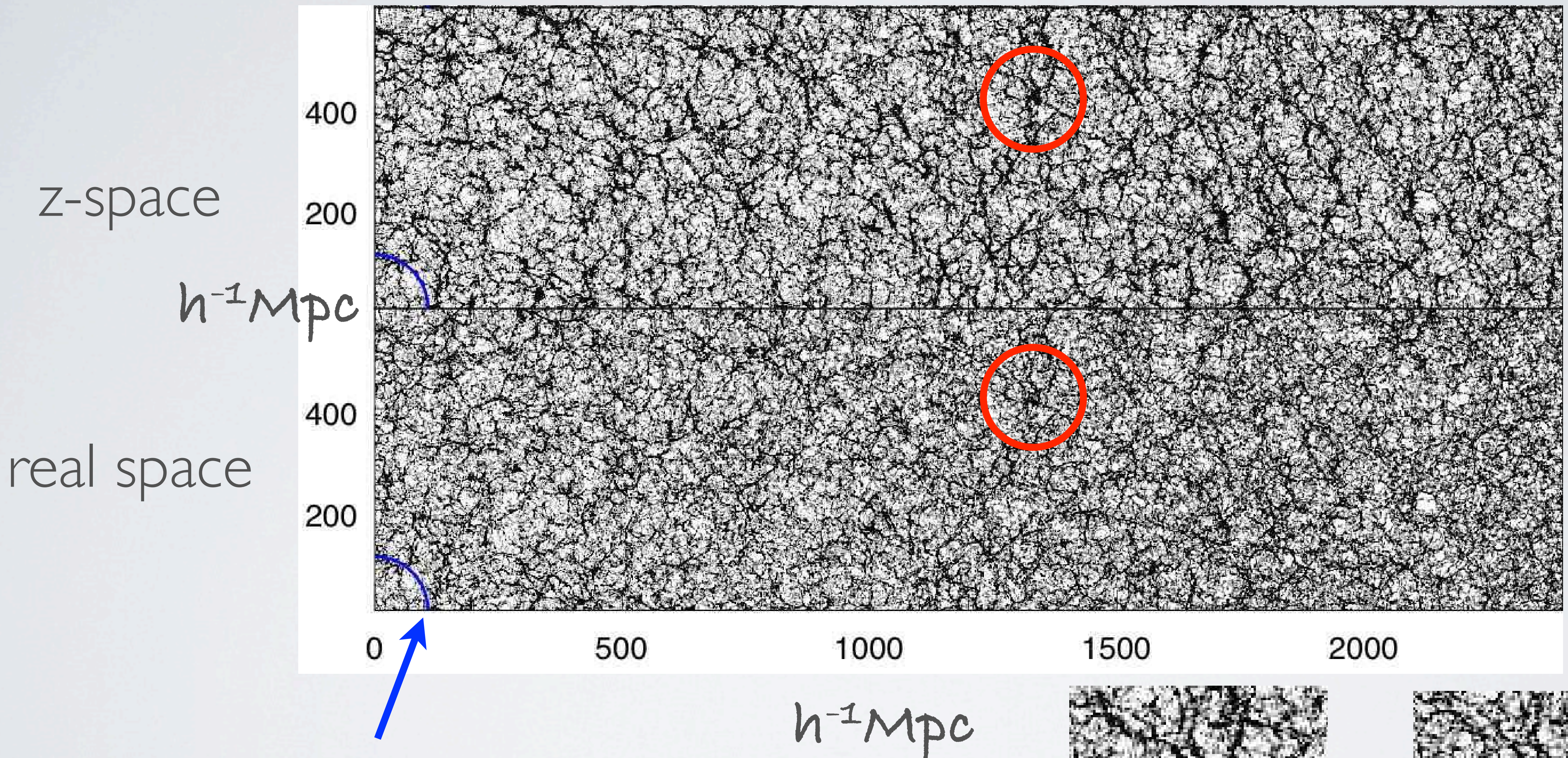

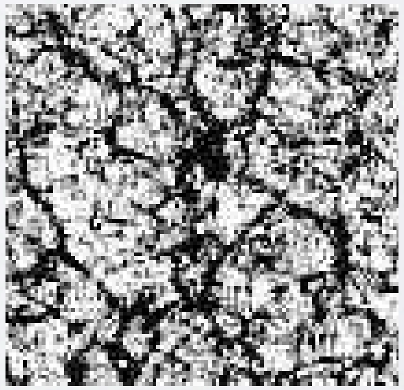

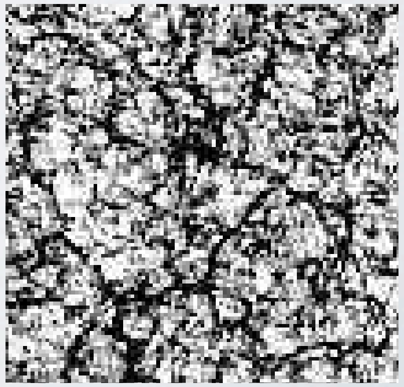

The Alcock&Paczynski Effect

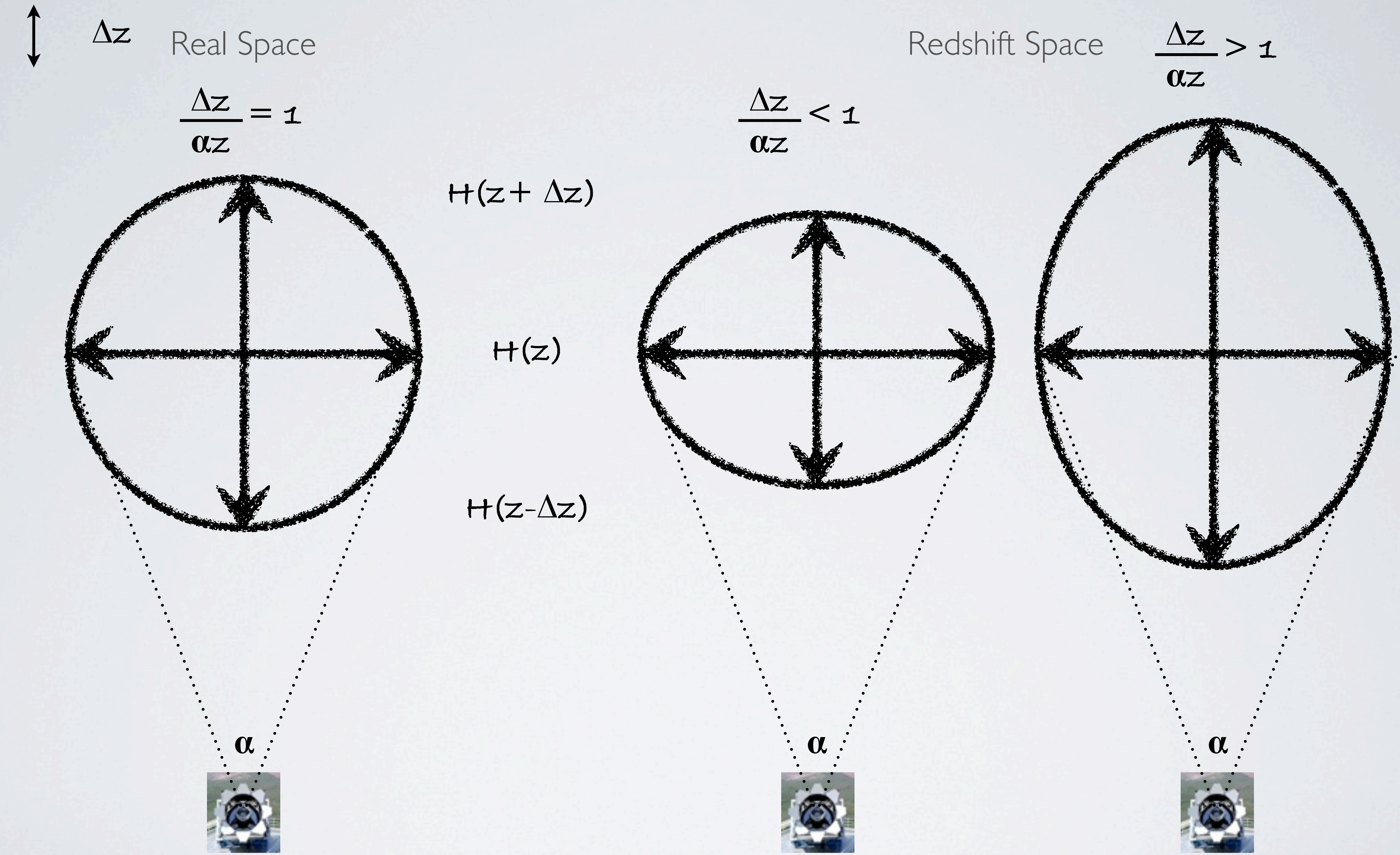

$$\frac{\Delta z}{\alpha z} = z^{-1}[\Omega_{\Lambda}+\Omega_{M0}(1+z)^{3}]^{1/2}\int_{1}^{z+1} dy\,(\Omega_{\Lambda}+\Omega_{M0}y^{3})$$

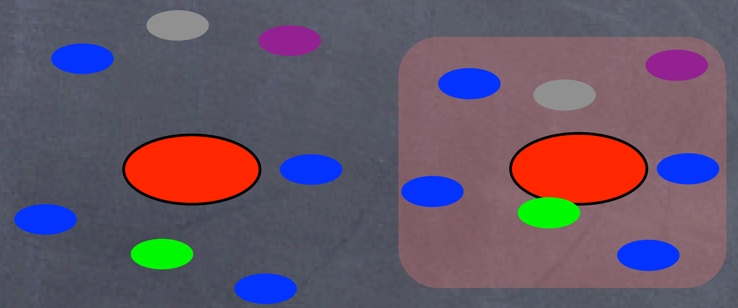

Quantifying the Squashing Effect

Kaiser 1987: Spherical Harmonics

$$P_{gal}^{(S)}(k,\mu) = (1+\beta\mu^2)^2 P_{gal}(k)$$

$$P_{gal}^{(S)}(k,\mu) = \mathcal{L}_0(\mu) P_0^{(S)}(k) + \mathcal{L}_2(\mu) P_2^{(S)}(k) + \mathcal{L}_4(\mu) P_4^{(S)}(k)$$

where

$$P_l(k) = 0.5(2l+1)\int P(\mu',k)\mathcal{L}_\ell(\mu')\, d\mu'$$

Legendre Polynomials

$$\mathcal{L}_0(\mu) = 1$$

$$\mathcal{L}_2(\mu) = 0.5(3\mu^2-1)$$

$$\mathcal{L}_4(\mu) = 0.125(35\mu^2-30\mu+3)$$

and

$\mu \equiv \cos(\theta)$

$f \equiv d\ln(D_1)/d\ln(a)$

$\beta \equiv f/b_1$

$\delta_{gal} \approx b_1 \delta$

observables!

$$P_0^{(S)}(k) = B_0(\beta)\, P_{gal}(k)$$

$$P_2^{(S)}(k) = B_2(\beta)\, P_{gal}(k)$$

$$P_4^{(S)}(k) = B_4(\beta)\, P_{gal}(k)$$

$$B_0(\beta) \equiv (1+2/3\beta+1/5\beta^2)$$

$$B_2(\beta) \equiv (4/3\beta+4/7\beta^2)$$

$$B_4(\beta) \equiv 8/35\beta^2$$

What Should We Expect from BOSS?

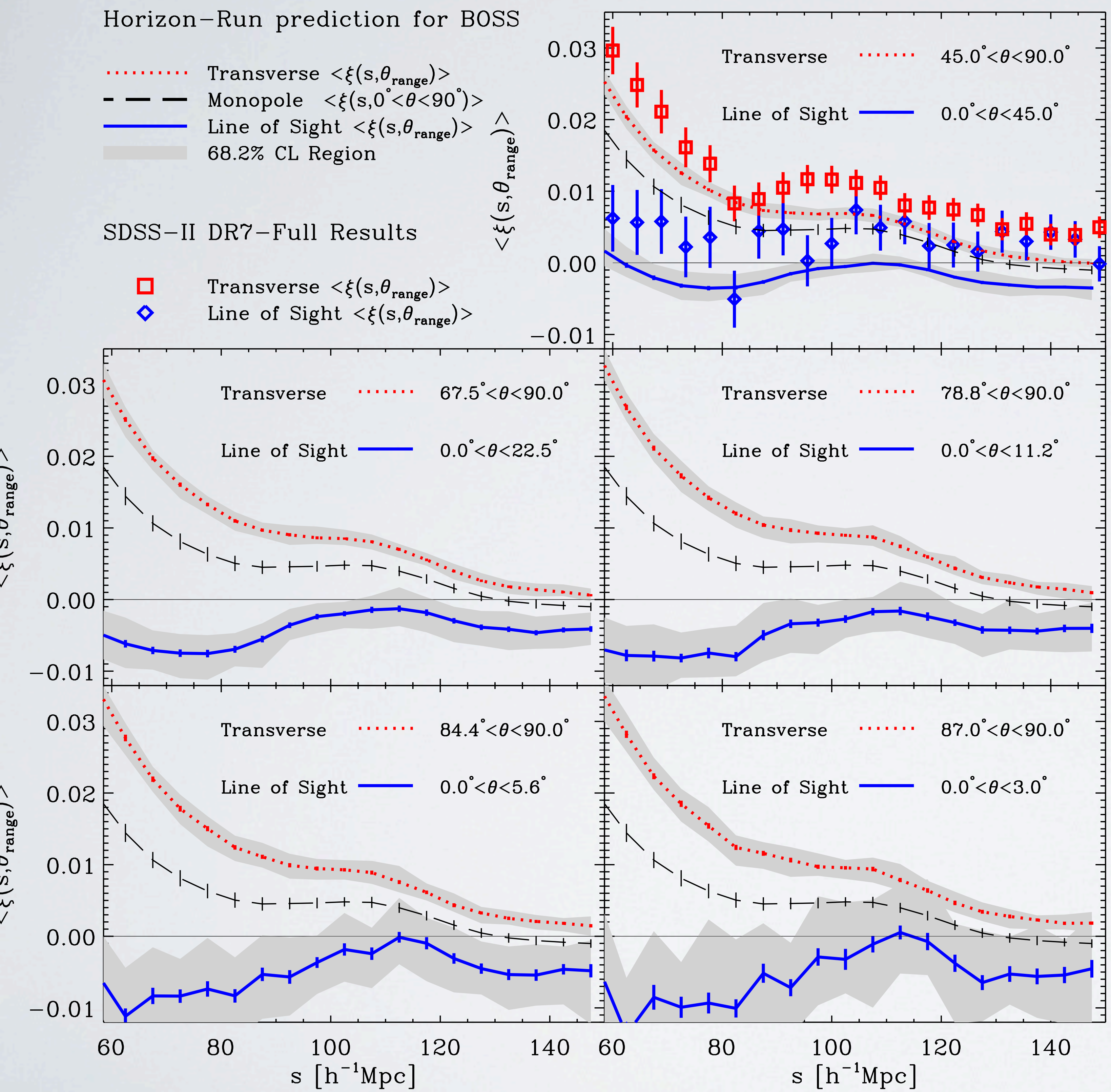

What Should We Expect from BOSS?

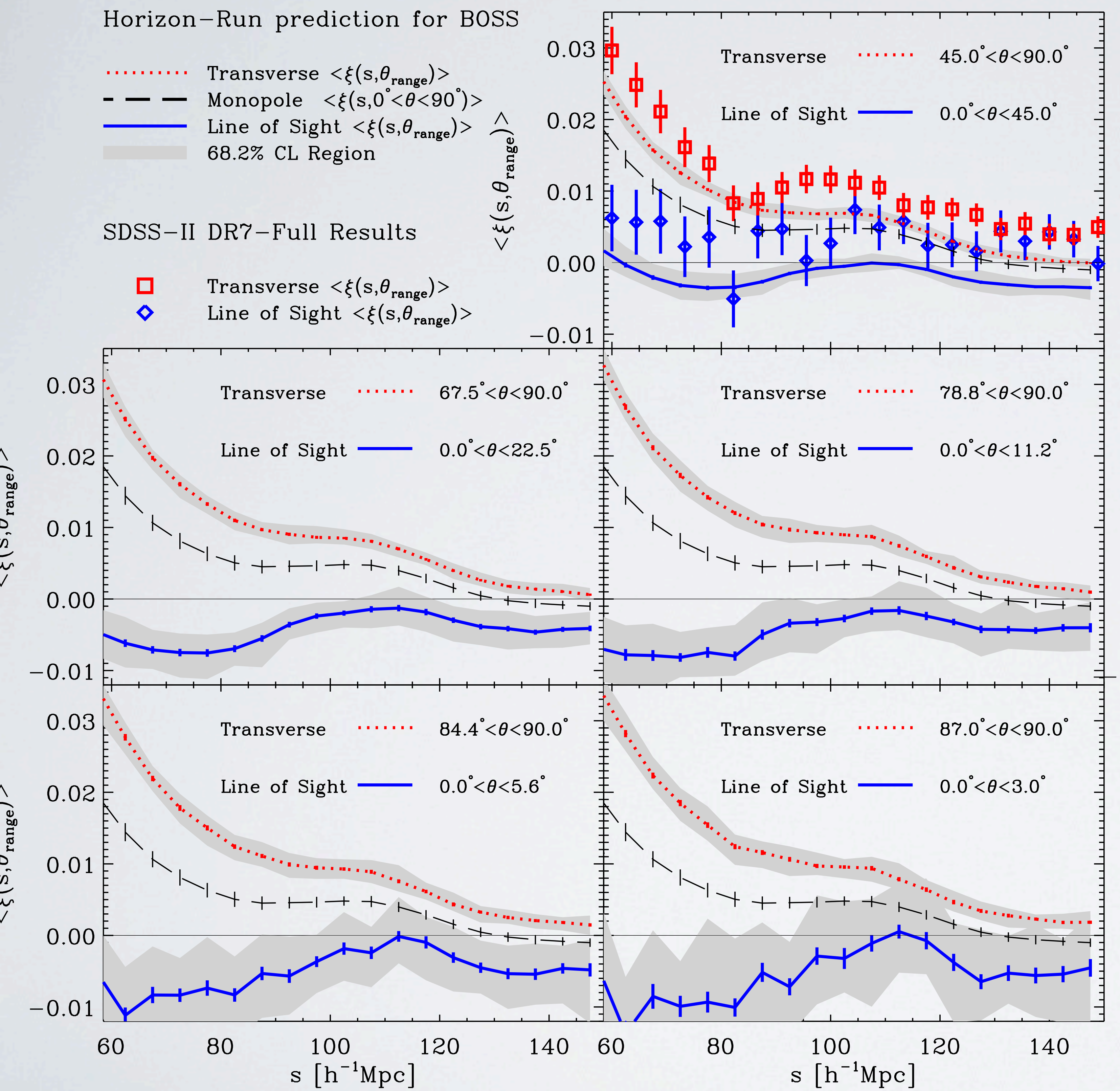

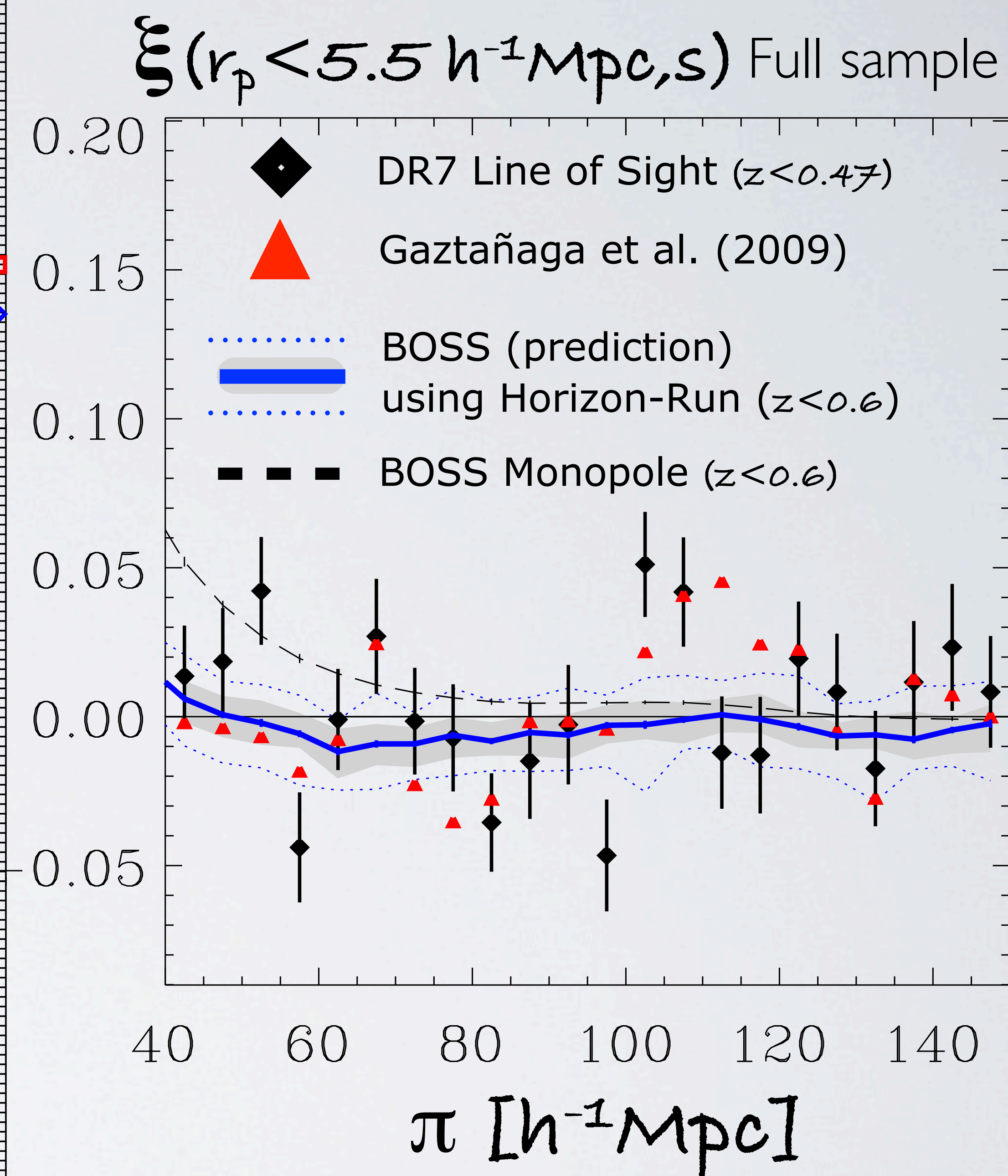

dotted: NL thoery
solid: SDSS-II